Lessons on Gas Detectors

A. Ranieri, «Gas Detectors Course», Scuola di Dottorato Bari 2017

Course's aim

- **Physics, architecture and construction techniques of Gaseous Detectors**
- Part I (Prof. F. Tessarotto)
  - Theoretical introduction (ionization, transport, multiplication, signal formation)
  - MPGDs in general (historical introduction, MSGCs, GEMs, Micromegas and other architectures)
  - GEMs, THGEMs and Micromegas (manufacturing, performance, applications)
  - PID (introduction, RICH principle, radiators, optics, photon detectors, example of RICHs)
  - Gaseous photon detectors (general characteristics, THGEMs + CsI, perspectives)

- **Part II (Prof. Verwilligen)**
- Simulation activity
- The students will face a few simulation aspects of micro-pattern gaseous detectors. During this part, the students will calculate and visualize the electric field of a GEM detector.
- Thereafter the students will use the calculated electric field to generate the response to a muon passing through the GEM detector.
- Therefore, they will simulate the gas with MAGBOLTZ, simulate the ionization of a muon passing through the GEM with HEED, and track the drifting ionization electrons with GARFIELD.
- GARFIELD will then be used to simulate the avalanches initiated by those ionization electrons and finally the students will calculate the signal induced by these avalanches.

- **Part III (A. Ranieri)**
- **Laboratory experiences**
- It will be performed a few classical measurements (gain, rates, sensitivity, etc..) based on a small planar GEM detector.

The gas ionization

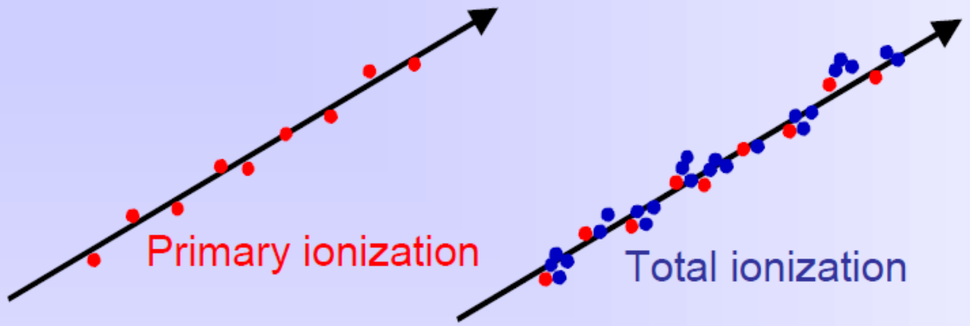

Lohse and Witzeling, Instrumentation In High Energy Physics, World Scientific,1992

Fast charged particles ionize atoms of gas. Often resulting primary electron will have enough kinetic energy to ionize other atoms.

$$n_{total} = \frac{\Delta E}{W_i} = \frac{\frac{dE}{dx}\Delta x}{W_i}$$

$$n_{total} \approx 3\ldots4 \cdot n_{primary}$$

n_{total} - number of created electron-ion pairs

Δ_E = total energy loss

W_i = effective <energy loss>/pair

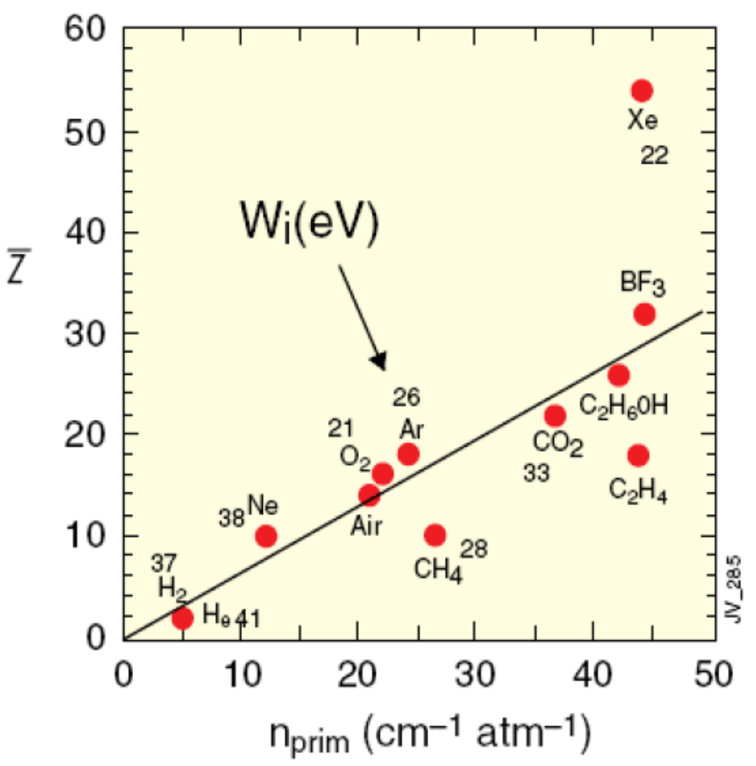

Number of primary electron/ion pairs in frequently used gases.

The gas ionization

The actual number of primary electron/ion pairs is Poisson distributed.

$$P(m) = \frac{\bar{n}^m e^{-\bar{n}}}{m!} \qquad \bar{n} = \frac{L}{\lambda} = LN\sigma_i$$

The detection efficiency is therefore limited to :

$$\varepsilon_{\text{det}} = 1 - P(0) = 1 - e^{-\bar{n}}$$

For thin layers ε_{det} can be significantly lower than 1.

For example for 1 mm layer of Ar $n_{primary} = 2.5 \rightarrow \varepsilon_{det} = 0.92$.

100 electron/ion pairs created during ionization process is not easy to detect.

Typical noise of the amplifier ≈ 1000 e^- (ENC) → gas amplification .

Charge moltiplication process in uniform field

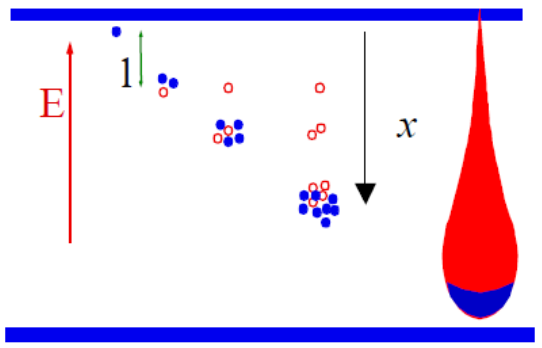

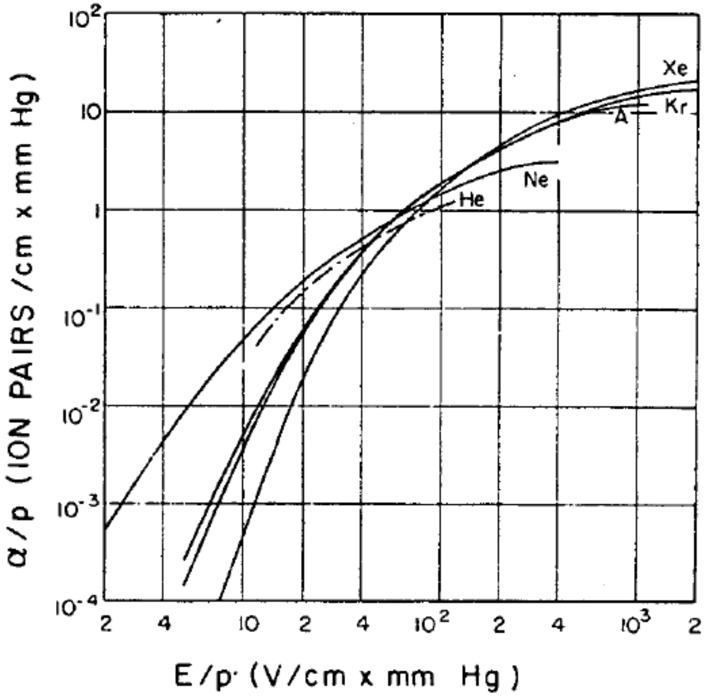

S.C. Brown, Basic Data of Plasma Physics (MIT Press, 1959)

Mean free path for ionization:

$$\lambda = \frac{1}{N\sigma} \qquad N\text{: molecules/cm}^3$$

Townsend coefficient:

$$\alpha = \frac{1}{\lambda} \qquad \text{Ionizing collisions/cm} \qquad \frac{\alpha}{P} = f\left(\frac{E}{P}\right)$$

$$\alpha = Ape^{-B\frac{p}{E}}$$

Incremental increase of the number of electrons in the avalanche:

$$dn = n\,\alpha\,dx$$

Multiplication factor (Gain): $M(x) = \frac{n}{n_0} = e^{\alpha x}$

Maximum Avalanche size before discharge (Raether limit):

Raether limit: $M < 10^8 \rightarrow \alpha x < 20$

H. Raether, Electron Avalanches and Breakdown in Gases (Butterworth 1964)

α(E) is determined by the excitation and ionization cross section of the electrons in the gas

α(E) depends also on various and complex energy transfer mechanisms between gas molecules.
It has to be measured for every gas mixtures

$$M = \exp\left[\int_{x_1}^{x_2} \alpha(x)dx\right]$$

Single wire proportional chamber

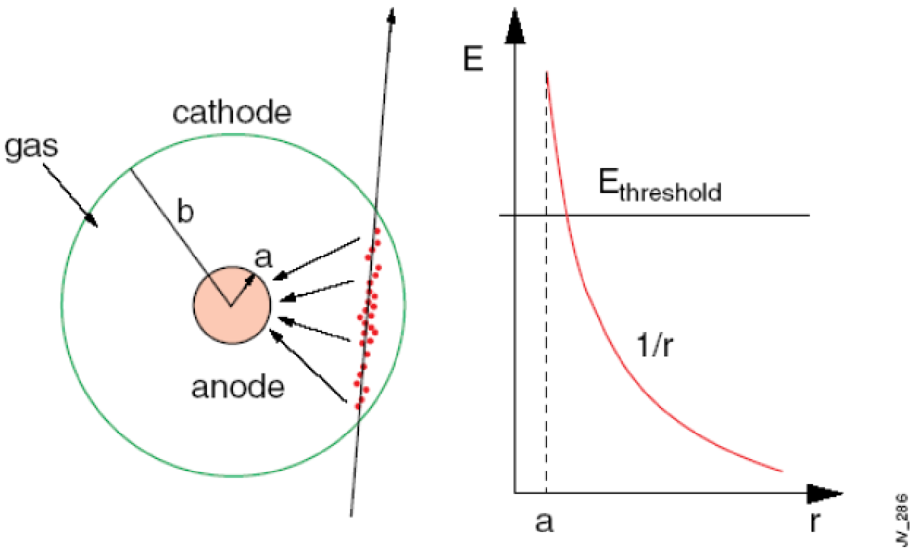

Electrons liberated by ionization drift towards the anode wire.

Electrical field close to the wire (typical wire Ø ~few tens of μm) is sufficiently high for electrons (above 10 kV/cm) to gain enough energy to ionize further → avalanche – exponential increase of number of electron ion pairs.

anode

e⁻ primary electron

$$E(r) = \frac{CV_0}{2\pi\varepsilon_0} \cdot \frac{1}{r}$$

$$V(r) = \frac{CV_0}{2\pi\varepsilon_0} \cdot \ln\frac{r}{a}$$

C – capacitance/unit length

Cylindrical geometry is not the only one able to generate strong electric field:

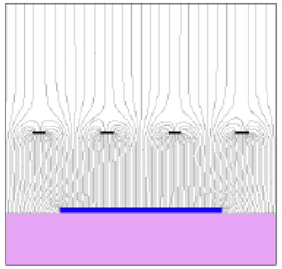

parallel plate

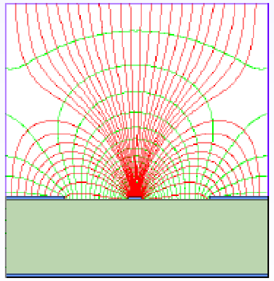

strip

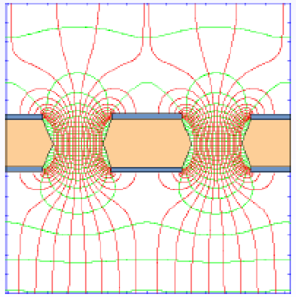

hole

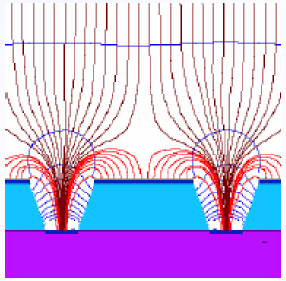

groove

SWPC – Operation Modes

ionization mode – full charge collection, but no charge multiplication;
gain ~ 1

proportional mode – multiplication of ionization starts; detected signal proportional to original ionization → possible energy measurement (dE/dx); secondary avalanches have to be quenched;
gain ~ $10^4 – 10^5$

limited proportional mode (saturated, streamer) – strong photoemission; secondary avalanches merging with original avalanche; requires strong quenchers or pulsed HV; large signals → simple electronics;
gain ~ 10^{10}

Geiger mode – massive photoemission; full length of the anode wire affected; discharge stopped by HV cut; strong quenchers needed as well

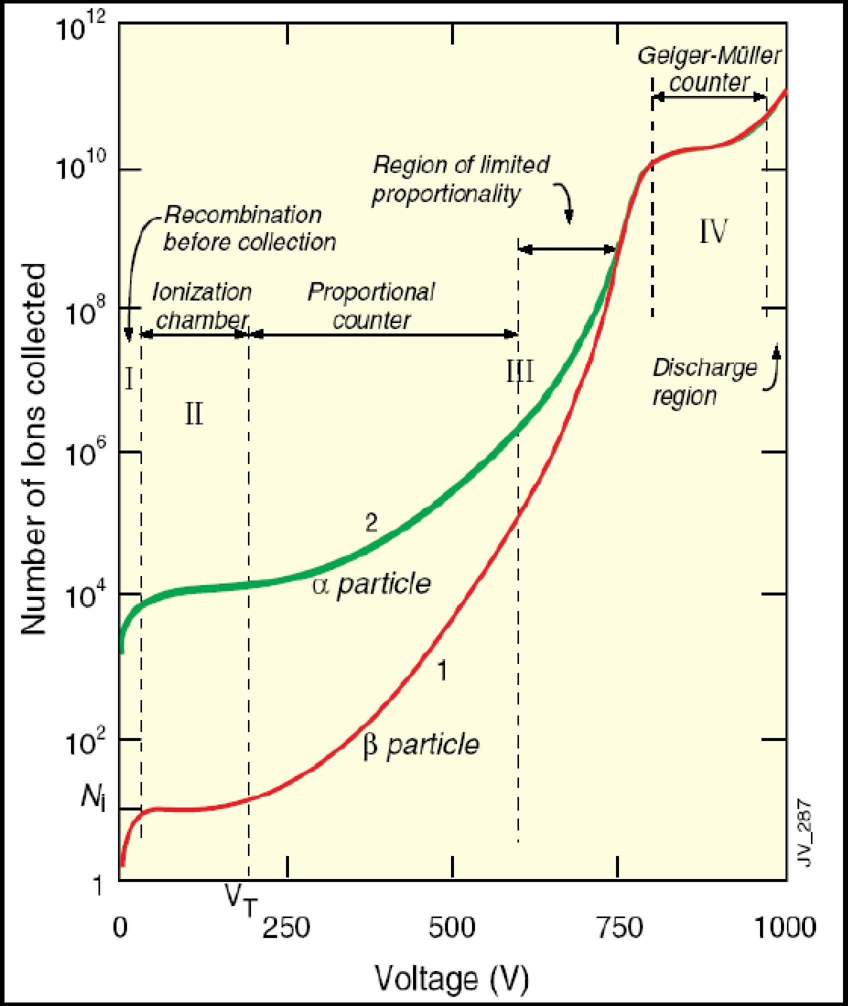

The invention of MWPC

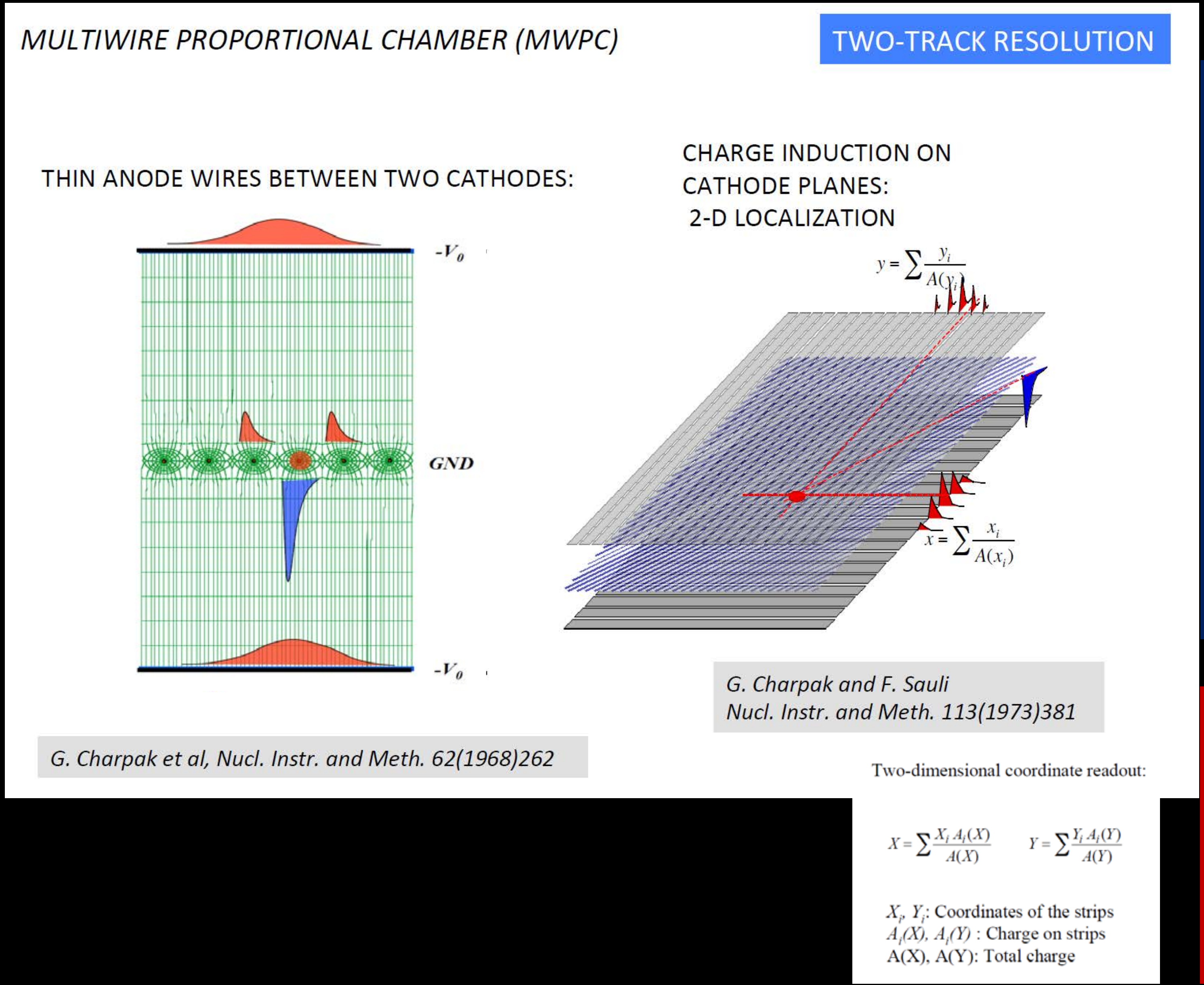

A major revolution occurred in 1968, when Georges Charpak invented the Multiwire Proportional Chamber(MWPC), a gaseous detector outperforming by orders of magnitude the rate capability of contemporary devices. Consisting of a grid of thin, parallel anode wires between two cathode planes, on application of suitable voltages the device collects and amplifies, by avalanche multiplication, the tiny ionization clusters released in a gas by Ionizing radiation, permitting detection with electronics means.

Pro’s:
Space resolution improvement ($\Delta x = d/\sqrt{12}$)
Good rate capability
Con’s:
Increasing of Electric field attraction for narrower wires distance (→ stability and mechanical issue)

Adding third dimension

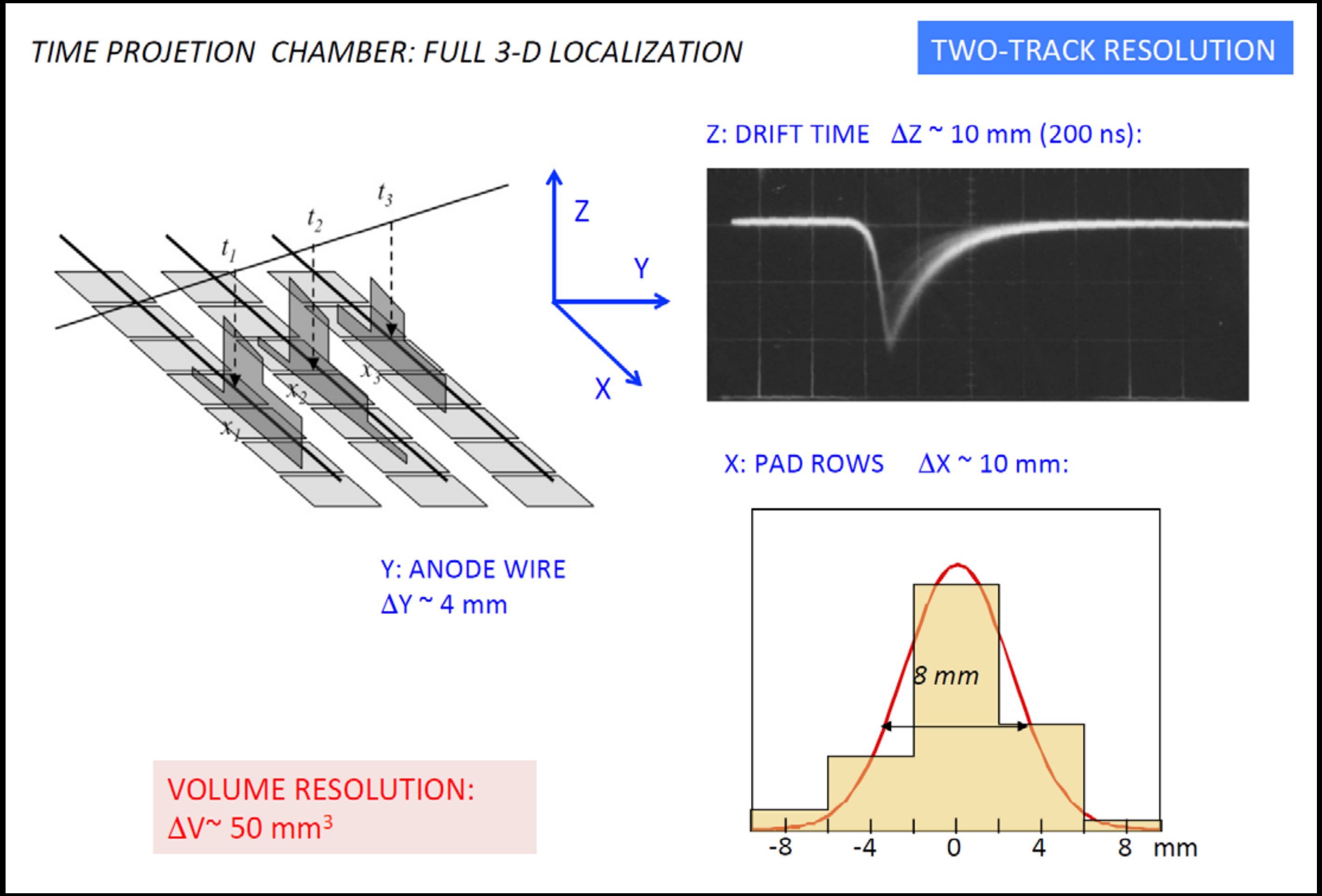

The MWPC was quickly adopted and successfully used by many experiments. Owing to the development work in many groups, the basic structure evolved and diversified into several more sophisticated devices exploiting the measurement of the collection or drift time of electrons to the anodes or the recording of the signals induced on cathodes to improve time and space resolutions.

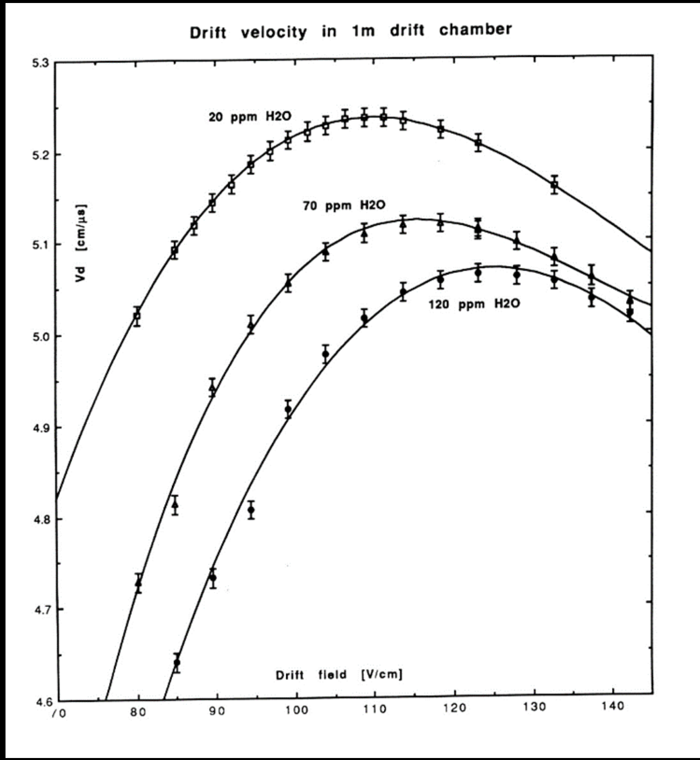

Big TPC construction

TIME PROJETION CHAMBER (TPC)

TWO-TRACK RESOLUTION

FIRST TPC: PEP-4 AT SLAC (1975)

D.R. Nygren and J. N. Marx, Physics Today No.31 Vol. 10(1978)

ALEPH TPC AT CERN-LEP (1989)

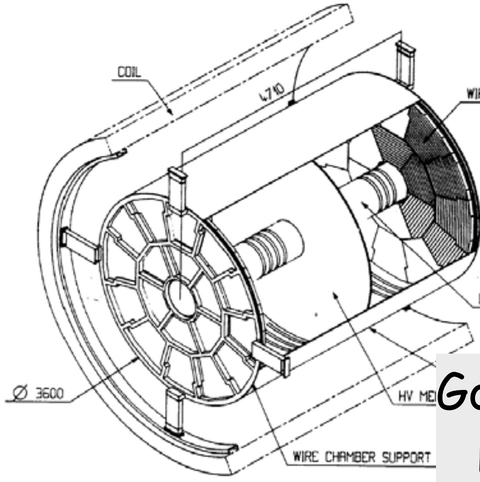

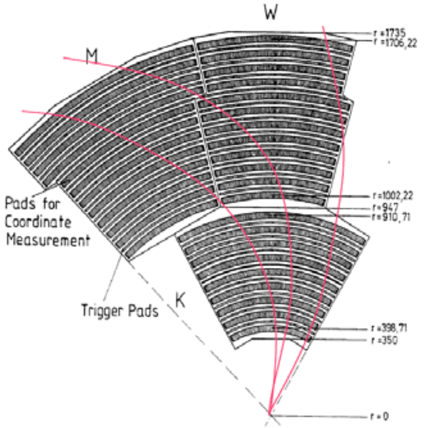

D. Decamp et al,Nucl. Instr.

- Field cage
- Gas system
- Wire chambers
- Gating
- Magnetic field
- Laser system
- Electronics

Dimensions

cylinder 4.7 x 1.8 m

Drift length

2x2.2 m

Electric field

110 V/cm

Electrodes

copper strips (35 μm & 19 μm thickness, 10.1 mm pitch, 1.5 mm gap) on Kapton

Good dE/dx resolution requires

long track length

large number of samples/track

good calibration, no noise, …

- Energy loss (dE/dx) depends on the particle velocity (Bethe-Block)
- The mass of the particle can be identified by measuring simultaneously momentum and dE/dx (ion pairs produced)
- Major problem is the large Landau fluctuations on a single dE/dx sample

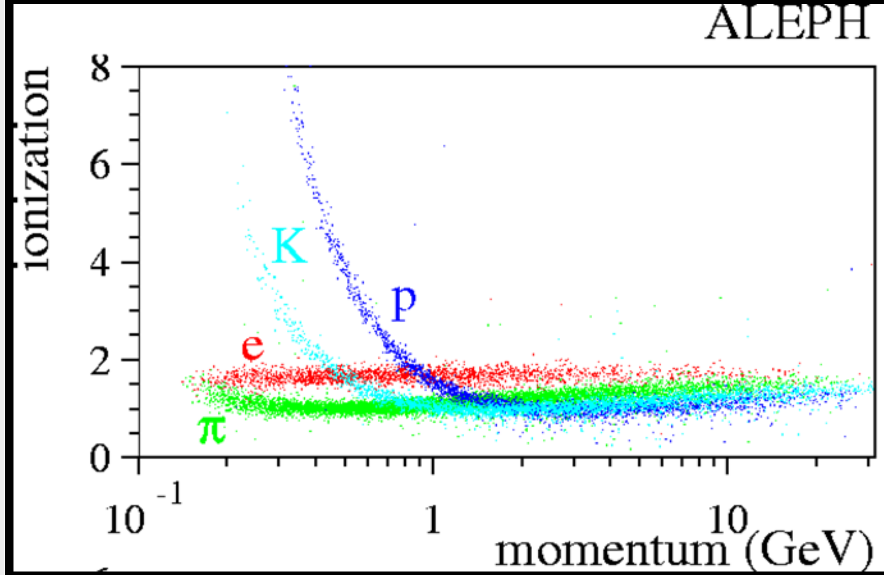

Space resolution:

$\sigma_{r\varphi} = 170\mu m$

$\sigma_z = 700\mu m$

Typical gas parameters & their influences on TPC performances

Typical mixtures: Ar(91%)+CH_4(9%),
Ar(90%)+CH_4(5%)+CO_2(5%)

Operation at atmospheric pressure

Properties:

- Drift velocity (~5cm/μs)
- Gas amplification (~7000)
- Signal attenuation (electron attachment) (<1%/m)

Parameters to control and monitor:

- Mixture quality (change in amplification)
- O_2 (electron attachment, attenuation)
- H_2O (change in drift velocity, attenuation)
- Other contaminants (attenuation)

Parameter change	Drift velocity, v_d	Effect on gas amplification, A	Signal ettenuation by electron attachment
0.1% ΔCH_4	0.4 %	-2.5% for $A = 1\times10^4$	
10 ppm O_2	Negligible up to 100 ppm	Negligible up to 100 ppm	0.15%/m of drift
10 ppm H_2O	0.5 %	Negligible at 100 ppm	< 0.03% /m of drift
1 mbar	Negligible if at max.	-(0.5%-0.7%)	

Lateral and longitudinal charge diffusion

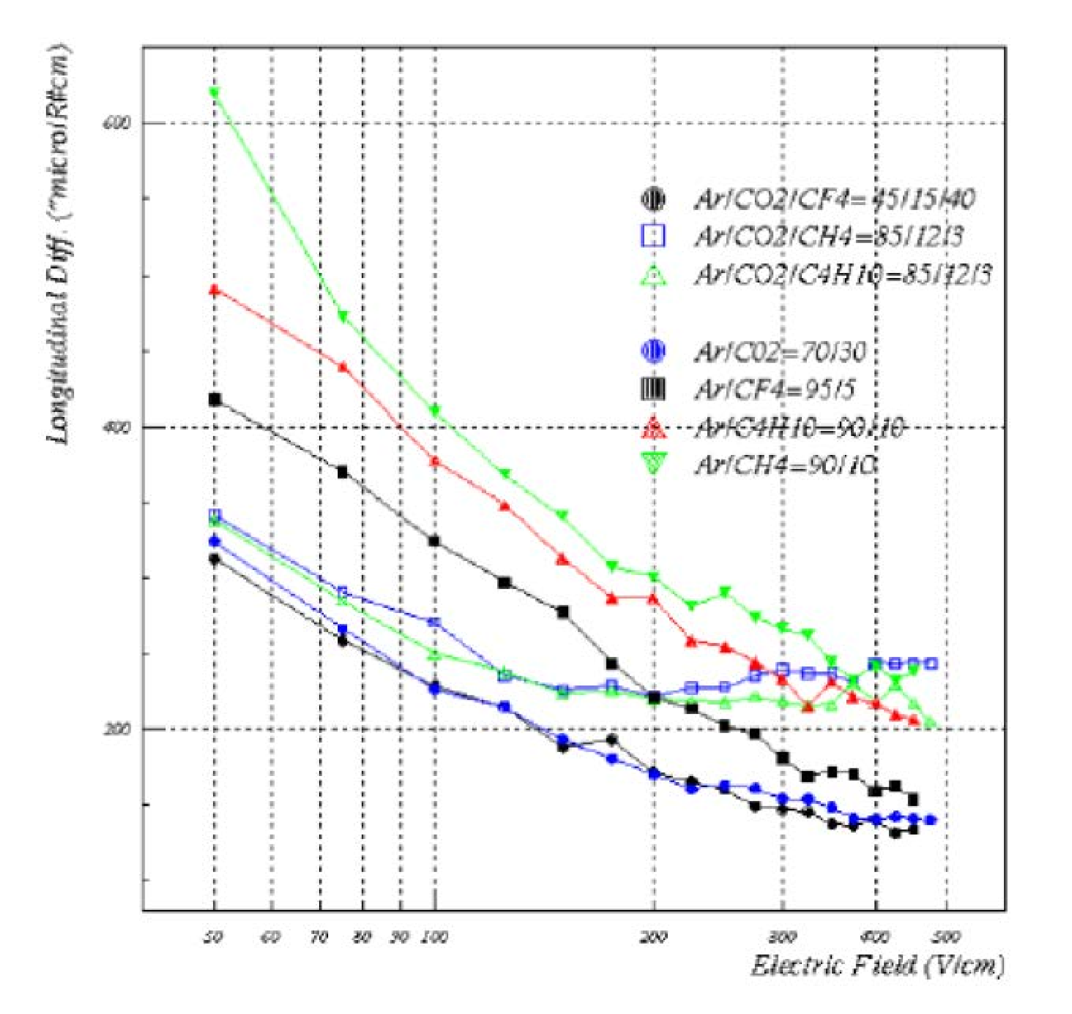

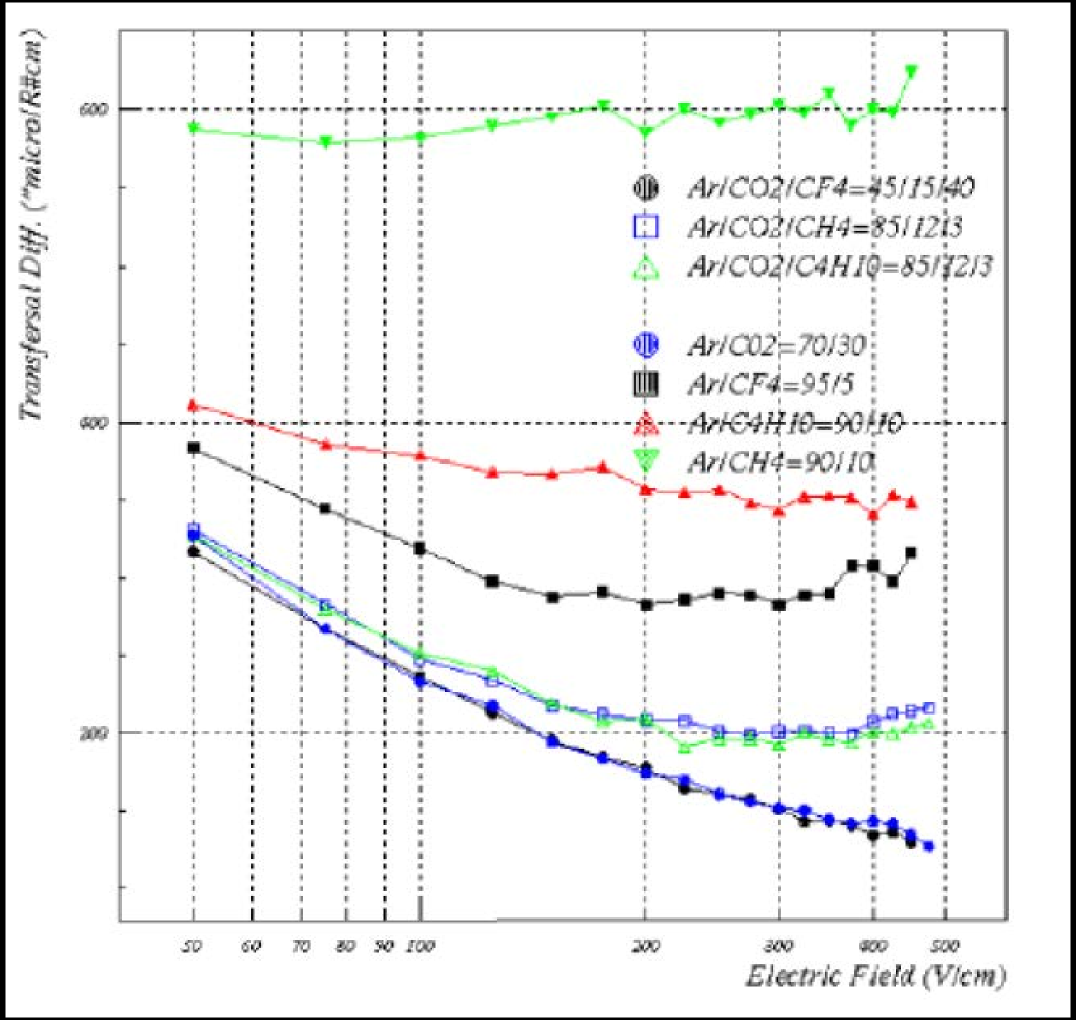

Review on TPC's

- TPC is a 3-D imaging chamber
  - Large dimensions. Little material
  - Slow device (~50 μs)
  - 3-D coordinate measurement ($\sigma_{xy} \approx 170\ \mu$m, $\sigma_z \approx 740\ \mu$m)
  - Momentum measurement if inside a magnetic field
- Reviewed some the main ingredients
  - Field cage, gas, wire chambers, gating grid, laser calibration, electronics, etc.
- History
  - First proposed in 1976 (PEP4-TPC)
  - Used in many experiments
  - Well established detecting technique

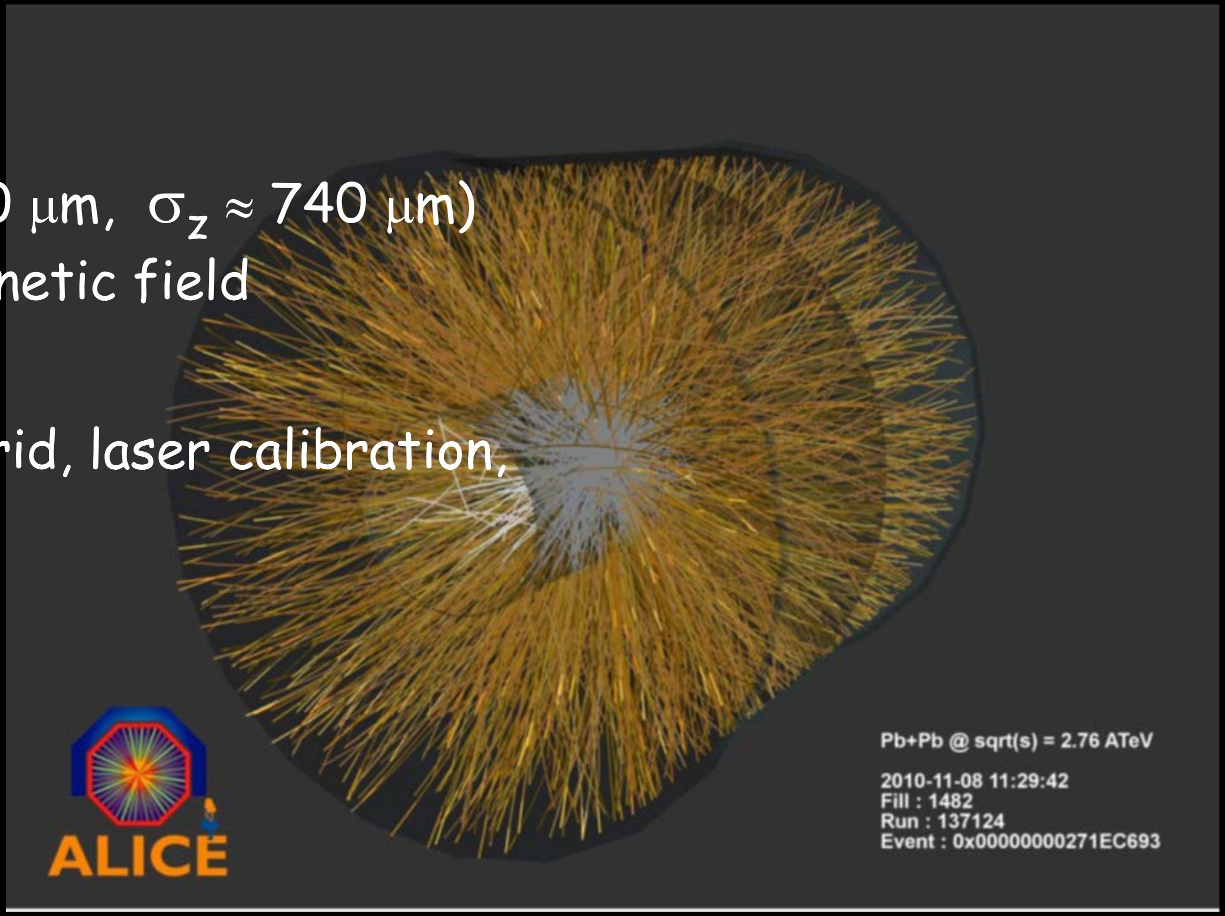

Limitation factors of MWPC: effects on the rate capability

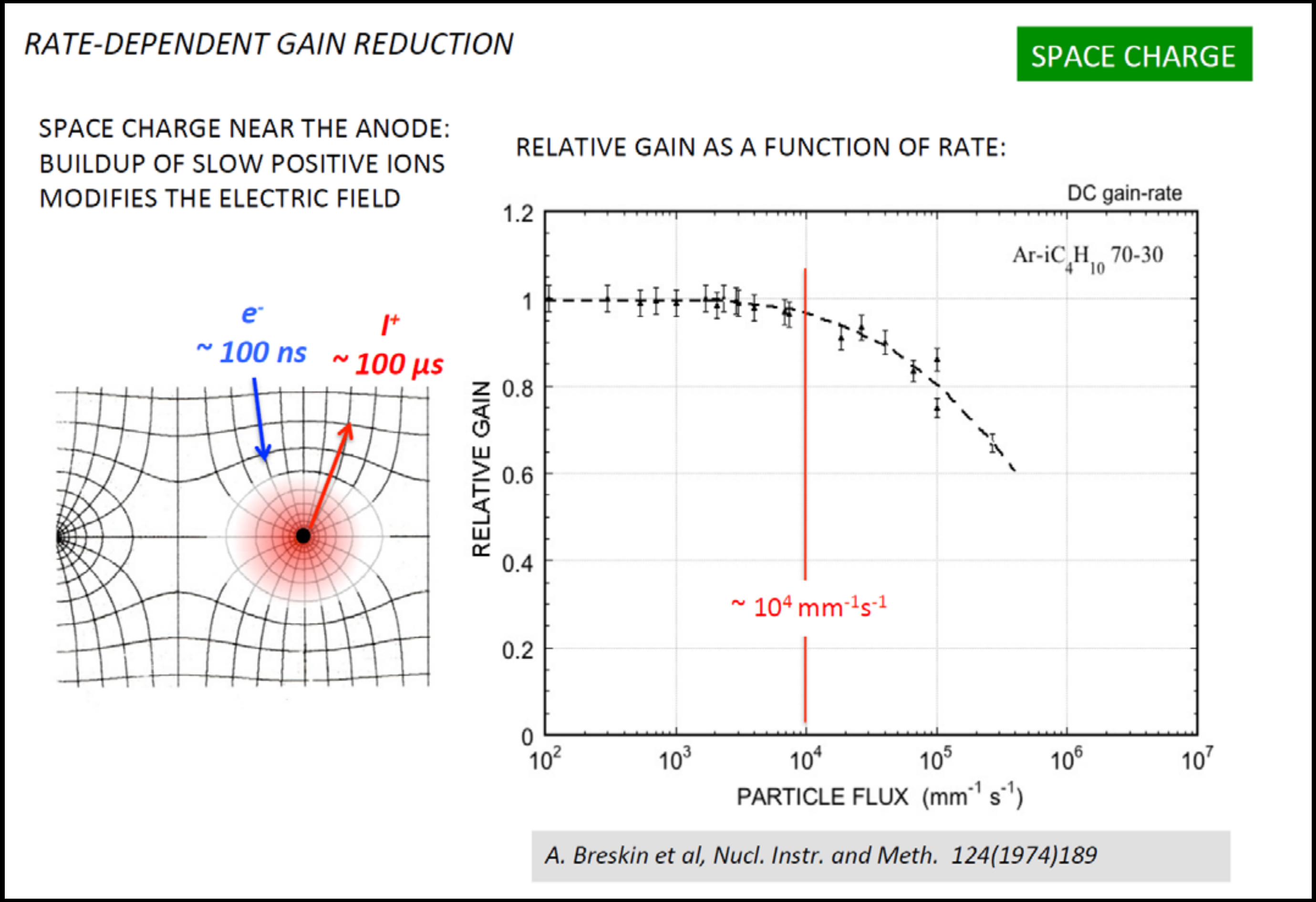

Despite their successful use in particle physics experiments and other fields, MWPCs have several limitations,intrinsic in their conception.The creation in the multiplication process of large amounts of positive ions, slowly receding towards the cathodes, causes a modification of the applied electric field, and results in a drop of gain and efficiency at particle fluxes above ~$10^4 mm^{-1}s^{-1}$.

The discrete wire spacing is itself a limitation to the multi-track resolution,essential at high particle rates and multiplicities.

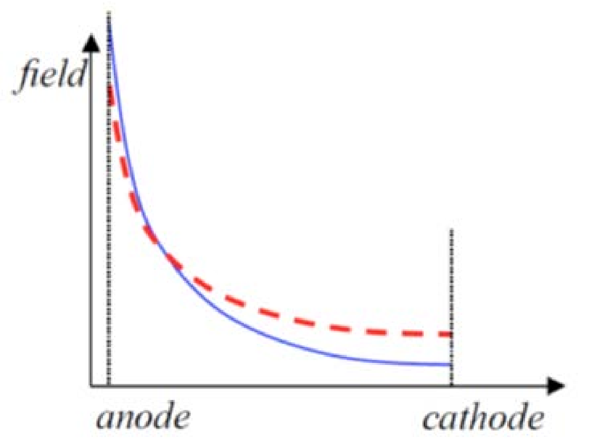

Limitation factors of MWPC: effects on the spatial coordinates determination

POSITIVE ION BACKFLOW

SPACE CHARGE

LATERAL DISPLACEMENT OF ELECTRONS DRIFTING NEAR A POSITIVE IONS COLUMN

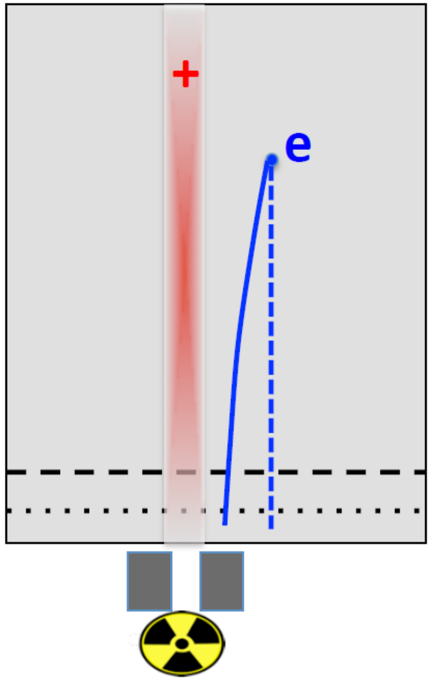

^{55}Fe SOURCE 1 cm FROM ION COLUMN
10 cm DRIFT

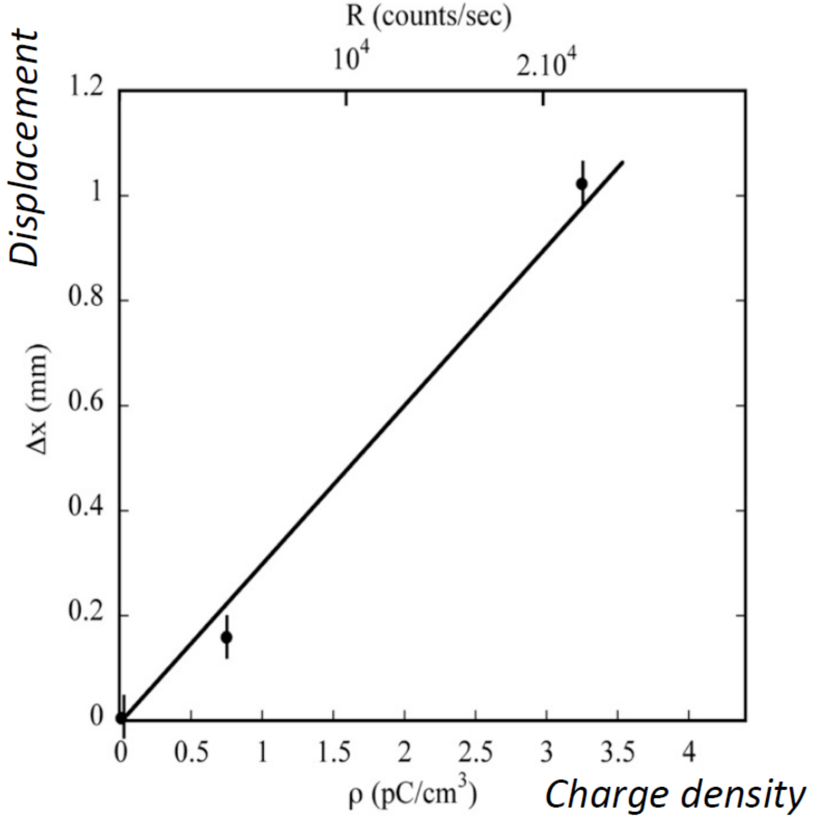

D. Friedrich, et al, Nucl. Instr. and Meth. 158(1979) 81

Limitation factors of MWPC:

POSITIVE ION BACKFLOW

SLOW POSITIVE IONS ACCUMULATE IN THE DRIFT VOLUME AND MODIFY THE FIELD RESULTING IN TRACKS DISTORTIONS:

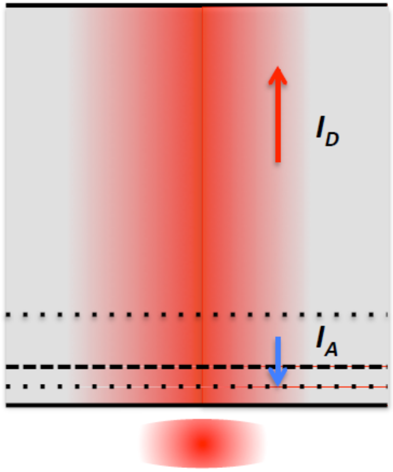

IONS BACKFLOW RATIO $IBF = \frac{I_{DRIFT}}{I_{ANODE}}$

THE WISH: $IBF \leq \frac{1}{GAIN} \approx 10^{-4}$

MWPC: IBF ~ 30%

RELATIVE DRIFT FIELD MODIFICATION (ALEPH MWPC-TPC)

SPACE CHARGE

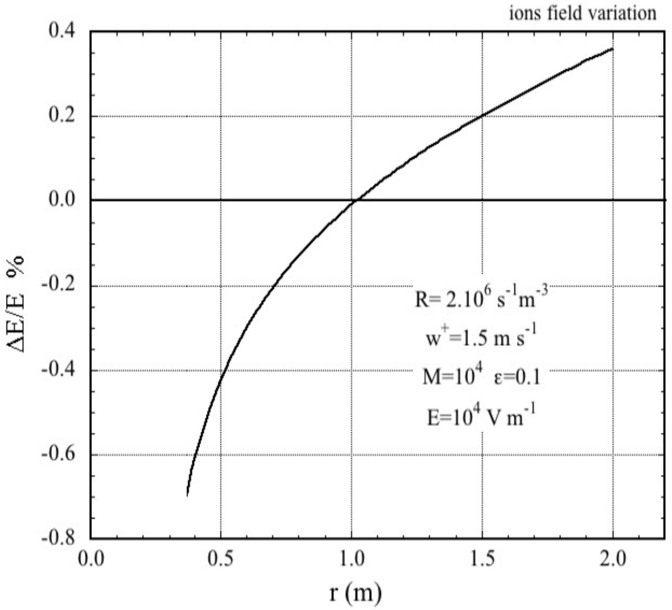

GATING:
ADD A WIRE MESH WITH VOLTAGE-CONTROLLED TRANSPARENCY

POSSIBLE AT LOW RATES:
Maximum electron drift time
< Time between events

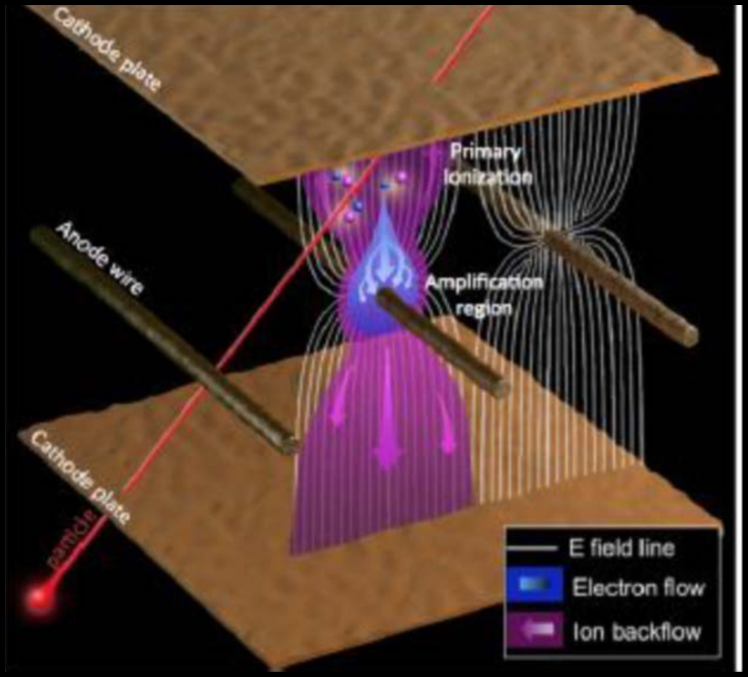

Limitation of Gas Detectors: the ageing

AGING

SECONDARY PROCESSES

Polymerization of organic compounds with formation of deposits on thin wires:

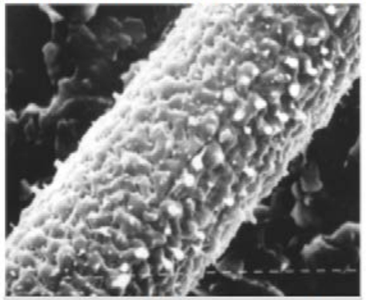

O. Ullaland, LBL-21170 (1986)107

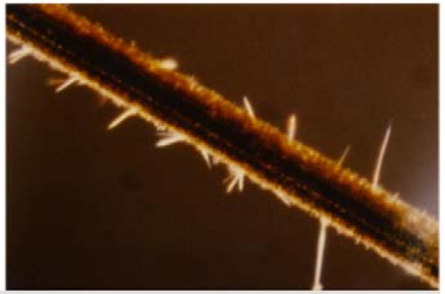

I. Juric and J. Kadyk, LBL-21170 (1986)141

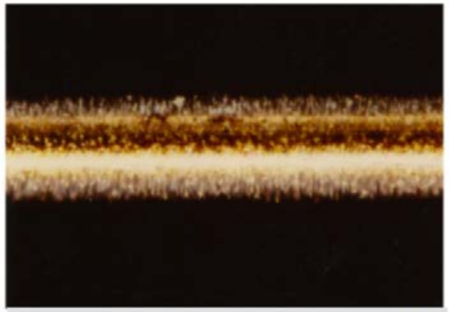

I. Juric and J. Kadyk, LBL-21170 (1986)141

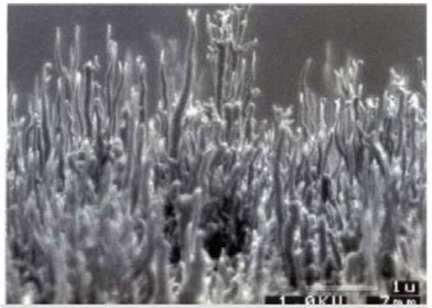

M. Binkley et al, Nucl. Instr. and Meth. A515(2003)53

Even more detrimental, the creation and deposit on the anode wires of thin insulating layers caused by the polymerization of organic gases or pollutants may result in an amazingly short operating life span

Classical ageing

Avalanche region → plasma formation (complicated plasma chemistry)

- Dissociation of detector gas and pollutants
- Highly active radicals formation
- Polymerization (organic quenchers)
- Insulating deposits on anodes and cathodes

Anode: increase of the wire diameter, reduced and variable field, variable gain and energy resolution.

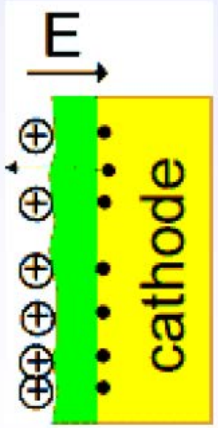

Cathode: formation of strong dipoles, field emmision and microdischarges (Malter effect).

An innovative structure of Gas Detector

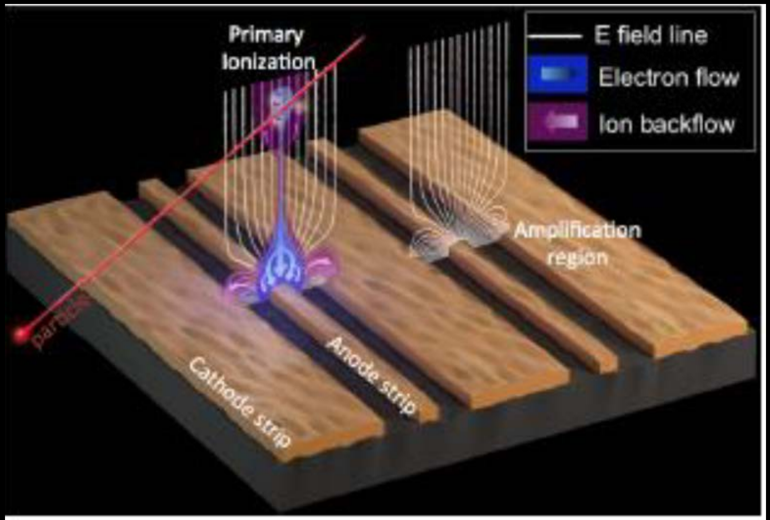

The Micro-Strip Gas Counter (MSGC), introduced by Anton Oed in 1988, seemed to overcome some of the above mentioned limitations. Consisting of a set of thin parallel metallic strips laid on an insulating substrate, alternatively connected as anodes and cathodes, MSGCs provide rate capabilities two orders of magnitude higher than MWPCs, and a tenfold improvement in the multi-track resolution. Disappointingly and despite the efforts by many groups, the device appeared to be rather susceptible to irreversible degradation due to occasional but destructive discharges.

MICRO-STRIP GAS COUNTER

MICRO-PATTERN GAS DETECTORS

MSGC

Anton Oed, 1988

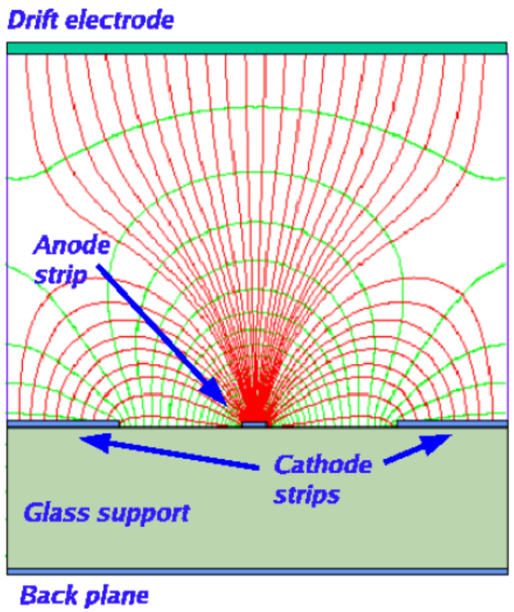

10 µm wide anode strips, 50 µm cathode strips at 100 µm pitch on glass substrate:

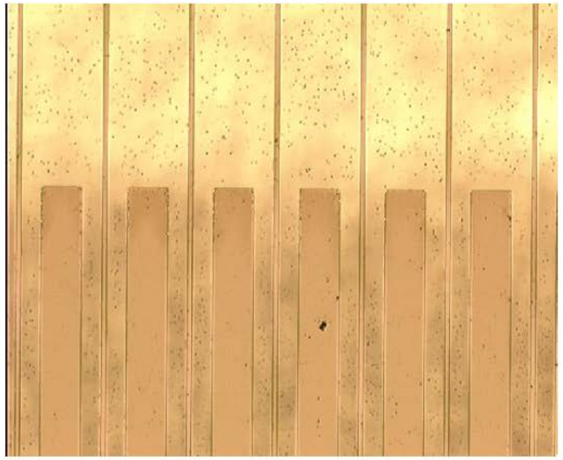

A. Oed, Nucl. Instr. and Meth. A263(1988)351

To compare a bit MWPC and MSGC

MWPC

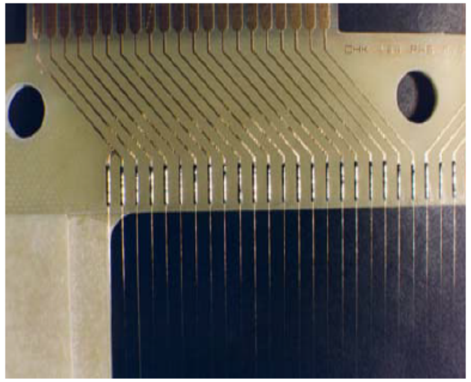

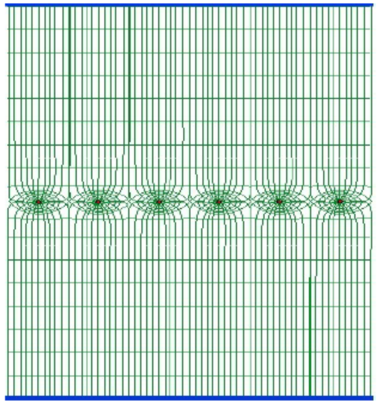

Typical distance between wires limited to 1 mm due to mechanical and electrostatic forces

MSGC

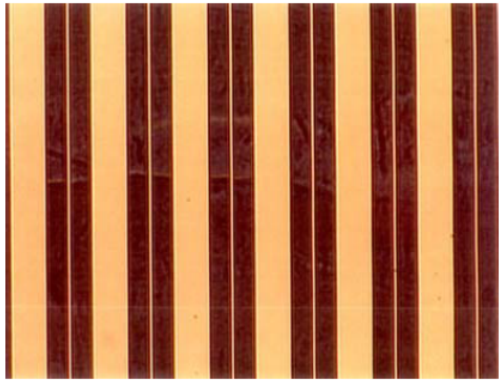

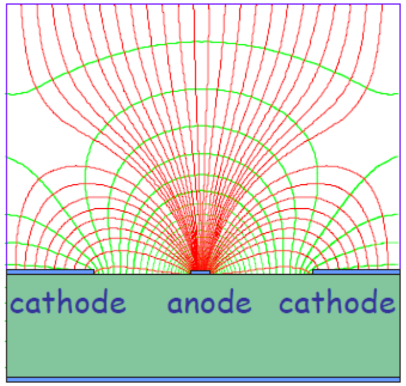

Typical distance between anodes 200 μm thanks to semiconductor etching technology

A. Oed
Nucl. Instr. and Meth. A263 (1988) 351.

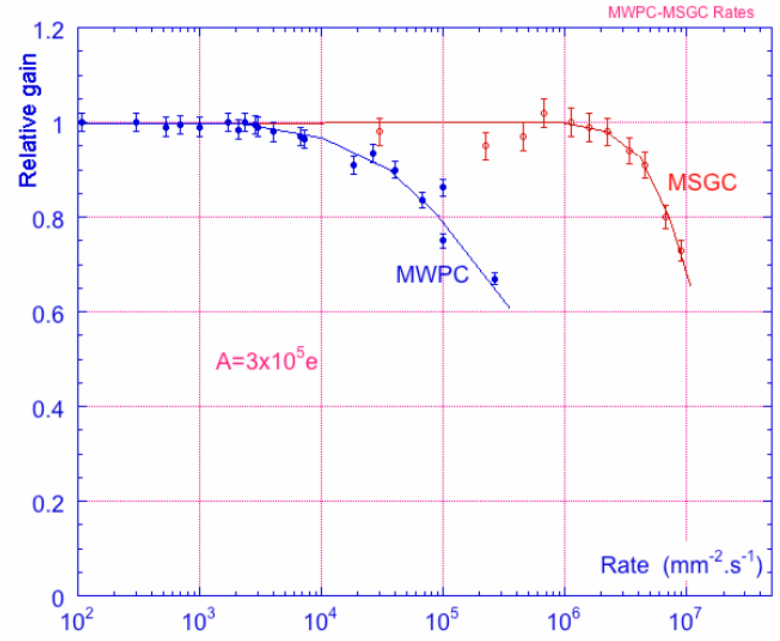

Rate capability limit due to space charge overcome by increased amplifying cell granularity

R. Bouclier et al, Nucl. Instr. and Meth. 367(1996)328

A few problems with MSGC: contamination

MSGC LIFETIME

MSGC

MSGC GAIN vs COLLECTED CHARGE:

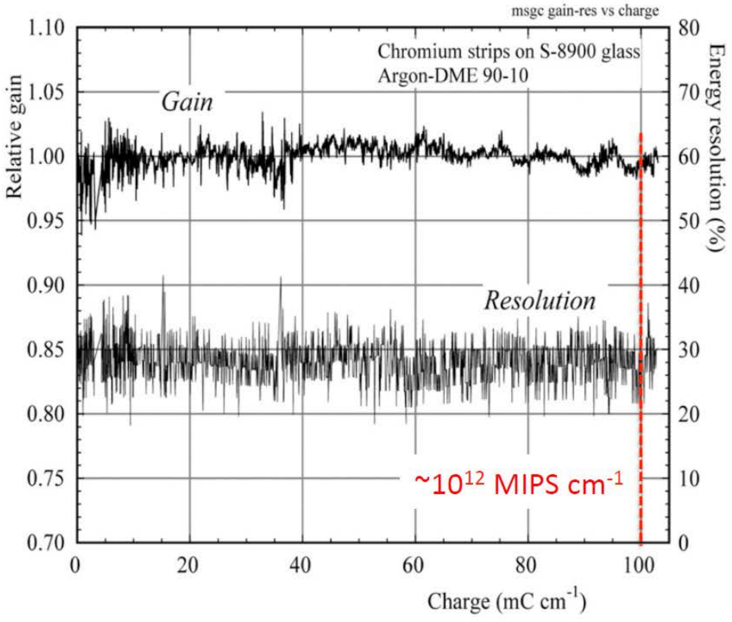

R. Bouclier et al, Nucl. Instr. and Meth. A367(1995)163

contaminations

BUT: EXTREME SENSITIVITY TO CONTAMINATIONS

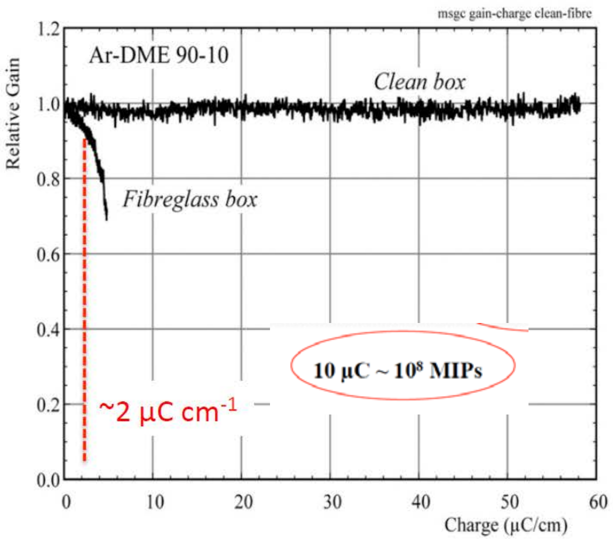

R. Bouclier et al, Nucl. Instr. and Meth. A348(1994)109

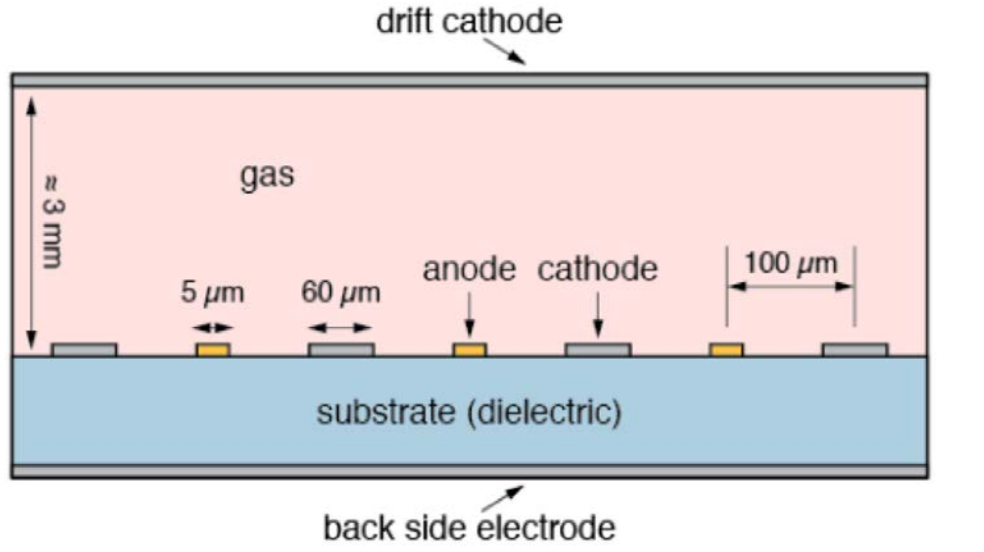

The problems met with the MSGCs resulted in a large effort devoted to the development of sturdier structures, preserving its rate and multi-track capabilities

A few problems with MSGC: discharge issue

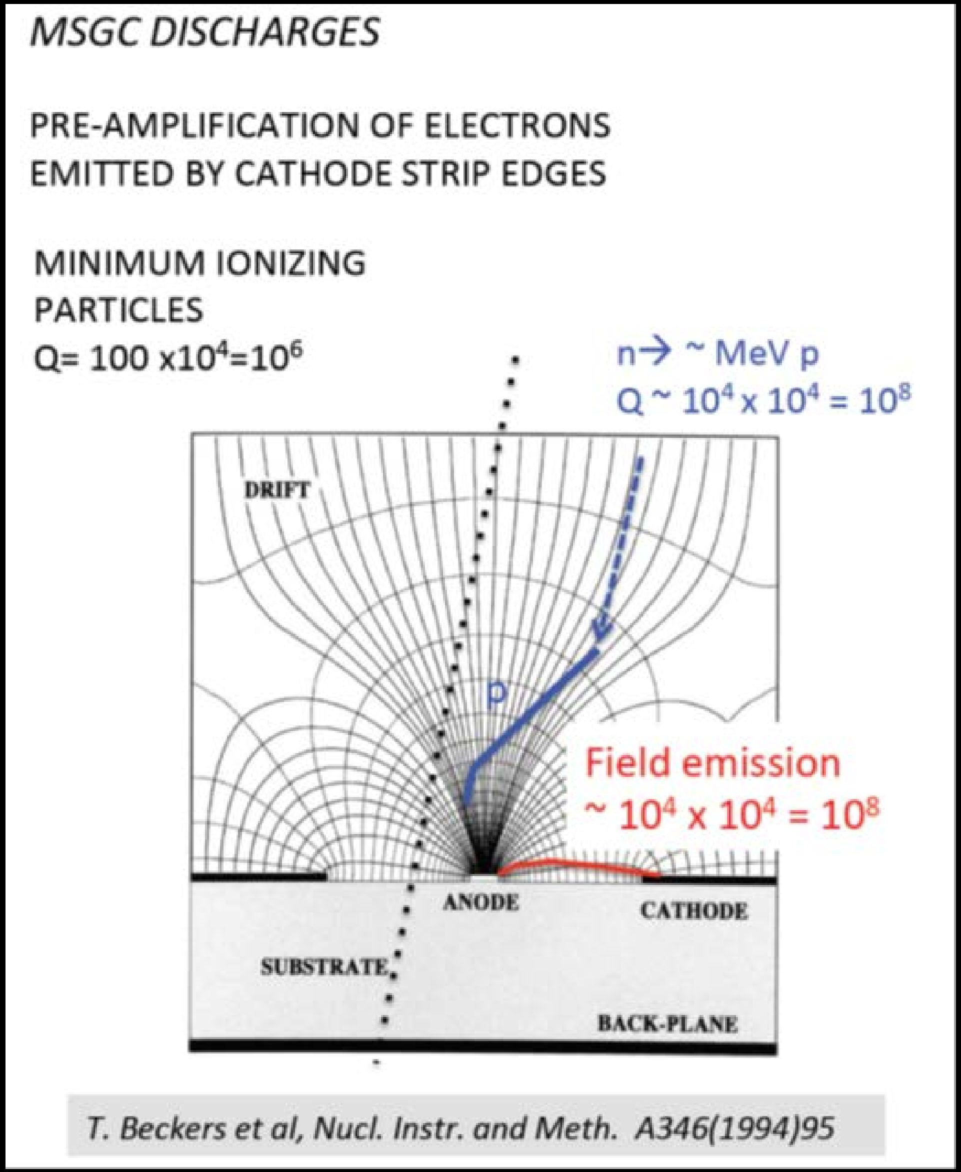

Many of the problems encountered with MSGCs are connected to the use of fragile electrodes exposed to the high electric fields needed to achieve the gains, typically around 10^4, needed for detection of small ionization yields. Under these condition,the occurrence in the gas of rare but highly ionizing events, due for example to neutron or gamma conversions, may lead to the creation of a local charge density exceeding the Raether limit (10^7 electron–ion pairs) leading to the formation of a streamer, and eventually to a discharge.

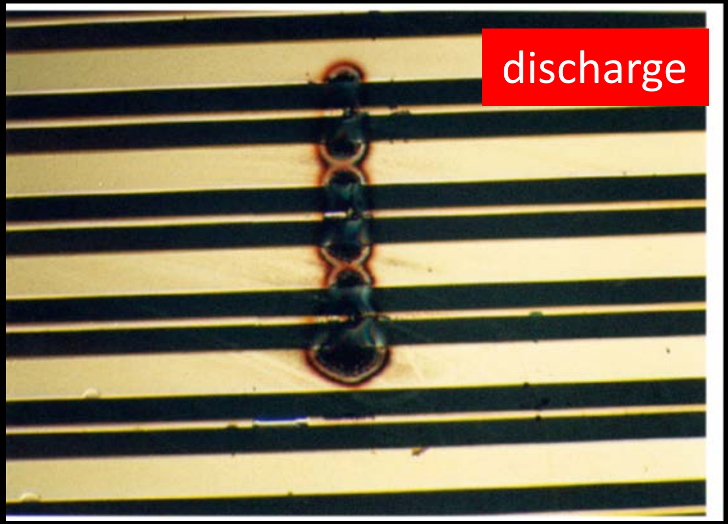

Discharge vs gain in MSGC

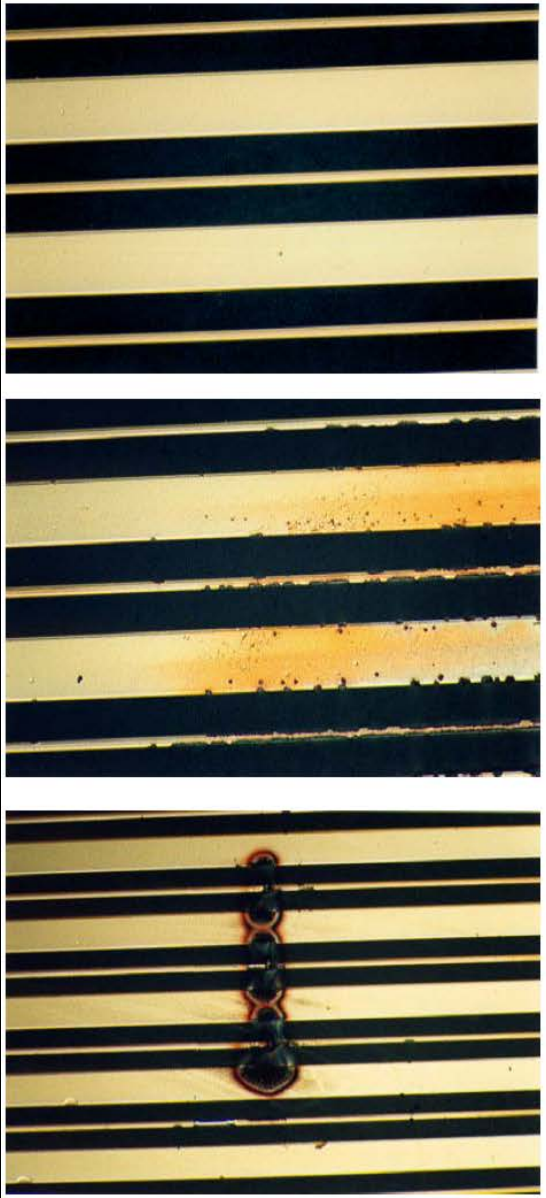

Surface charging

Bulk resistivity of the support material
Surface modification by doping or deposition

Ageing

Gas, Gas system, MSGC support, Construction material

Discharges

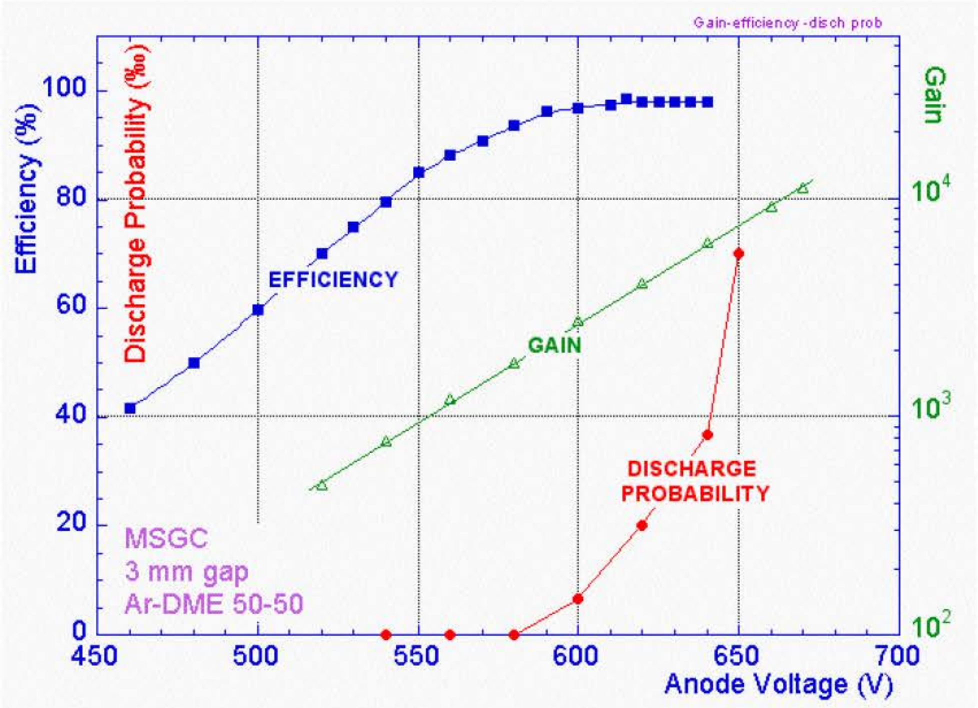

New MPGDs (exploiting micro-litographic technique)

Semiconductor industry technology:

Photolithography
Etching
Coating
Doping

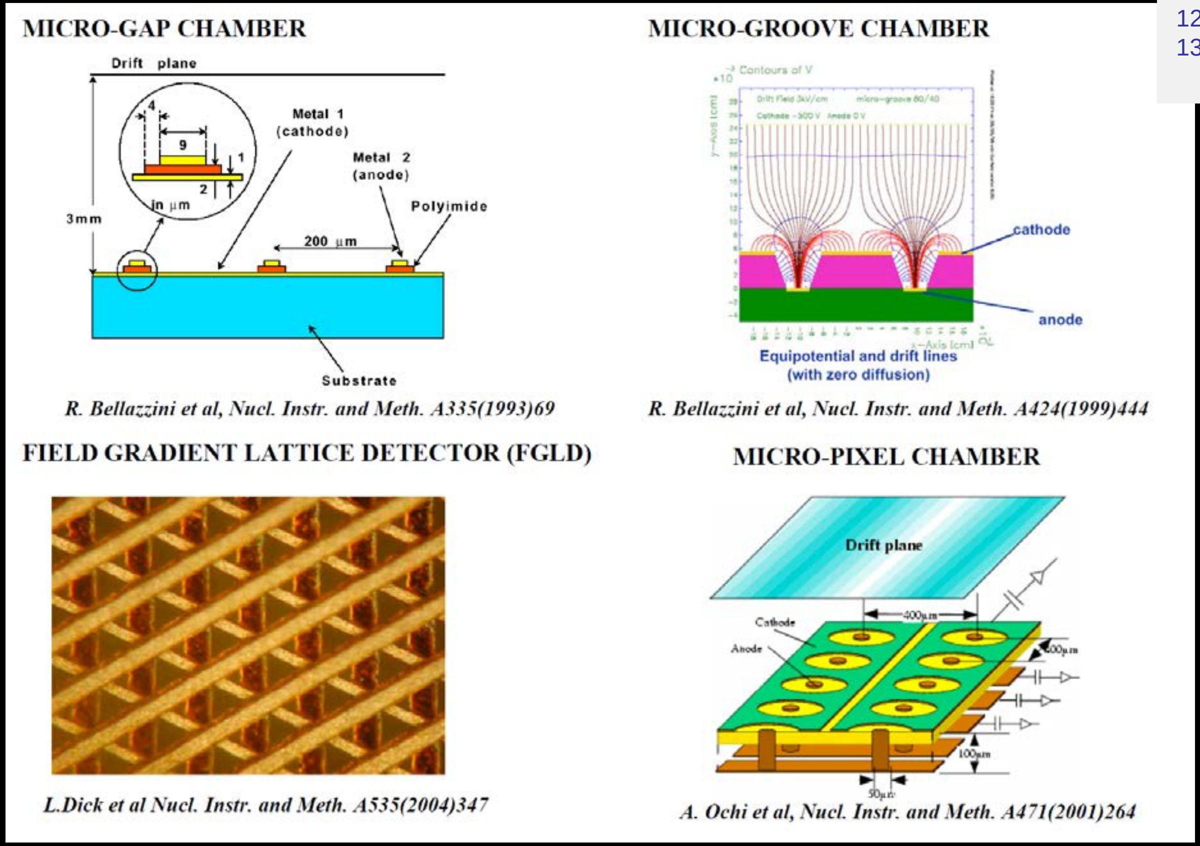

Advantages of MPGDs

1. Rate Capability
2. High Gain
3. Space Resolution
4. Time Resolution
5. Energy Resolution
6. Ageing Properties
7. Low Material Budget
8. Geometrical Flexibility
9. Readout Structures
10. Ion Backflow Reduction
11. Photon feedback Reduction
12. Large area at low prices
13. Flexible geometry

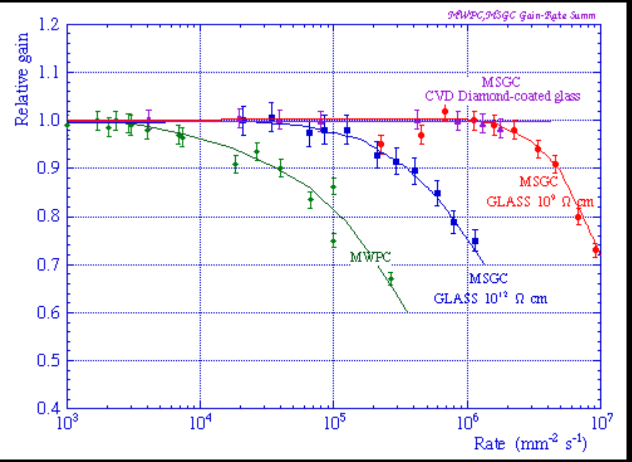

Problem:

- rate capability limited by space charge defined by the time of evacuation of positive ions

Solution:

- reduction of the size of the detecting cell (limitation of the length of the ion path) using chemical etching techniques developed for microelectronics and keeping at same time similar field shape.

scale factor

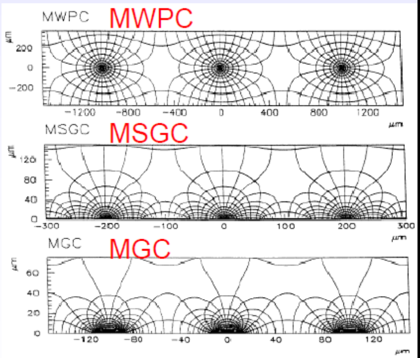

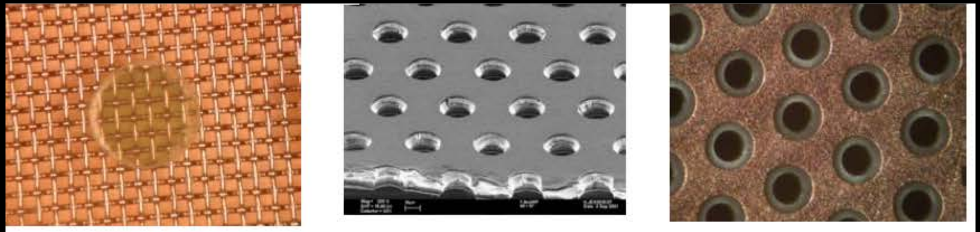

Current Trends in Micropattern Gaseous Detectors

1. Manufacturing Technologies
2. Micromegas
3. GEM
4. ThickGEM/RETGEM
5. MPDG with CMOS pixel ASICs
6. Ingrid Technology

Applications (HEP, Astrophysics, Nuclear Physics, Industrial and Medical)

1. Charged Particles Tracking
2. Triggering
3. TPC Readout
4. Calorimetry, Muon Detectors
5. Photon Detectors (UV and Visible Light Detection)
6. X-Ray Astronomy
7. Soft X-Ray Imaging
8. Neutron Detection
9. Cryogenic Detectors

New MPGD structures

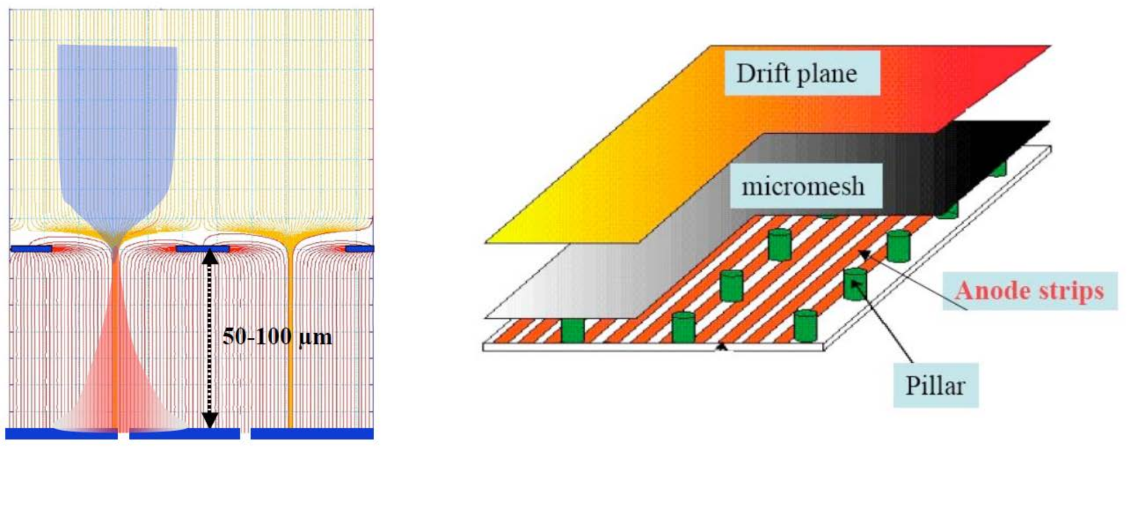

Y. Giomataris et al, Nucl. Instr. and Meth. A376(1996)29

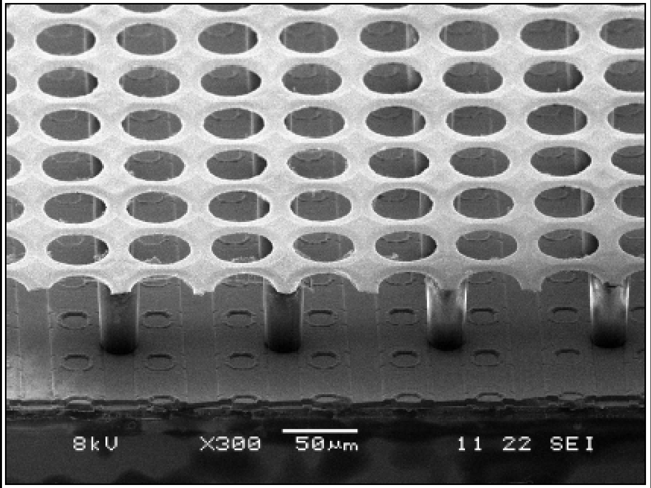

GAS ELECTRON MULTIPLIER

Holes pattern on Cu-plated polymer 50 µm thich

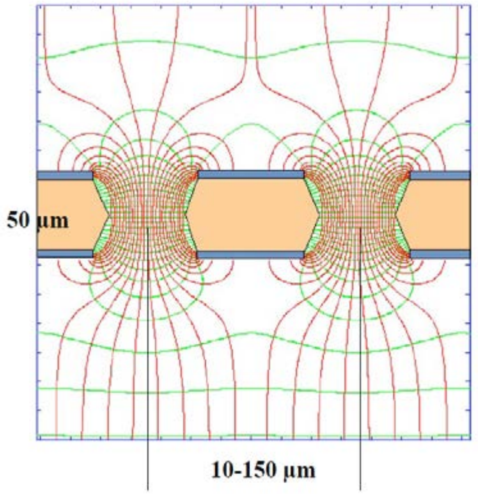

80 µm Ø holes at 140 µm pitch

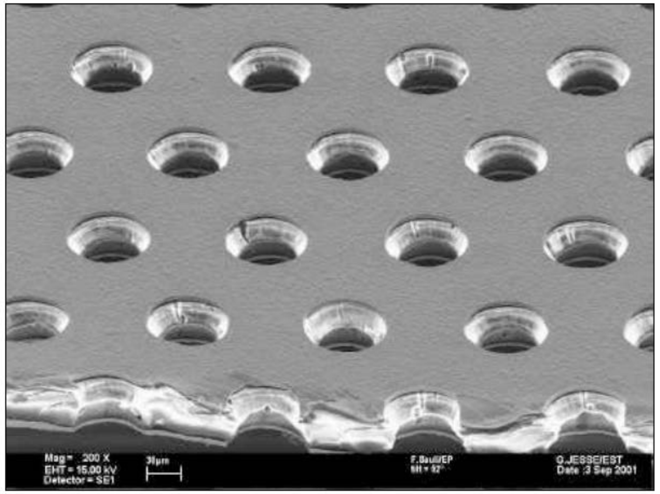

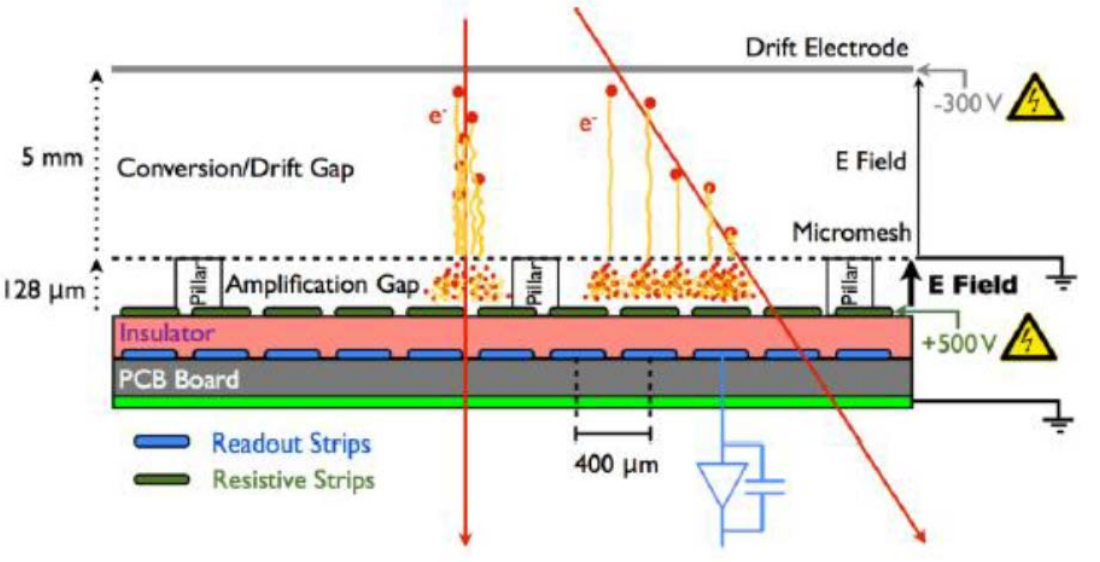

The structure of MMEGAS

NEW MICRO-PATTERN GAS DETECTORS

MICROMEGAS

MICROMEGAS
Thin (50-100 µm) multiplication gap:

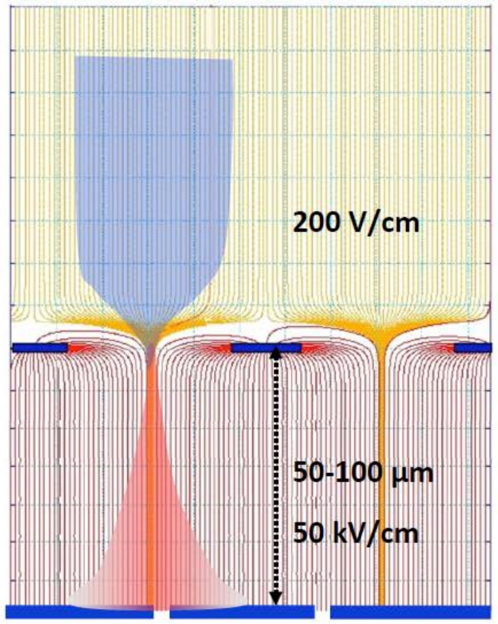

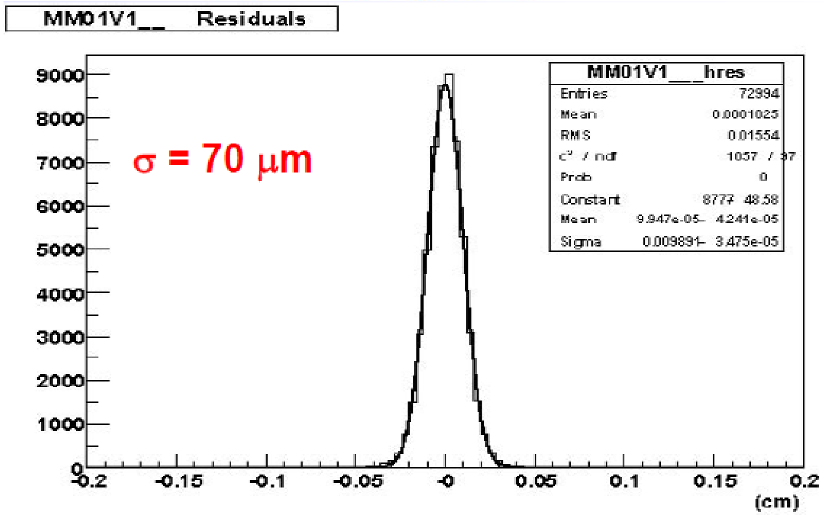

Space resolution

E field similar to parallel plate detector.
E_a/E_i ~ 50 to secure electron transparency
and positive ion flowback supression.

Y. Giomataris et al,
Nucl. Instr. and Meth. A 376(1996)29

J. Derré et al,
Nucl. Instr. and Meth. A459(2001)523

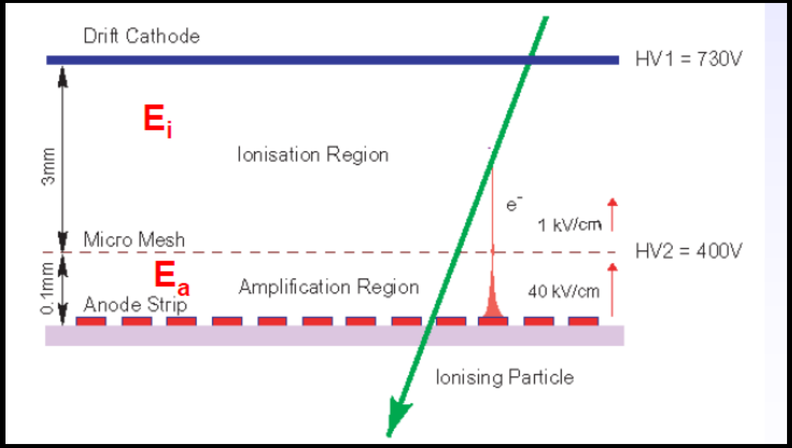

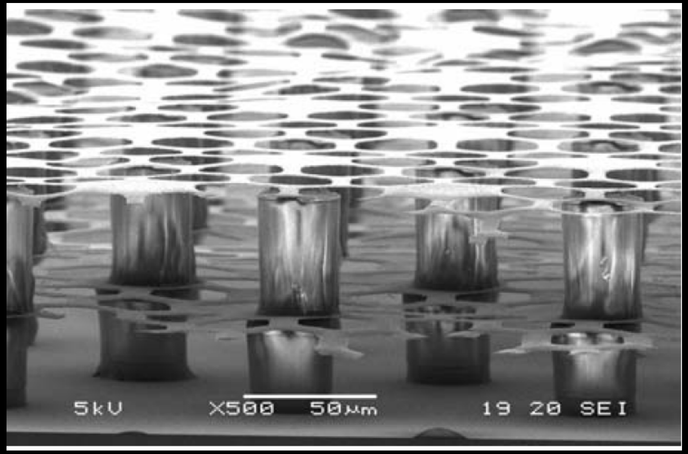

Discharge mitigation technique in MMEGAS

DISCHARGES: RESISTIVE MICROMEGAS

MICROMEGAS

BUILT ON A HIGH-RESISTIVITY POLYMER

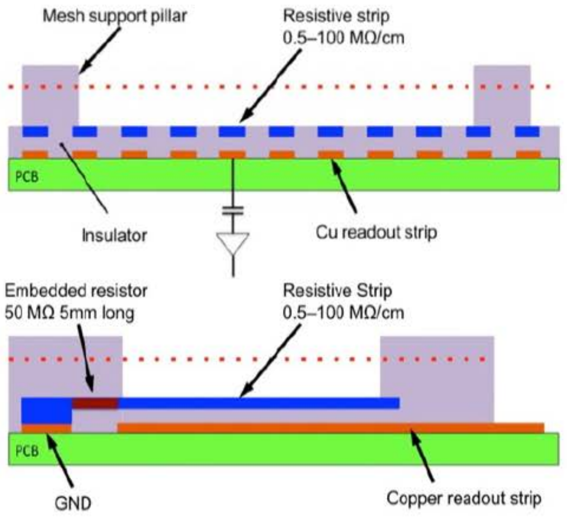

Orthogonal view

SPARK RATES IN NEUTRON BEAM EXPOSURE:

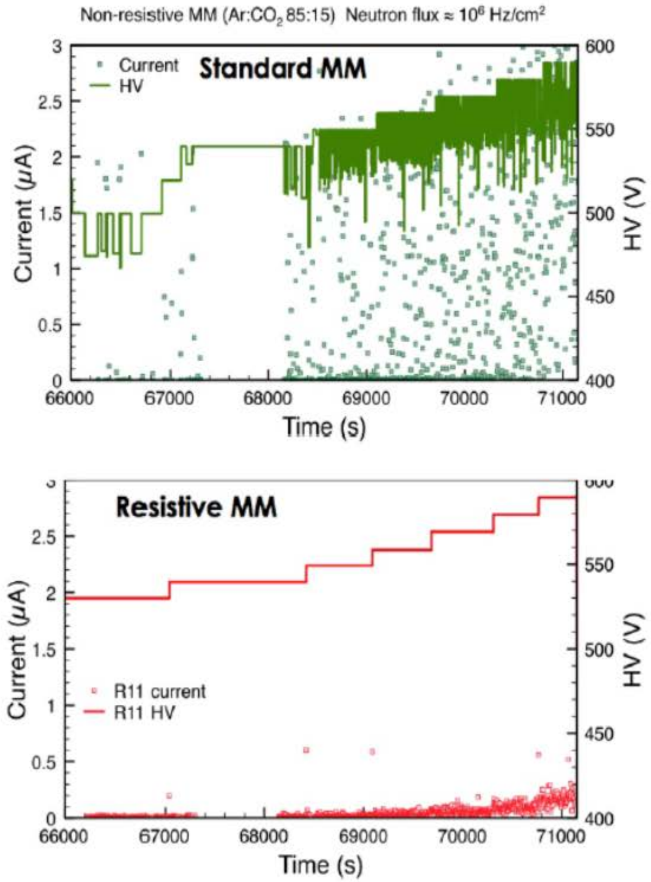

T. Alexopolous et al, Nucl. Instr. and Meth. A640(2011)110

Gas Electron Multiplier detectors

From 1997 MPGDs have played a fundamental role in **HEP** and Nuclear Physics. Today their applications are being extended beyond fundamental Science:

Astrophysics
Material analysis
Heritage and Art
Homeland security
Industrial
Risk alert
Medicine
Environment

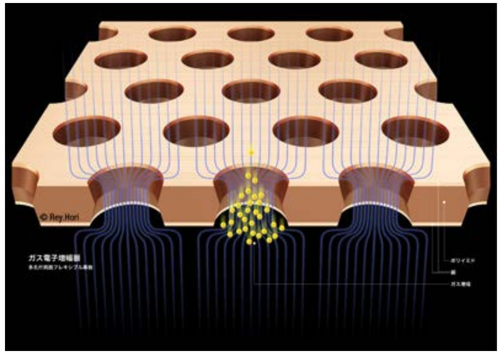

GEM foil.

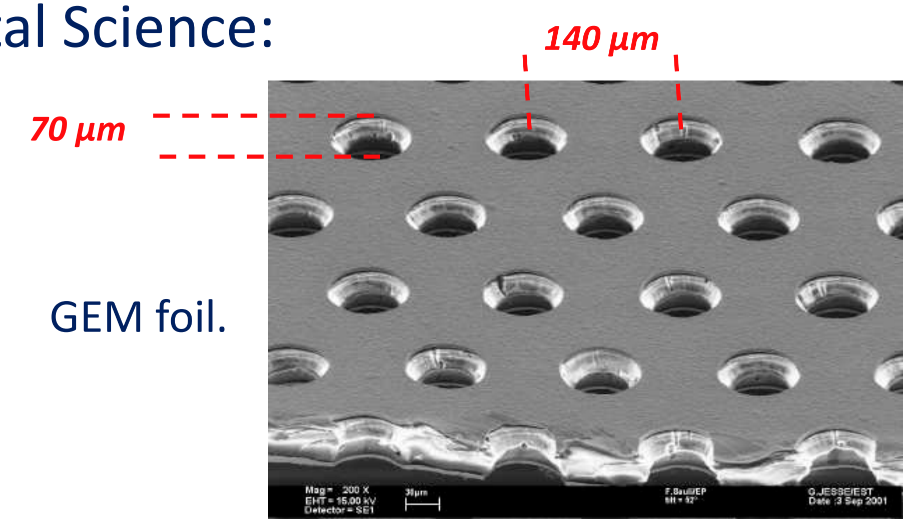

Triple GEM detector layout.

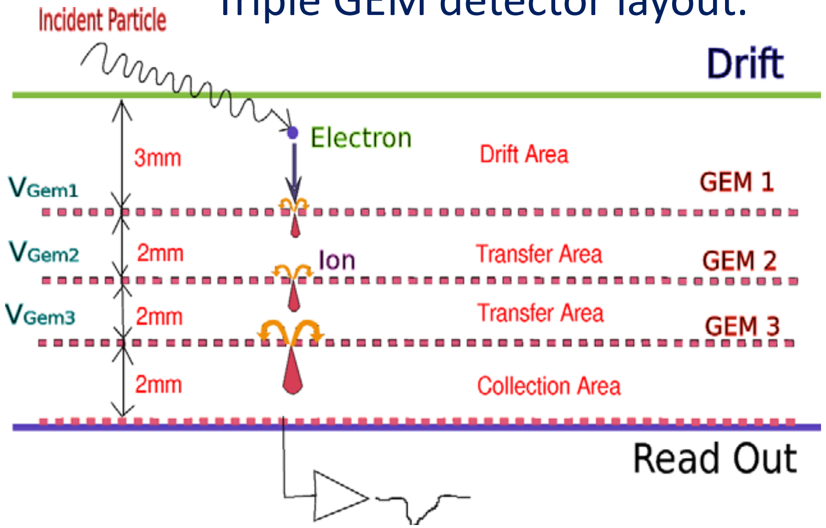

- ✓ **high detection efficiency (>98%);**
- ✓ **good 2D imaging capability by read-out segmentation;**
- ✓ **excellent spatial resolution typically 100 μm;**
- ✓ **good time resolution (4-5 ns);**
- ✓ **high radiation flux resistance;**
- ✓ **high rate capability (50 MHz/cm^2)**
- ✓ **flexibility, robustness and low costs.**

GEM foil construction technology

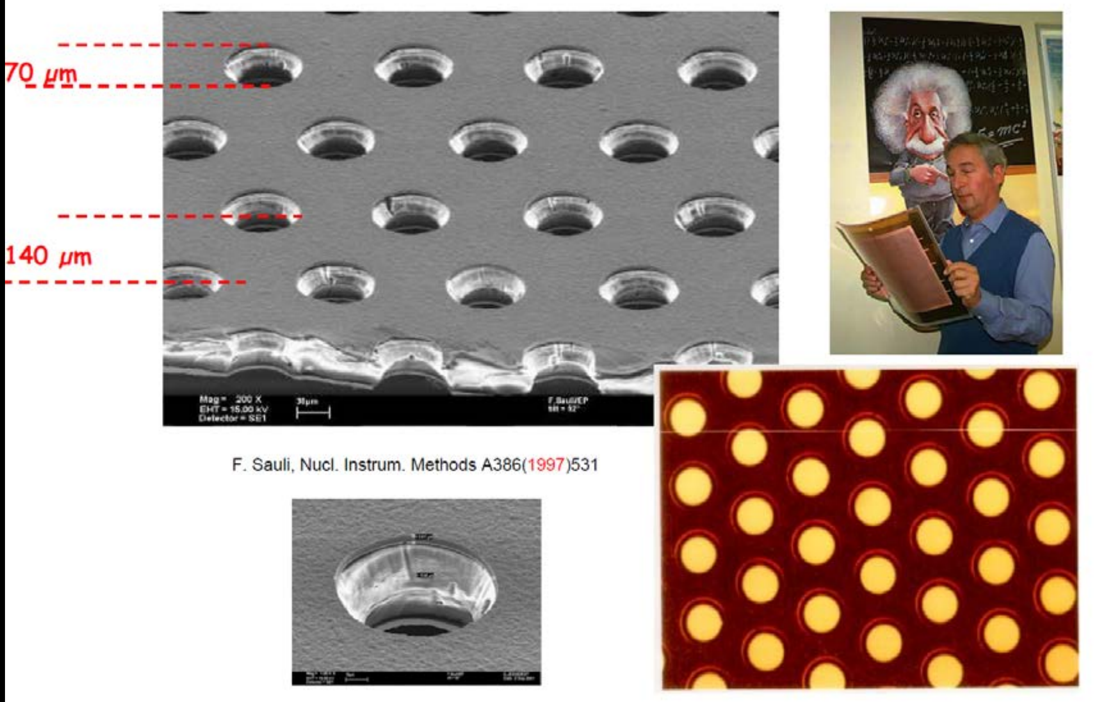

F. Sauli, Nucl. Instrum. Methods A386(1997)531

Thin-metal coated polymer foil Pierced by a high density of holes (50-100/mm^2).
Typical geometry: 5µm Cu on 50µm Kapton, 70µm holes with 140µm pitch

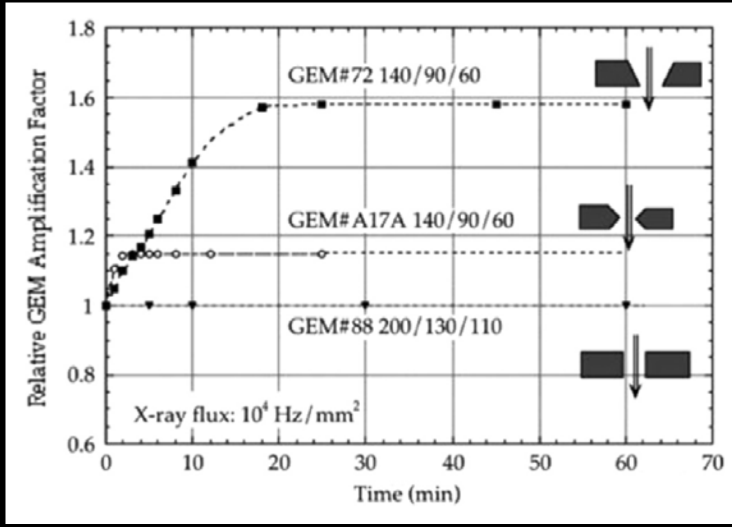

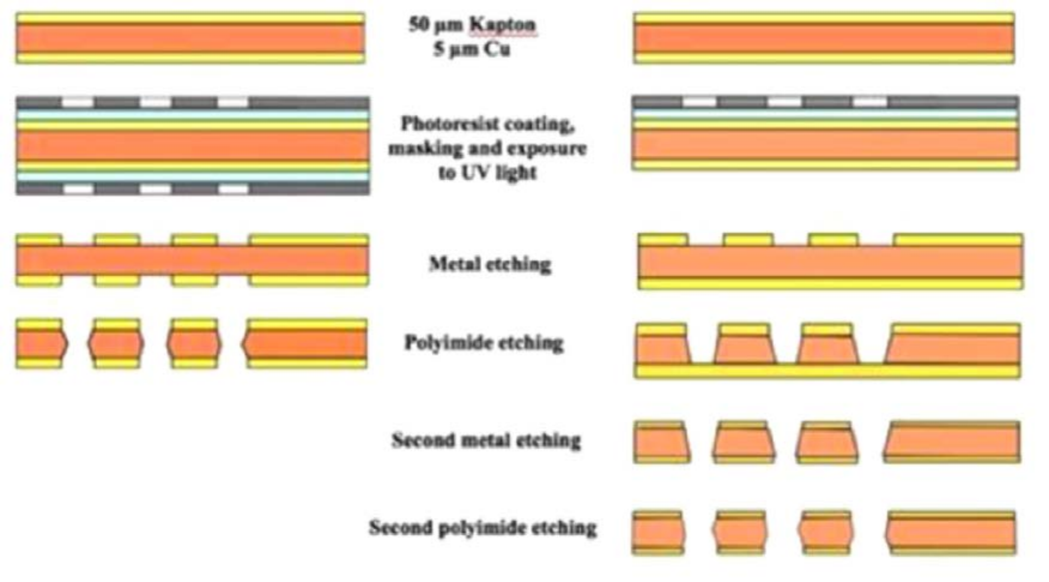

Double mask and single-mask tecnology

Single GEM structure

GAS ELECTRON MULTIPLIER (GEM)

GEM

Thin (50 µm) metal-coated polymer foil with high density of holes:

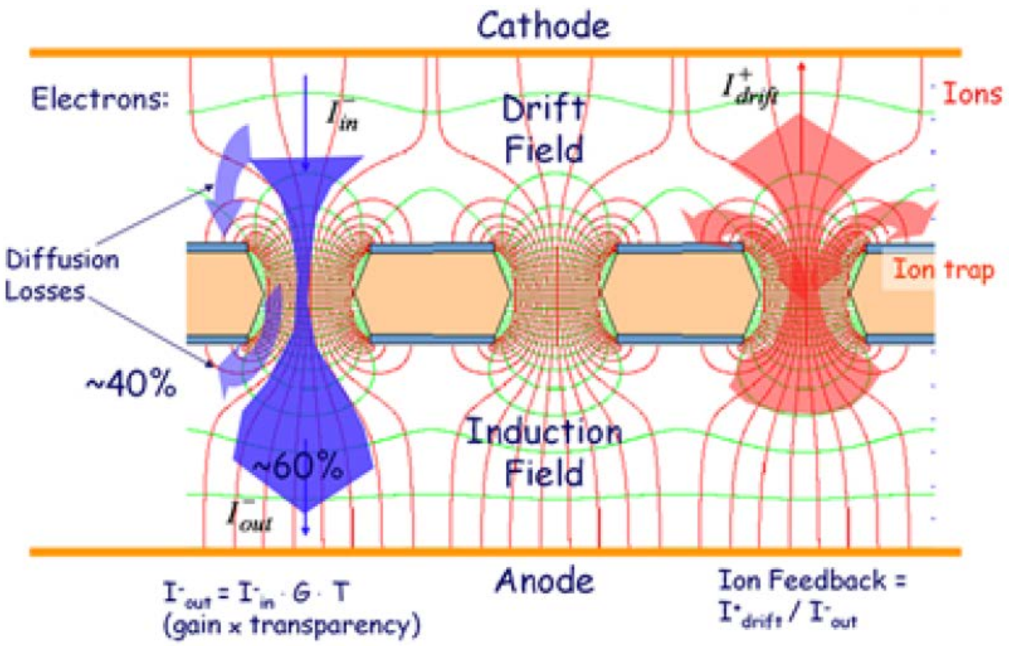

FAST ELECTRON SIGNAL ON ANODE STRIPS (NO ION TAIL):

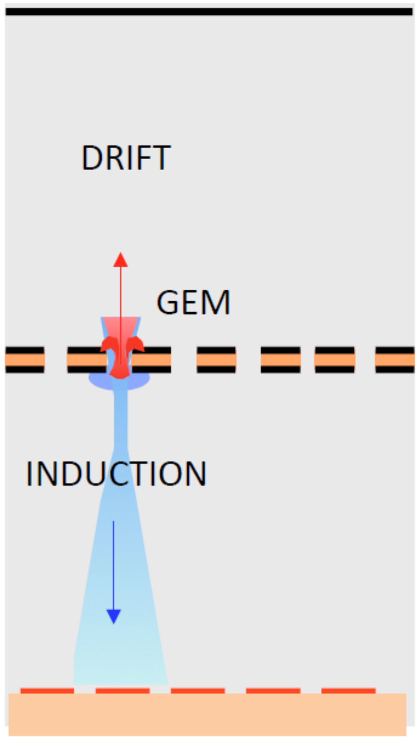

F. Sauli, Nucl. Instr. and Meth. A386(1997)531

1. Electrons are collected on patterned readout board.
2. A fast signal can be dected on the lower GEM electrode for triggering or energy discrimination.
3. All readout electrodes are at ground potential.
4. Positive ions partially collected on the GEM electrode

The choice of parameters in a single GEM foil detector

To study gain in GEM we have to analyze which are the mechanisms of charge amplification first

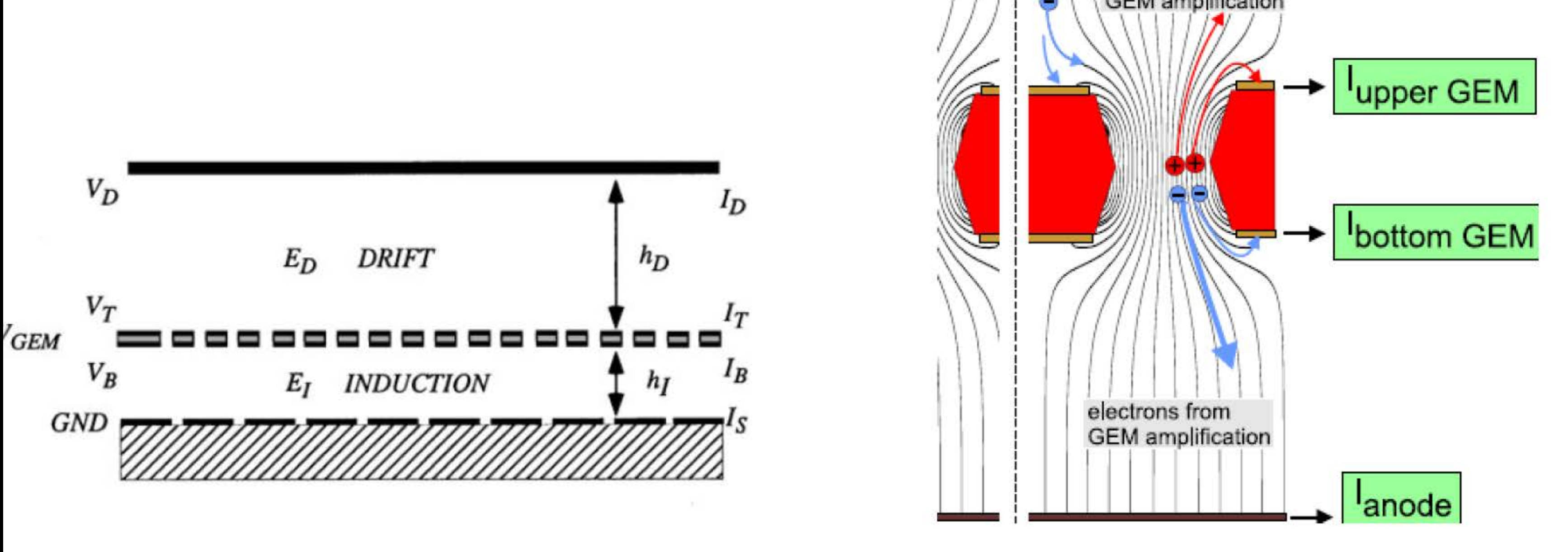

(a) (b)

We identify three electric fields:
The *drift field*, the *moltiplication field* and the *induction field*

The electron Transparency

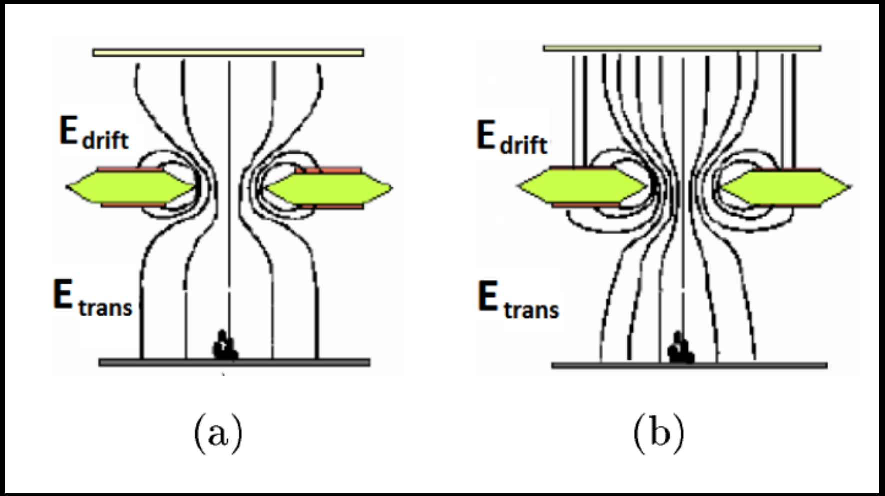

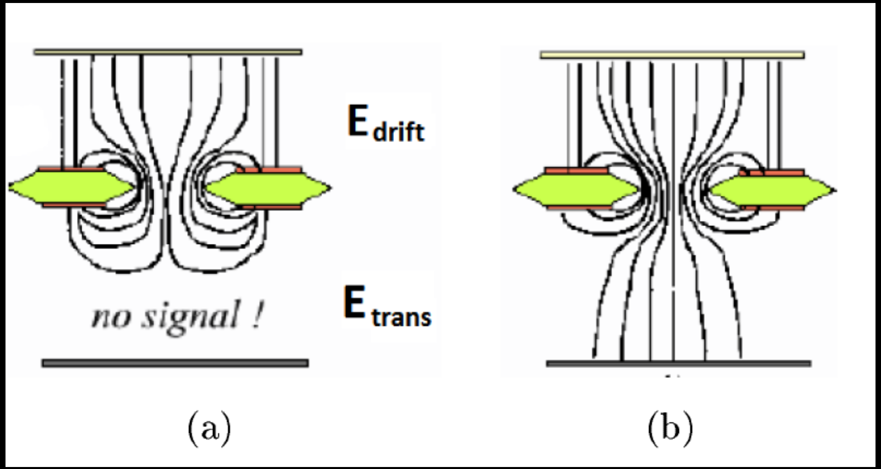

1. The electric fields (drift and induction) play a crucial role to define the so called *Transparency*
2. Another important parameter is the geometry of holes

Focusing (a) or undefocusing (b) effect on electron determines the *sticking* ε_{coll} and the *transfering* ε_{extr} efficiencies

The intrinsic gain of GEM foil can be defined as:

$$G_{intr} \propto e^{<\alpha> V_{GEM}}$$

The effective gain is defined as:

$$G_{eff} = G_{intr} \bullet \varepsilon_{coll} \bullet \varepsilon_{extr}$$

Rigorous formula of Gain

$$G = \exp(\int (\alpha(x) - \eta(x))\delta x),$$

Gain determination

$$\epsilon^{coll} = \frac{electrons\ collected\ in\ the\ holes}{electrons\ produced\ above\ the\ holes}$$

Collection efficiency

$$\epsilon^{extr} = \frac{electrons\ extracted\ from\ the\ holes}{electrons\ produced\ in\ the\ holes}$$

Extraction efficiency

$$G_{int} \propto e^{\overline{\alpha} \Sigma V_{GEM}}$$

Intrinsic gain

$$G_{eff} = G_{intr} * \varepsilon^{coll} * \varepsilon^{extr} = G_{intr} * T$$

Effective gain

Influence of Electric Fields on the electron transparency

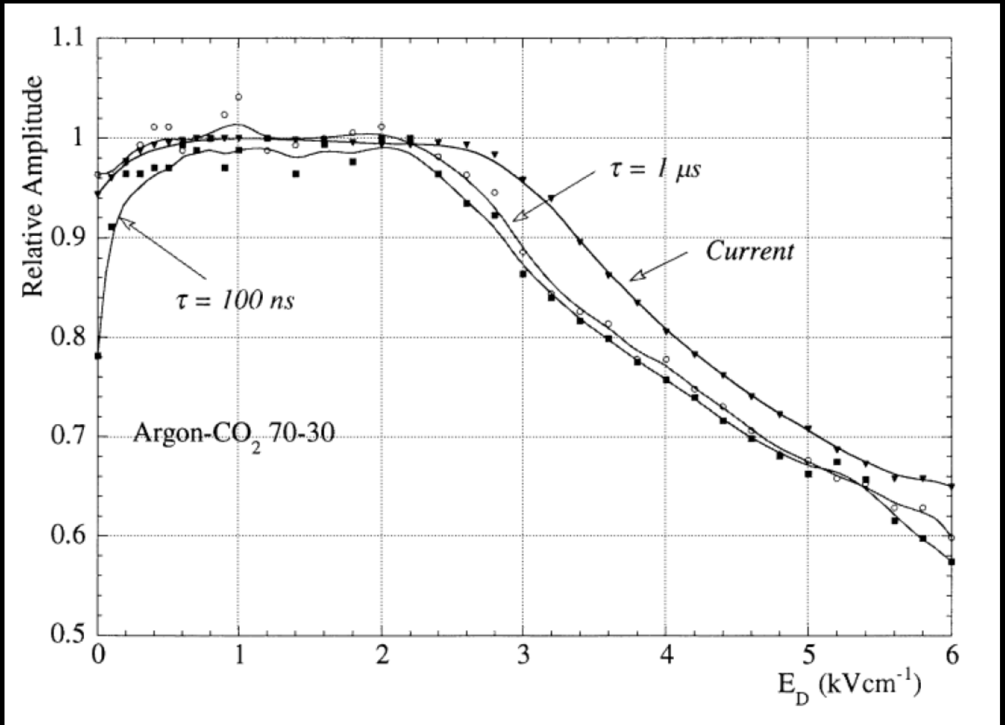

Owing to the structure of the detector, the sharing of collected charges (electrons and ions) between electrodes depends on the value of fields and holes geometry charateristics

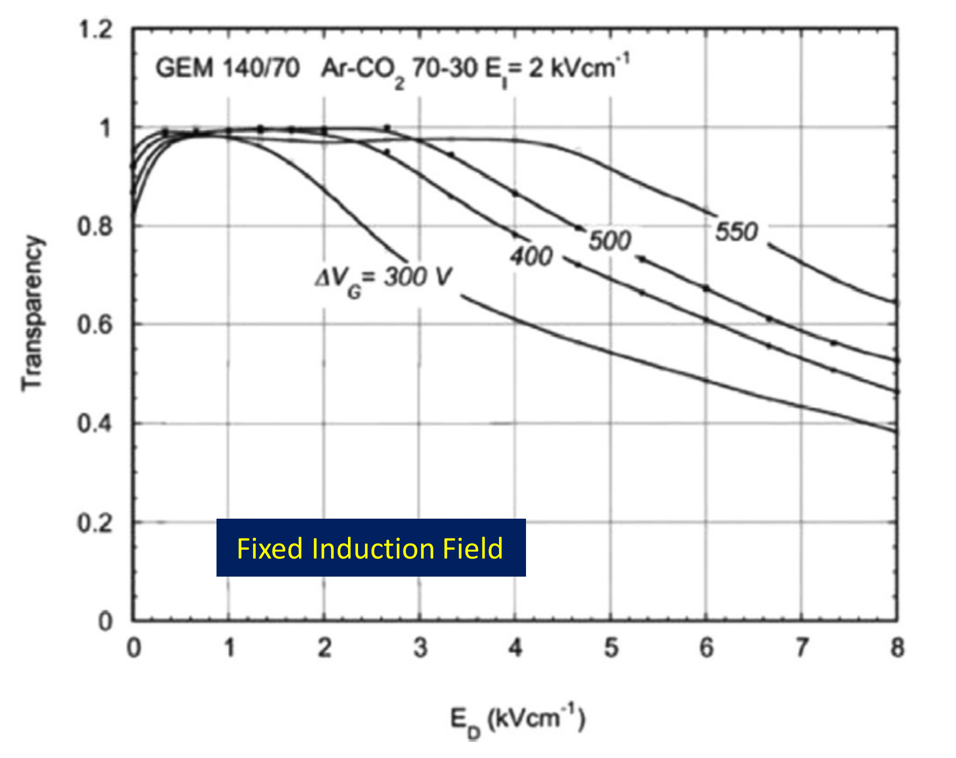

Electron transparency of a standard GEM electrode (70 um holes at 140 um pitch) as a function of drift field for fixed induction field, for several values of GEM voltage.

Influence of Electric Fields on the electron transparency

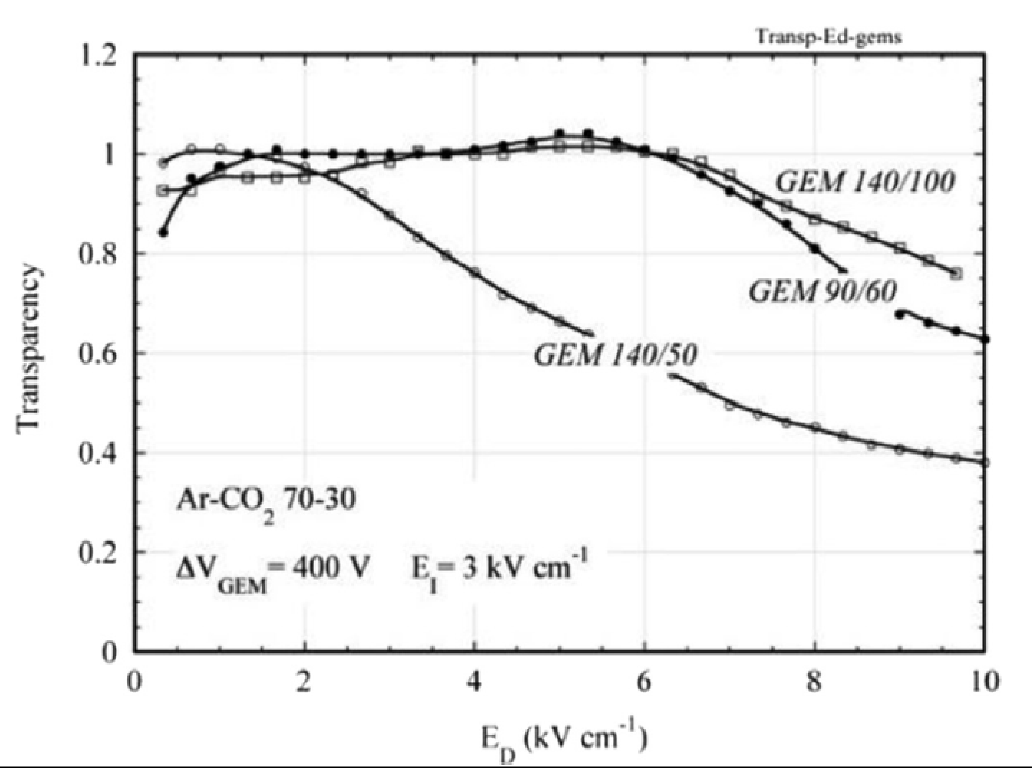

Electron transparency for different GEM geometry labeled as pitch/holes diameter.

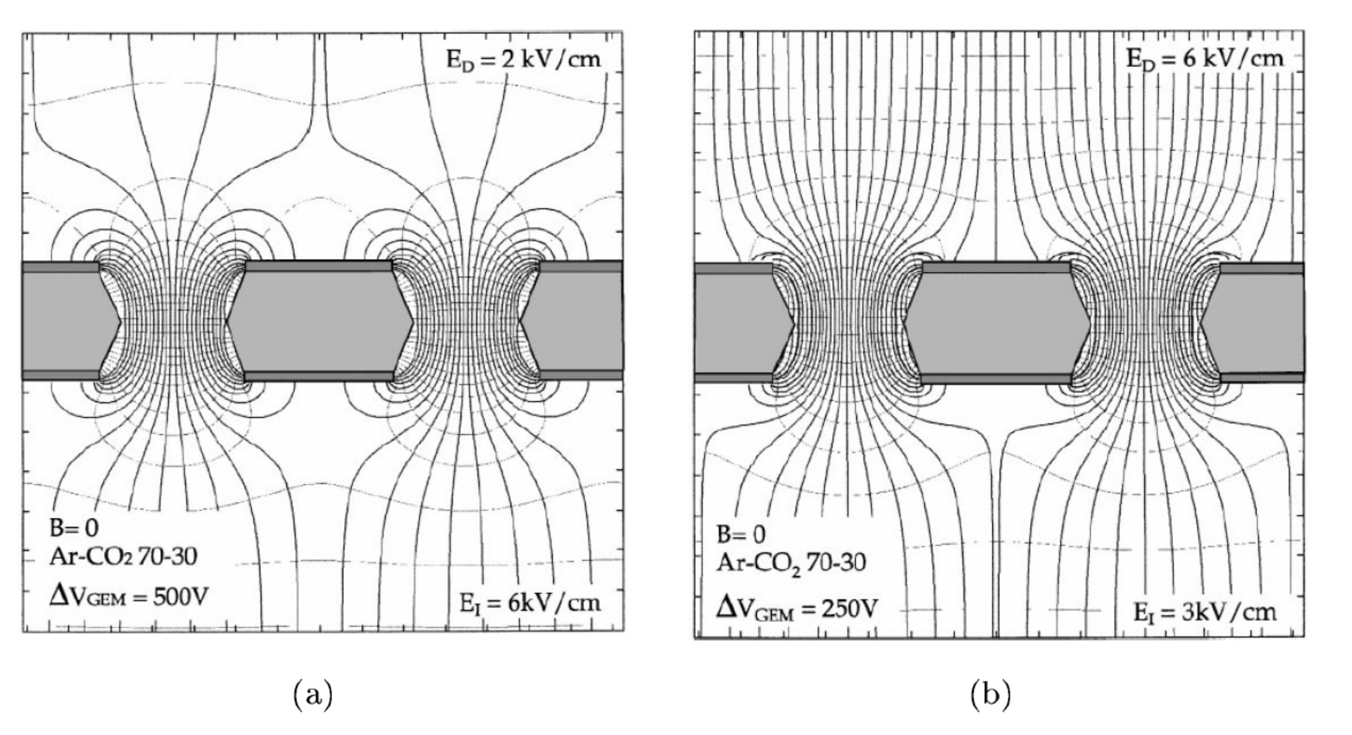

Electron transparency dependence vs Different drift and induction electric field

Effect of hole dimension on the Gain

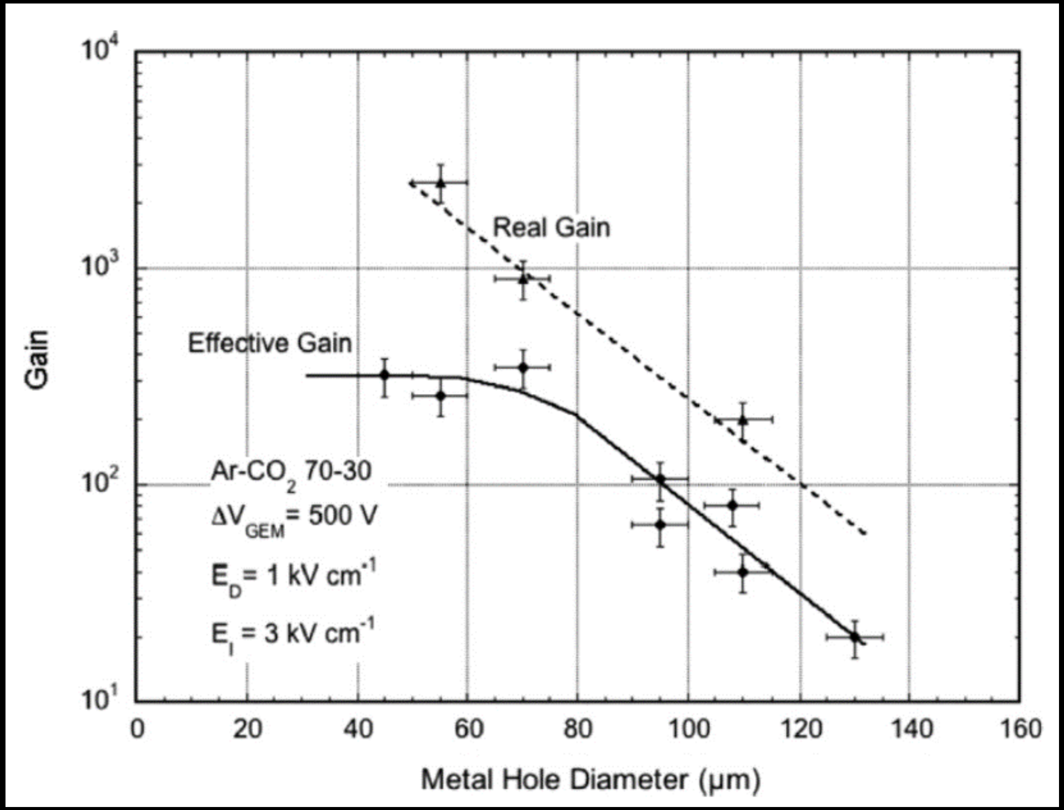

Reduce too much the hole diametr is not beneficial on the gain value

Choice of drift and induction gaps thicknesses: current signal on a single GEM detector

The drift region thickness is chosen such to guarantee an appropriate number *of primary ionization pairs* and to reduce *pile-up* event in order to have a good *event rate*

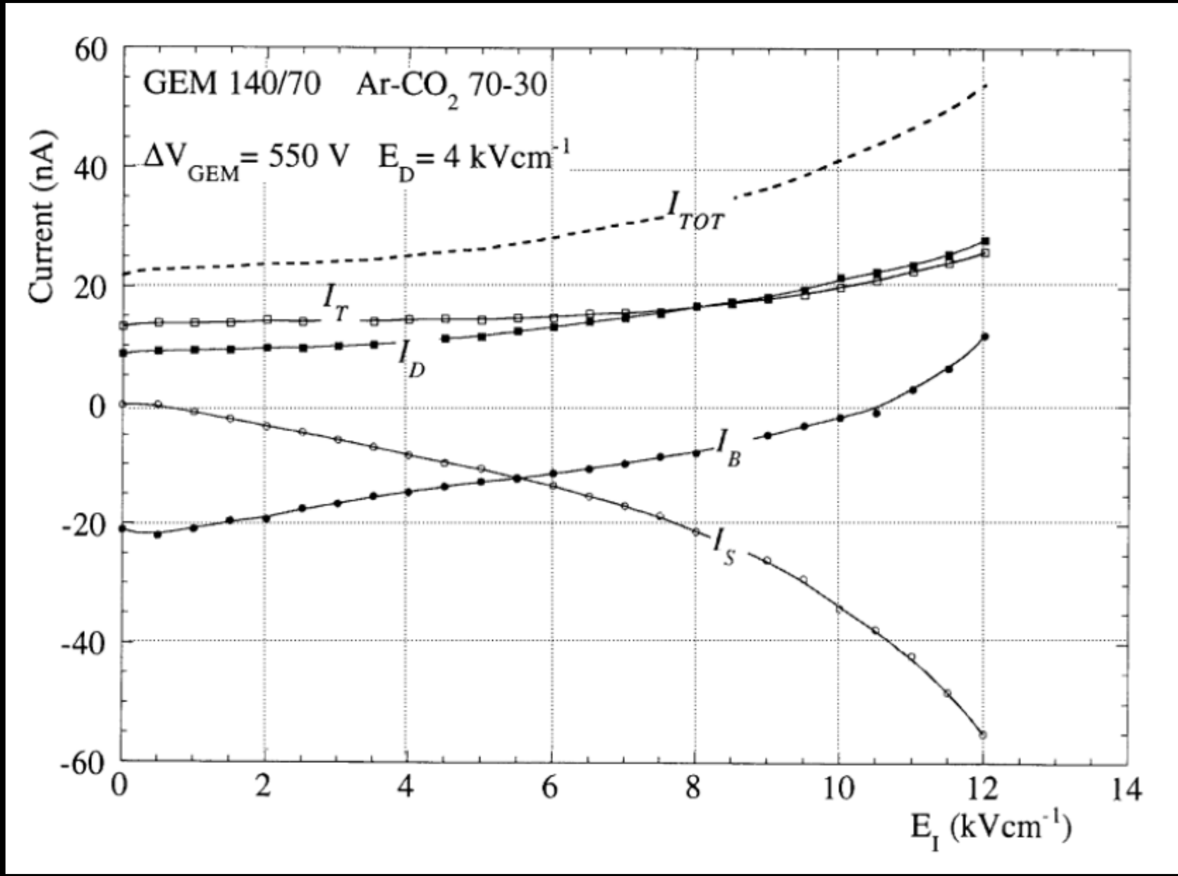

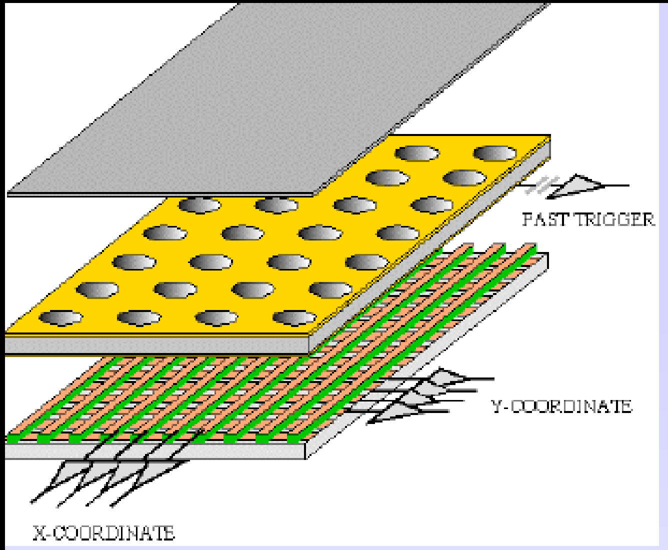

The induction gap thickness is such that to avoid the formation of sparks

Gain dependence on gas mixture composition

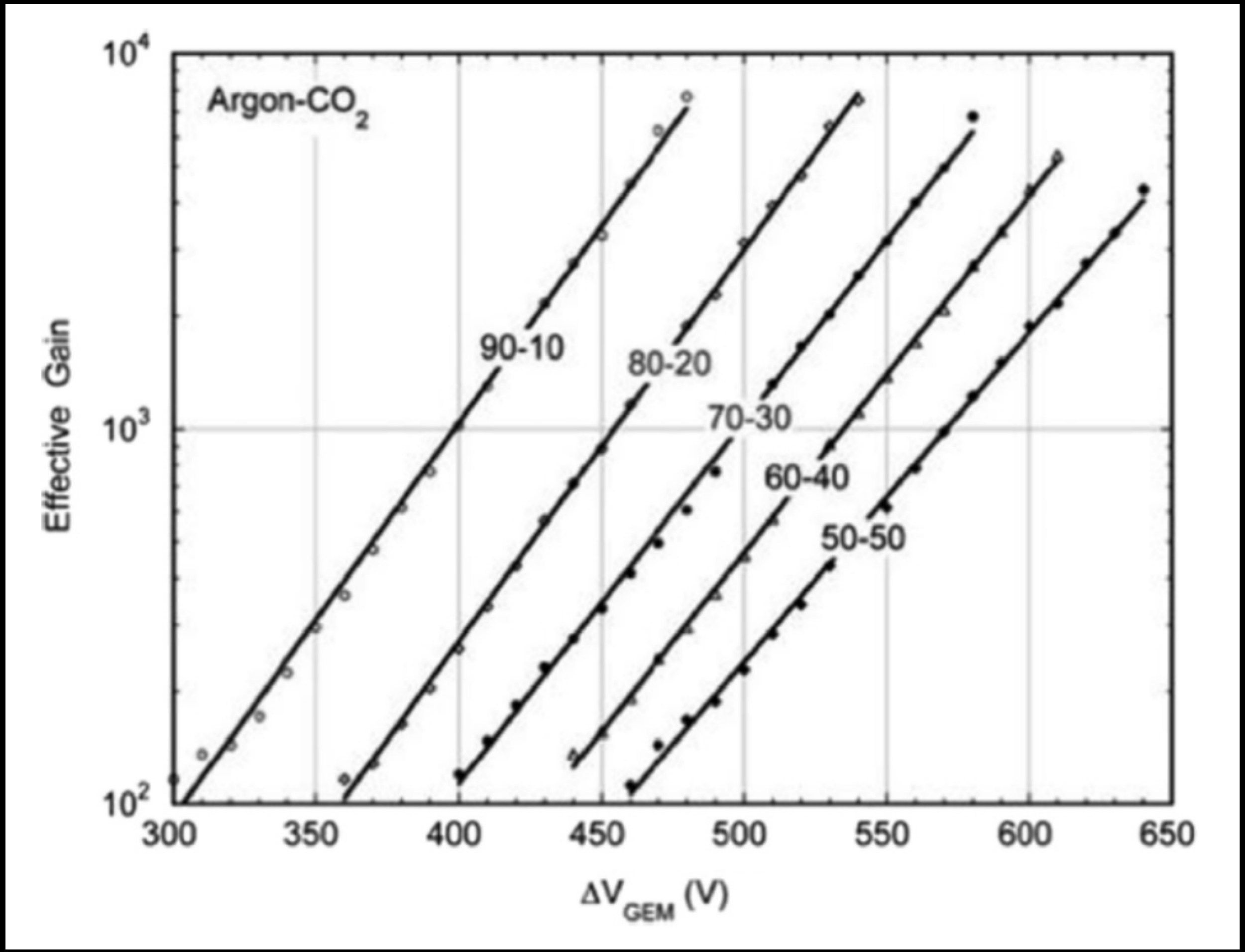

Single GEM effective gain as a function of voltage in Ar–CO_2 mixtures at atmospheric pressure as a function of HV

Energy resolution for a single GEM detectors

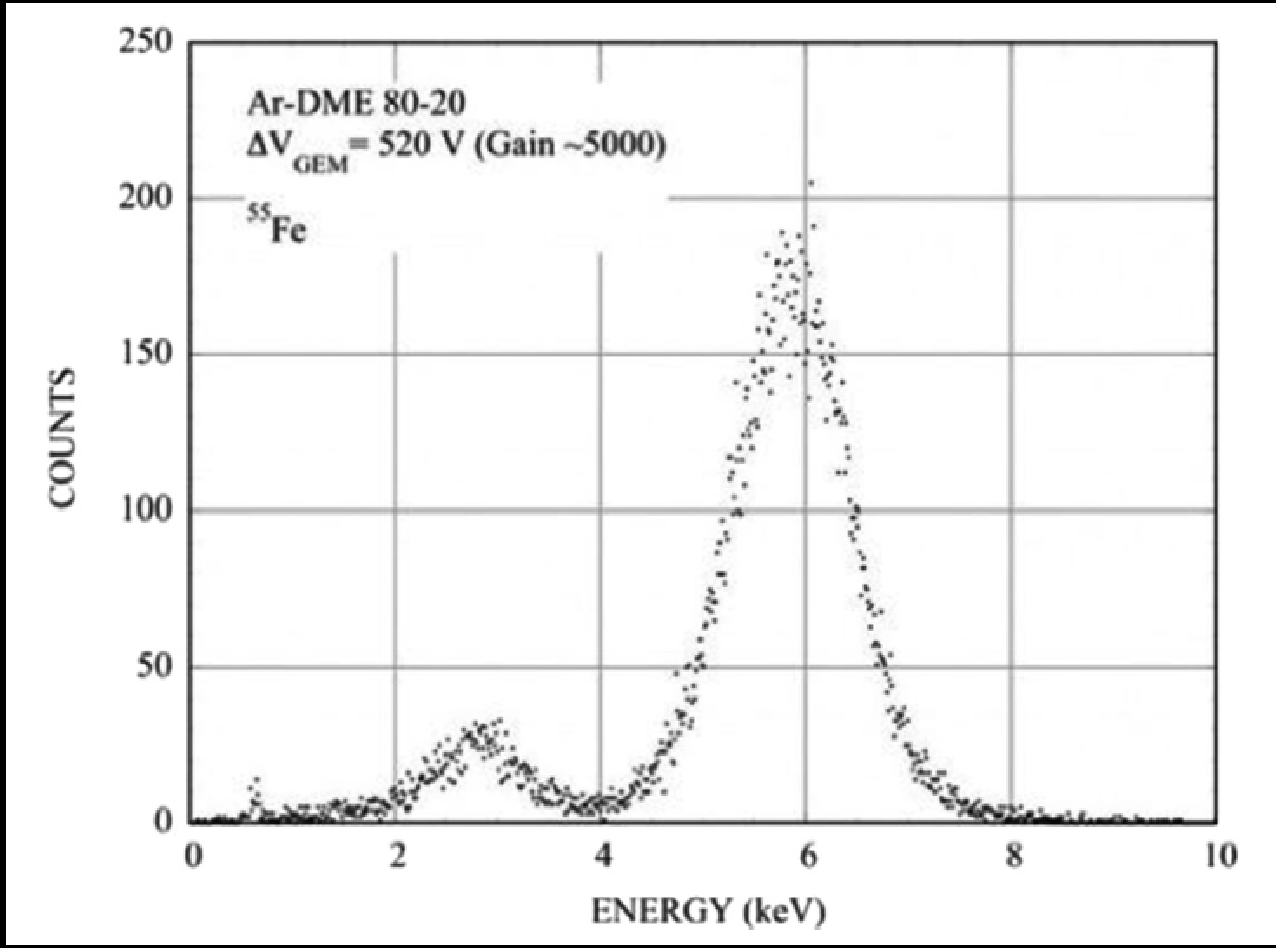

Pulse height spectrum on 5.9keV for a single GEM.
The relative energy resolution is 17%FWHM.

Effective Gain in Triple-GEM detector

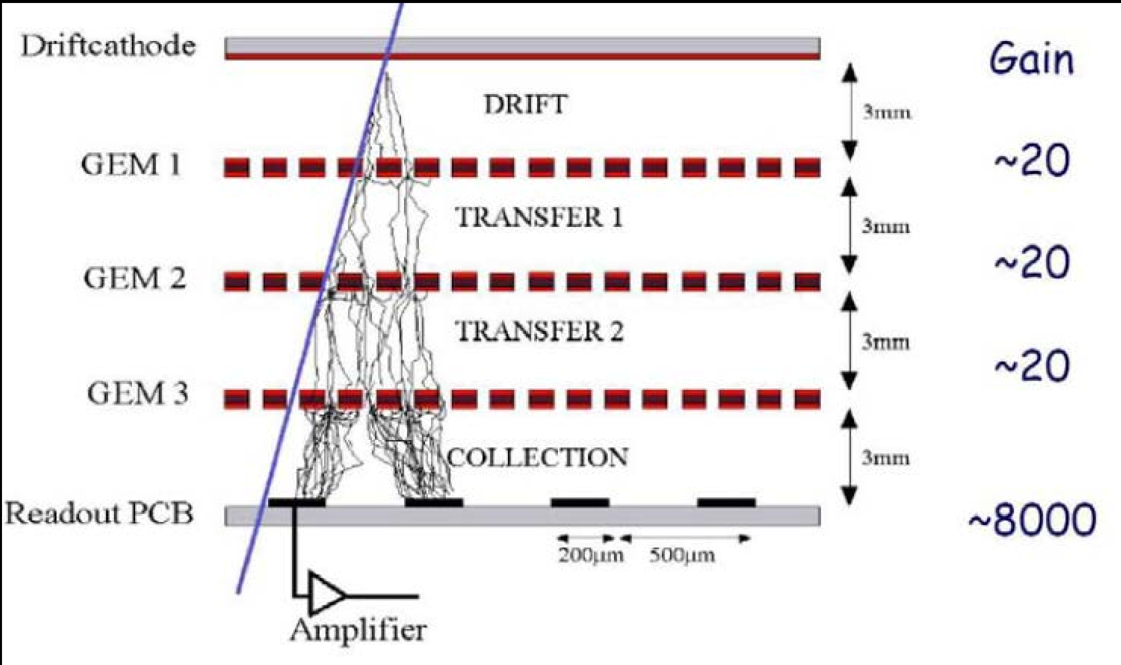

- Multiple structures provides equal gain at lower voltage
- Discharge probability on exposures to α particles is strongly reduced

$$G_{intr} \propto e^{<\alpha> V_{GEM_{TOT}}}$$

$$G_{eff} = \prod_{i=1}^{3} G^i_{intr} \cdot \epsilon^i_{infil} \cdot \epsilon^i_{estr}$$

$$\epsilon^i_{infil} \cdot \epsilon^i_{estr} = T^i$$

Dimensions of different regions

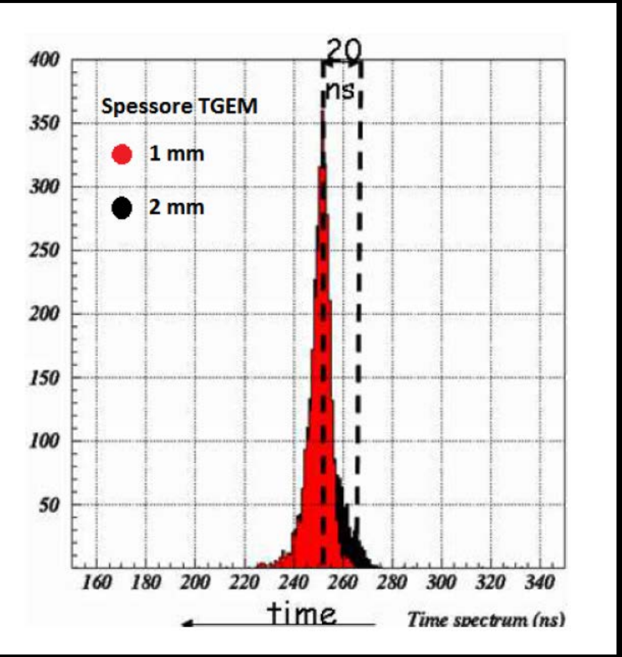

The *bi-GEM* effect → Important on the first transfer gap thickness

Limitations of sparks → Important on the second transfer gap thickness

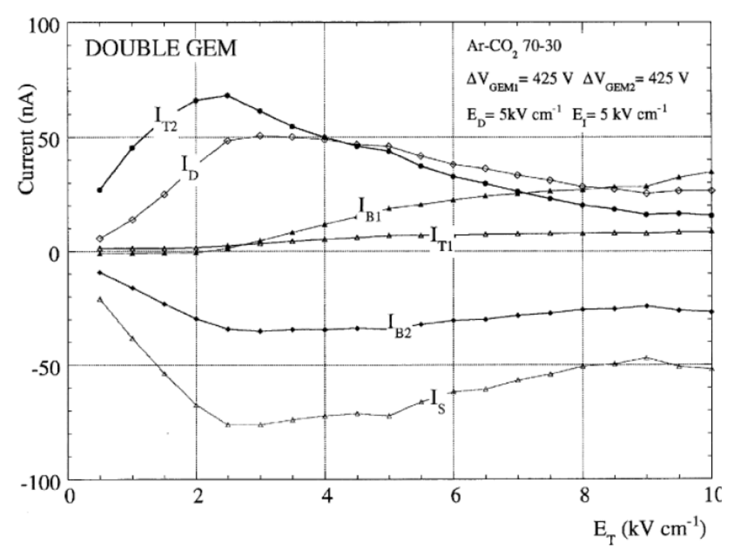

Dependence of current signal on Transfer Electric Field in a double-GEM

Multi-GEM detector
Gain and discharge probability with 5 MeV α particles

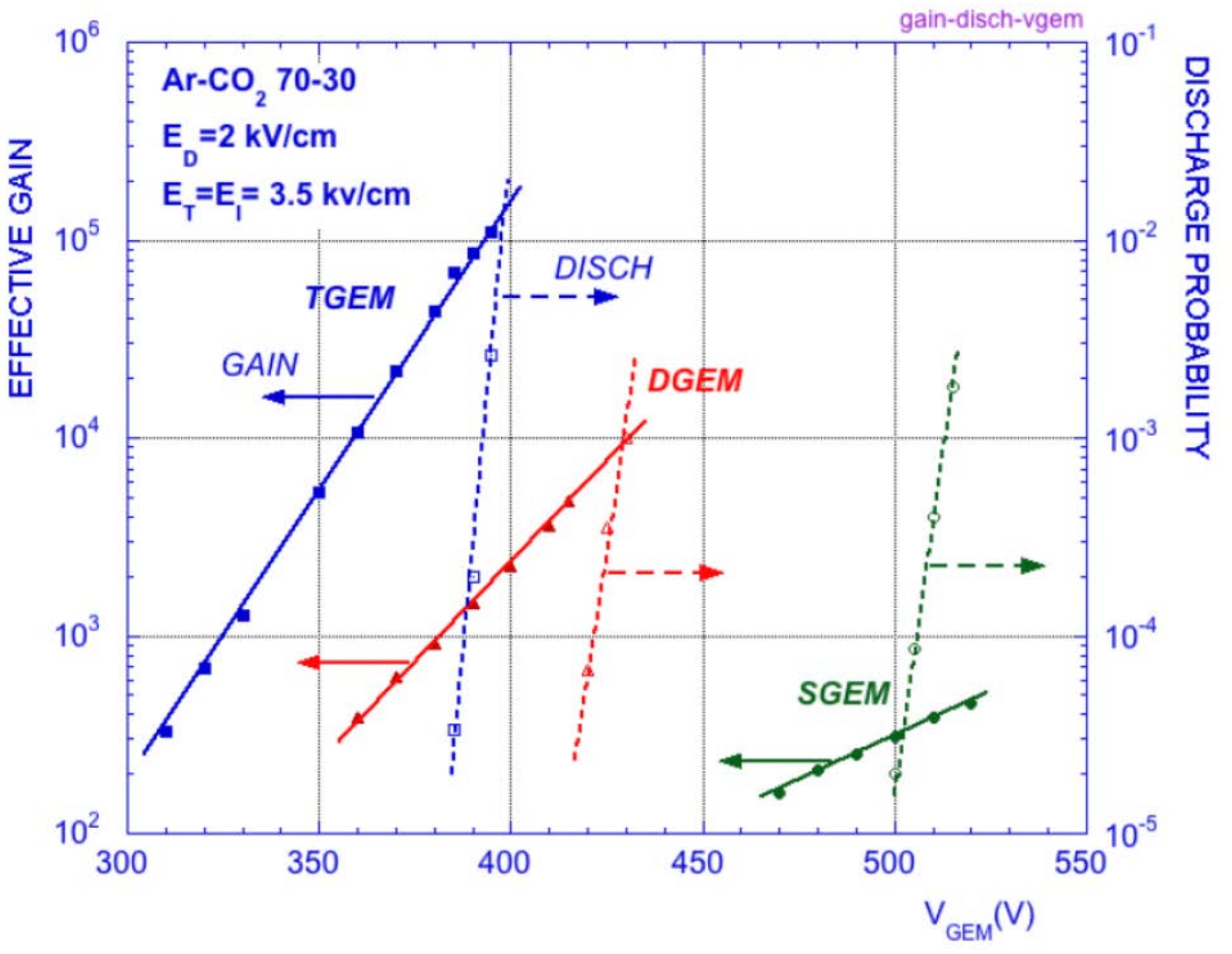

S. Bachmann et al Nucl. Instr. and Meth. A479(2002)294

Performances comparison MMEGAS vs GEM

FAST ELECTRON SIGNALS WITH SLOW ION TAIL:

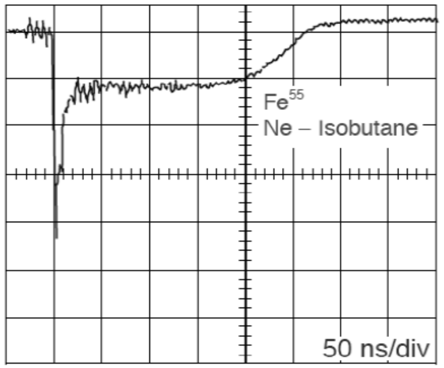

GEM TIME SEPARATION (electron signal only):

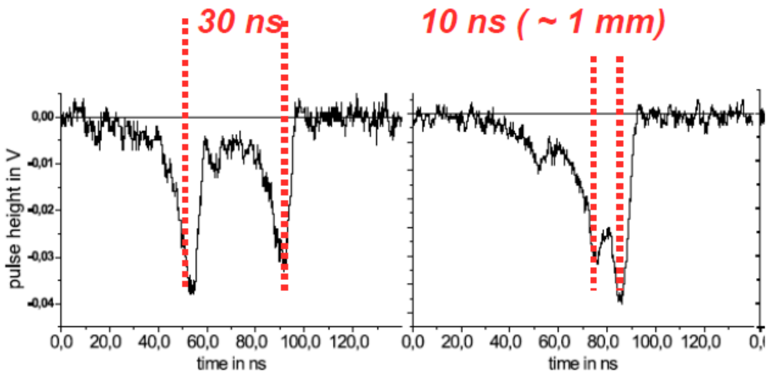

GAIN AND DISCHARGE PROBABLILITY ON HIGHLY IONIZING TRACKS

^{220}Rn -> 6.4 MeV α

GEM:

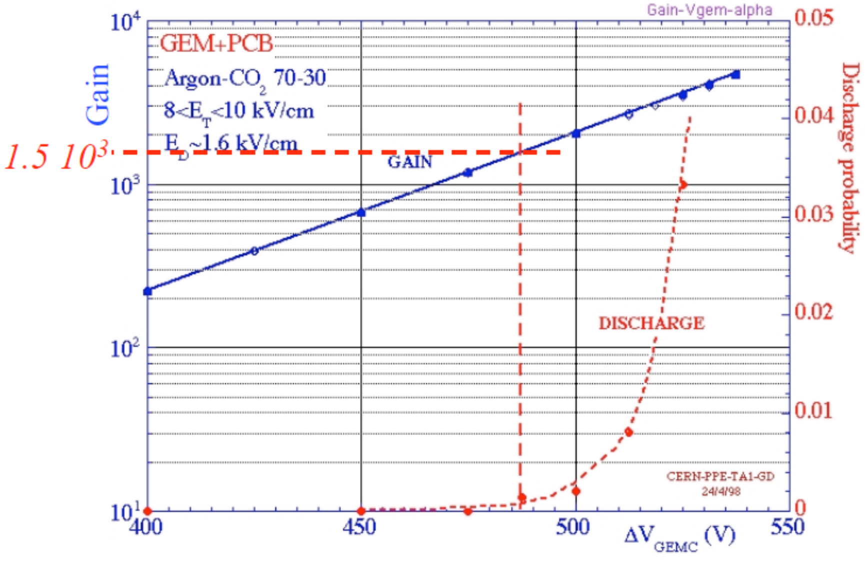

MICROMEGAS:

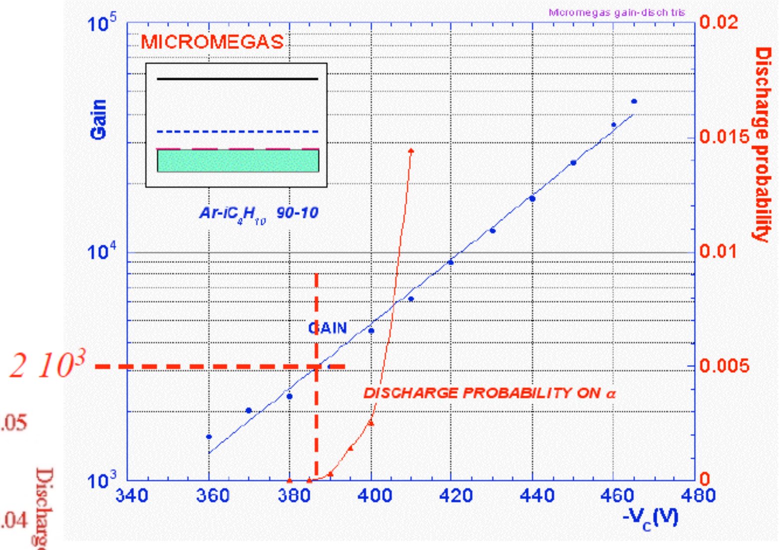

A. Bressan et al
Nucl. Instr. and Meth. A424(1999)321

$\Delta E_\alpha \sim 500$ keV $\sim 10^4$ e

$Q \sim 2\ 10^7$

Discharge probability vs effective gain

DISCHARGES: MULTI-GEM

MULTI-GEM

DISCHARGE PROBABILITY VS GAIN:

IN MULTI-GEMs, THE CHARGE SPREADS BY DIFFUSION OVER MANY INDEPENDENT HOLES!

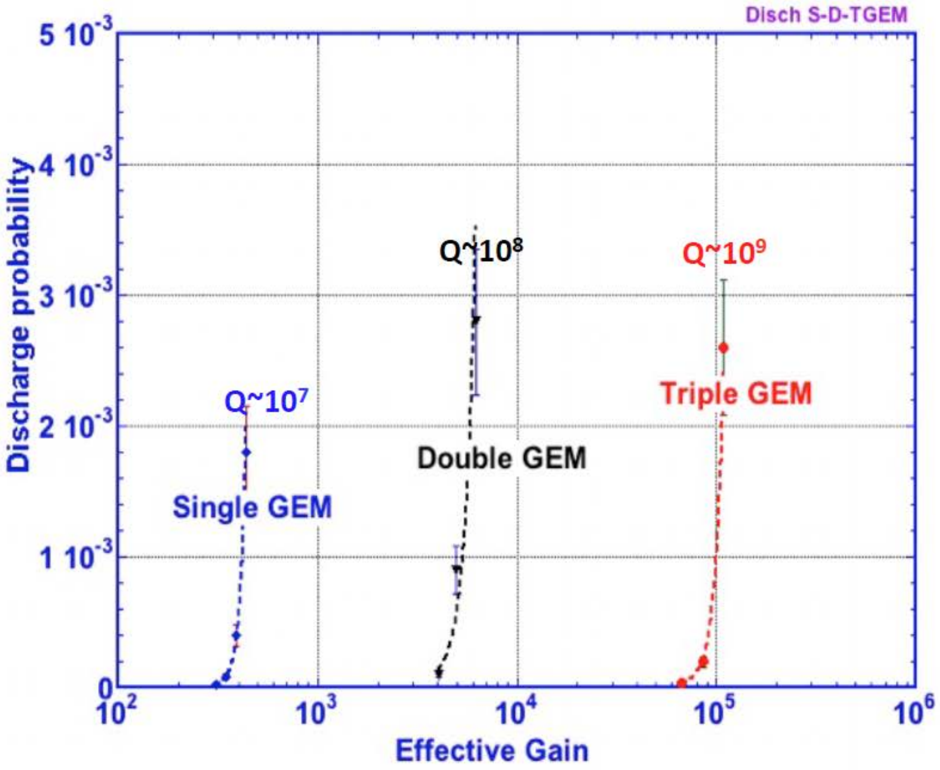

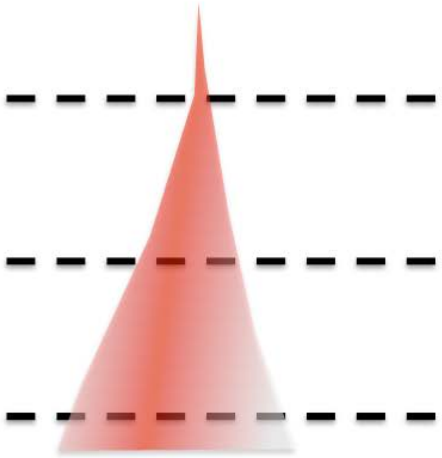

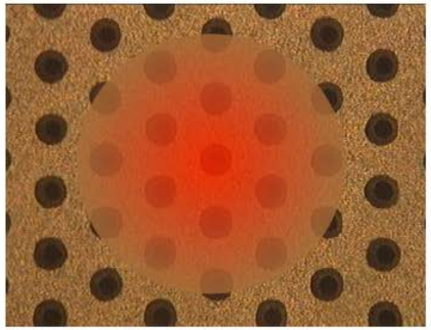

Standard GEM typical spatial & timing resolution

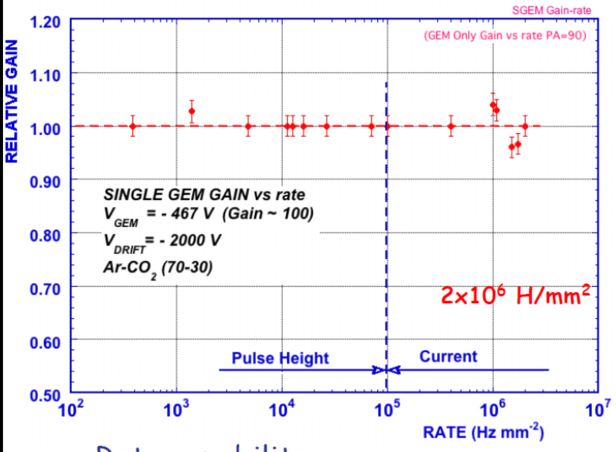

Rate capability

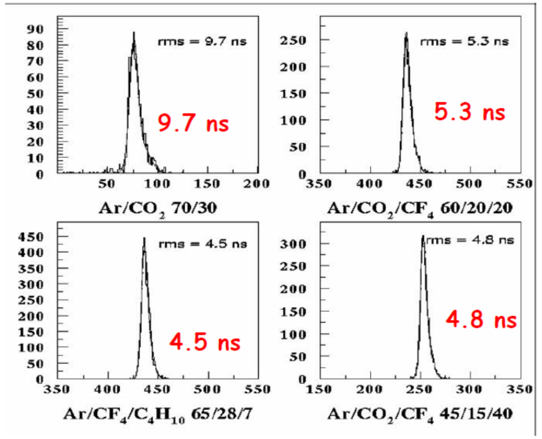

Time resolution

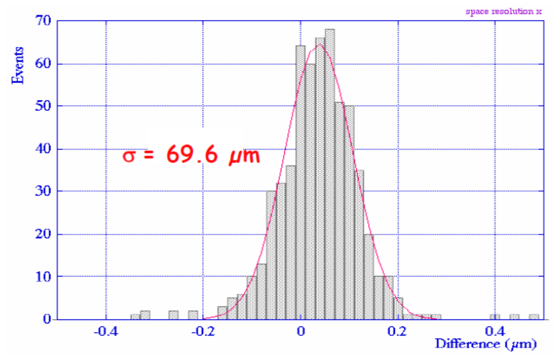

Space resolution

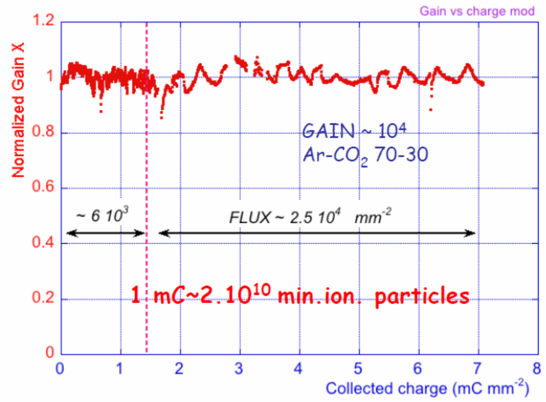

Ageing properties

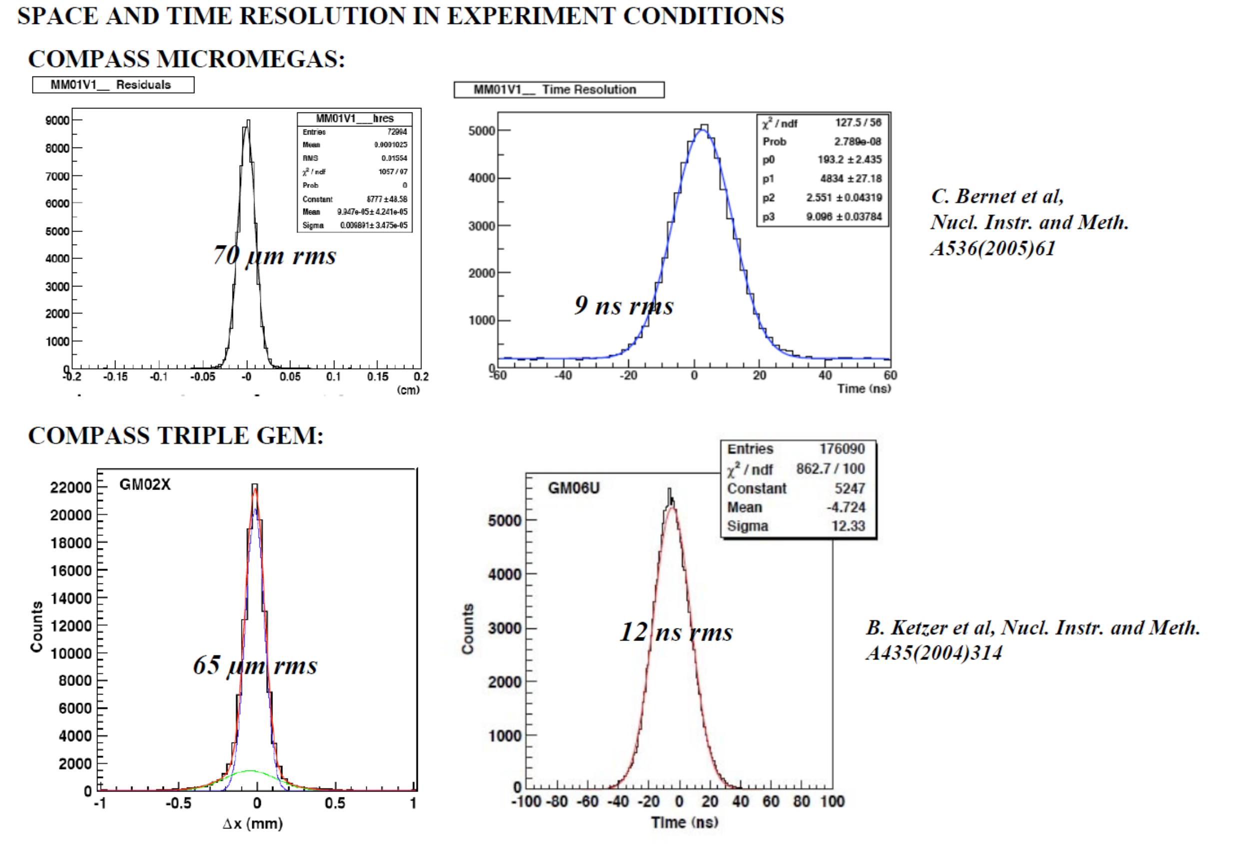

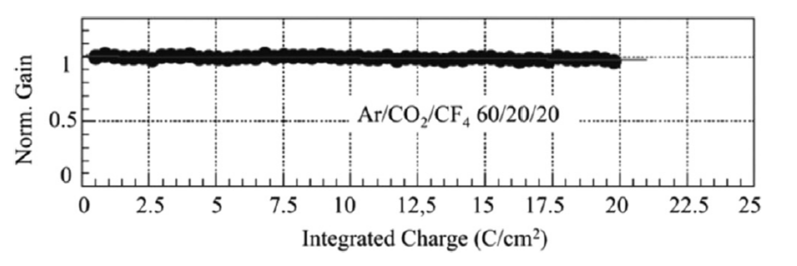

Extended lifetime with addition of CF_4 to standard mixture Ar/CO2

Timing performances

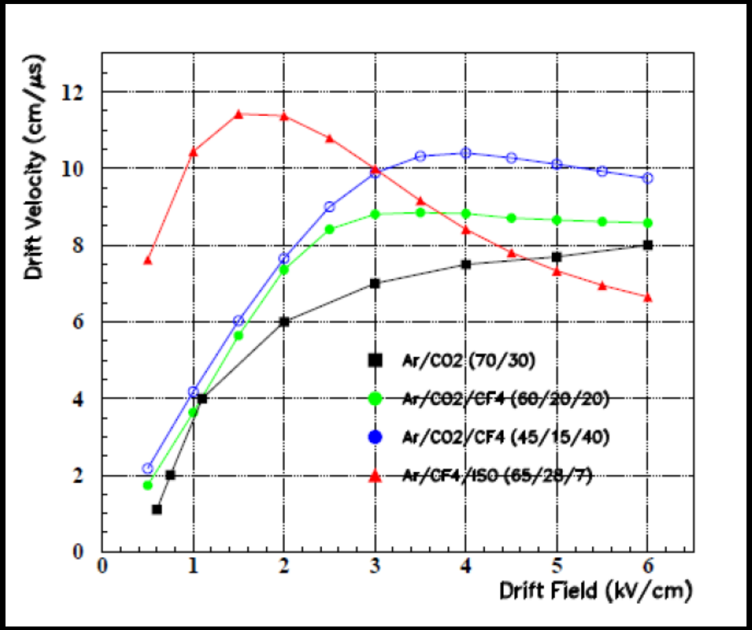

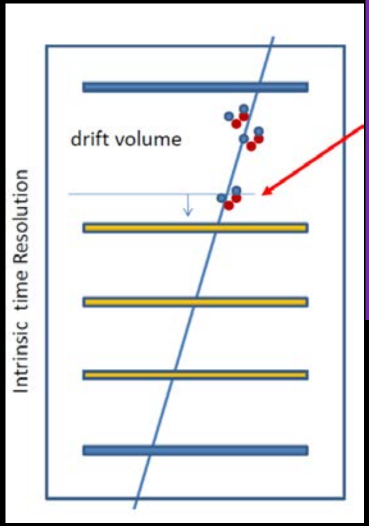

the time resolution is dominated by fluctuations of the nearest distance of the primary ionisation processes to the region where the gain is acquired, d_{near}.
Defining λ as the average number of primary clusters generated by an ionising particle inside the gas, this distance follows a classical exponential distribution

d= exp(-λx)/λ

The **contribution** to the time resolution of the **drift velocity** is:

$$\sigma_t = (\lambda v_d)^{-1}$$

With a drift gap of the order of 3-4 mm and with a proper choice of the gas mixture, these detectors can reach a time resolution of the order of **5-10 ns**.

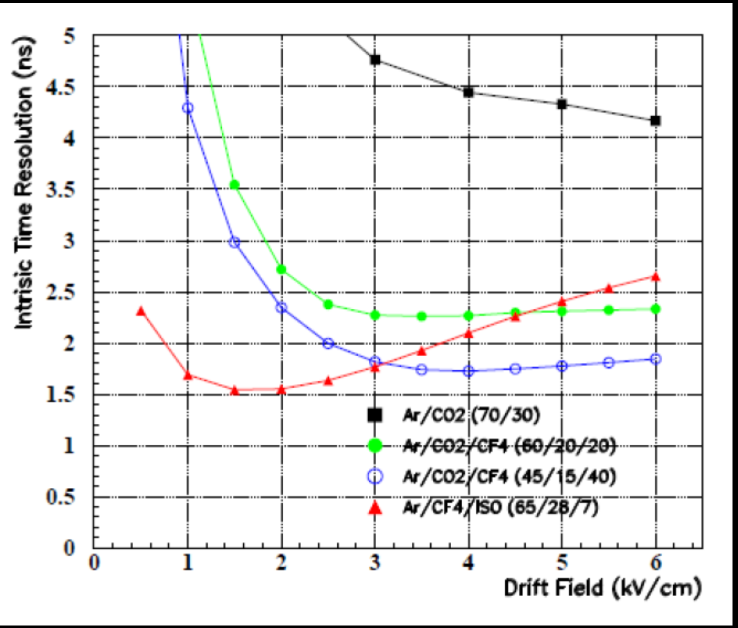

Typical values for gases employed in MPGDs are λ = 3 mm^{-1} and v_d up to 0.12 mm/ns leading to few **ns time resolution** with the best choice of gas mixtures and operating voltages

Timing performances

…moreover the contribution of the gain fluctuation is governed by the *gas time constant* (*effective* Townsend coefficient)

$(\eta_{eff} v_d)^{-1}$

In the multiplication volume the field is very high (50 -100 kV/cm) and consequently $\eta_{eff} > 100\ mm^{-1}$ e con $v_d = 0.12\ mm/ns$ → time resolution contribution < 100 ps

In order to improve the time resolution new configurations are proposed. The improvement is obtained by using several drift regions each one coupled to its multiplication stage

The reduction of the time resolution, in fact, is proportional to the number of the layers N_D employed. In this case the time resolution transforms in:

$$\sigma_t = (\lambda v_d N_D)^{-1}$$

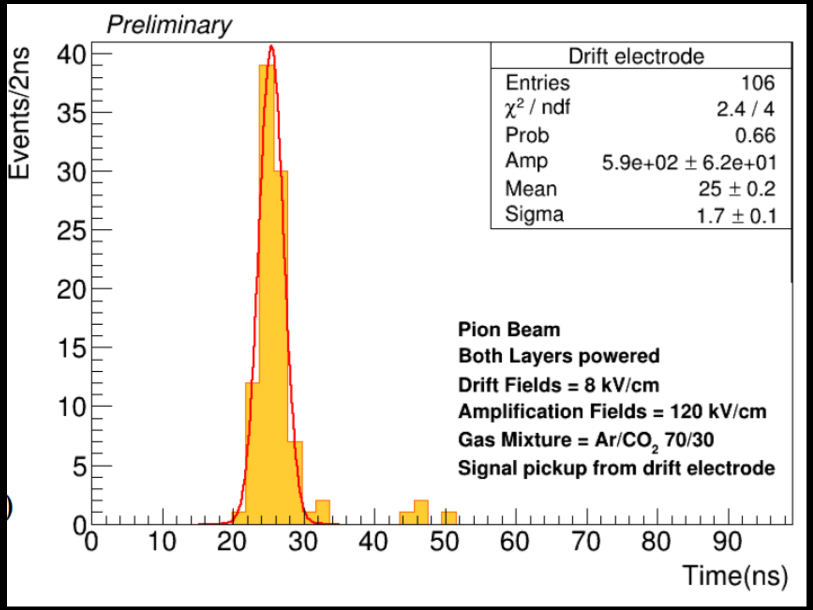

I. Vai et.al. CMS Collaboration
Vienna Conference on Instrumentation2016

R. De Oliveira et.al. *«A novel fast timing micropattern gaseous detector:FTM» CERN-OPEN 2015-002 INFN-15-01/BA*

IBF effect in multi-GEM

$$IBF = \frac{N_C^+}{N_A^-}$$

$$\epsilon = \frac{N_G^+}{N_I}$$

$$IBF = \frac{N_I + \epsilon N_I}{N_I G_{eff}} = \frac{1+\epsilon}{G_{eff}}$$

POSITIVE IONS BACKFLOW: MULTI-GEM

MULTI-GEM

THE IBF VALUE RESULTS FROM THE INTERPLAY OF GEOMETRY, FIELDS AND DIFFUSION:

Strong dependence of IBF from drift Electric field

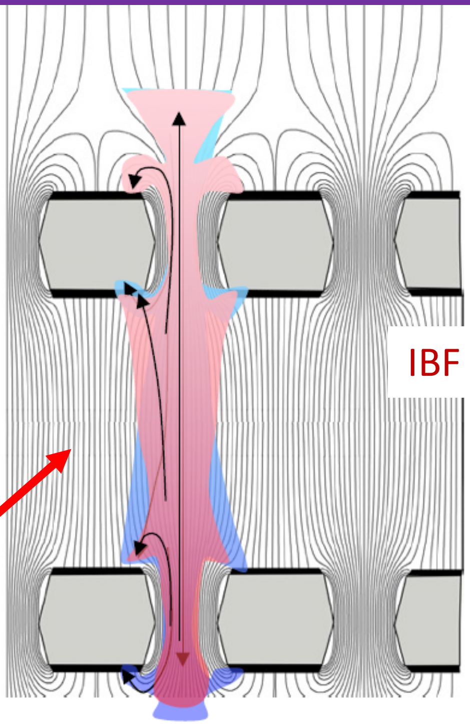

The extraction of electrons is more efficient of the recombination of ions in the drift region. This mechanisms is favoured in GEM than in others gas detectors

IBF AS A FUNCTION OF GAIN:

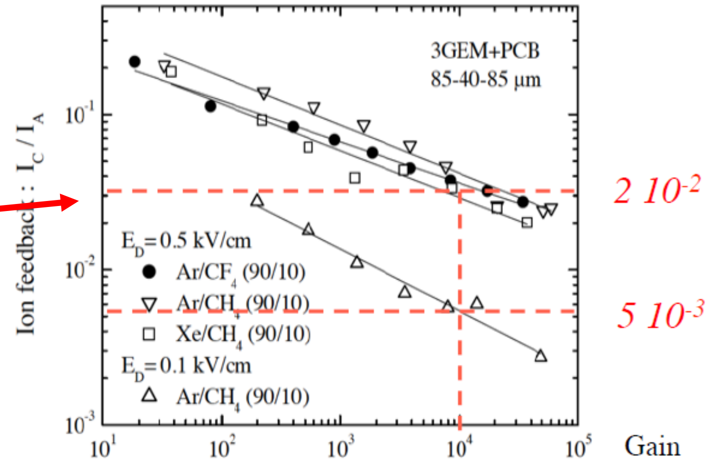

A. Bondar et al, Nucl. Instr. and Meth. A496(2003)325

IBF and Energy Resolution

THE WISH:

$$IBF \leq \frac{1}{GAIN} \approx 10^{-4}$$

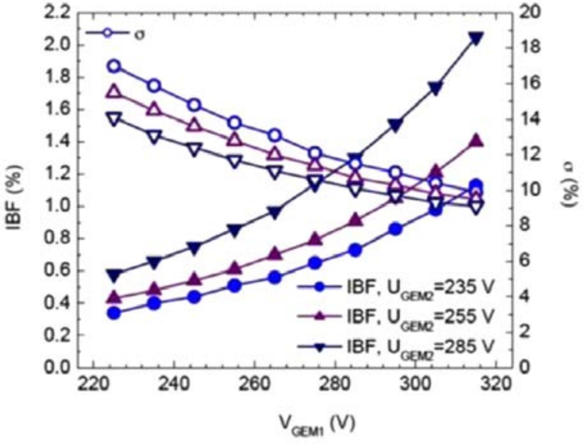

M. Killenberg et al, Nucl. Instr. and Meth. A530(2004)251

Space Charge effect on GEM rate capability

GEM RATE CAPABILITY

GEM GAIN vs RATE (SOFT X-Rays)

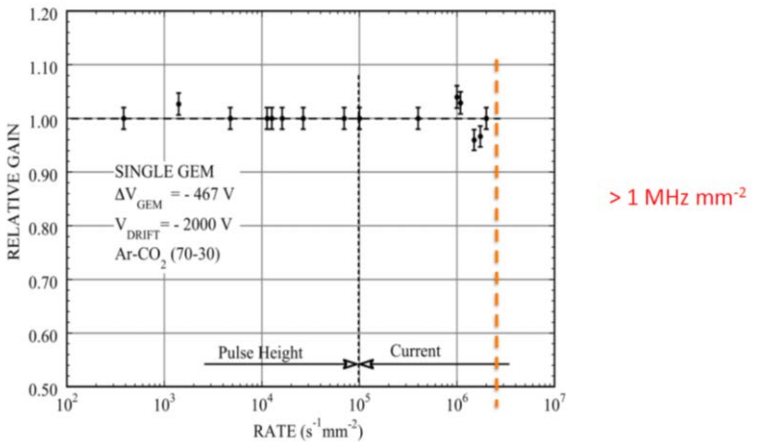

J. Benlloch et al, IEEE NS-45(1998)234

GEM RATE CAPABILITY

A STRANGE OBSERVATION: GAIN INCREASE AT VERY HIGH RATES (2006, UNPUBLISHED)

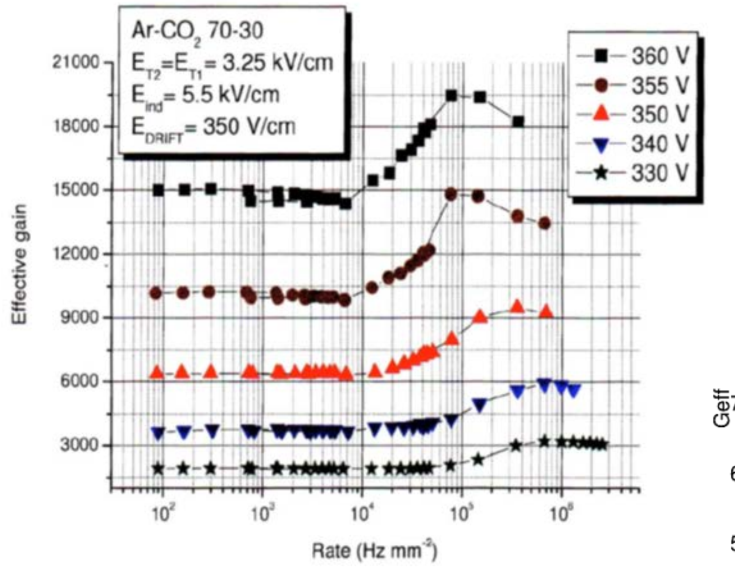

Peter Everaerts, PhD Thesis Gent University (2006)

$$\rho \sim \frac{(\epsilon + 1) \cdot n_{prim} \cdot e}{v_{ion}}$$

Spatial charge density

GEM RATE CAPABILITY (SIMULATION)

GEM

- COMSOL Finite Element Analysis
- GARFIELD

SPACE CHARGE BUILDUP:

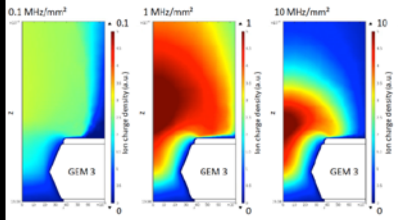

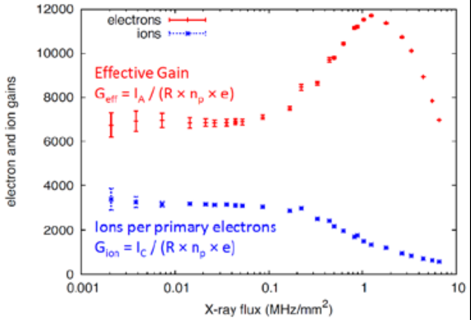

S. Franchino et al, IEEE Nucl. Sci. Symposium (San Diego, Oct. 31, 2015)

$$E(z) \sim E_D - \frac{\rho d}{2\epsilon_0} + \frac{\rho z}{\epsilon_0}$$

Electric field in drift region on the top of 1'st GEM

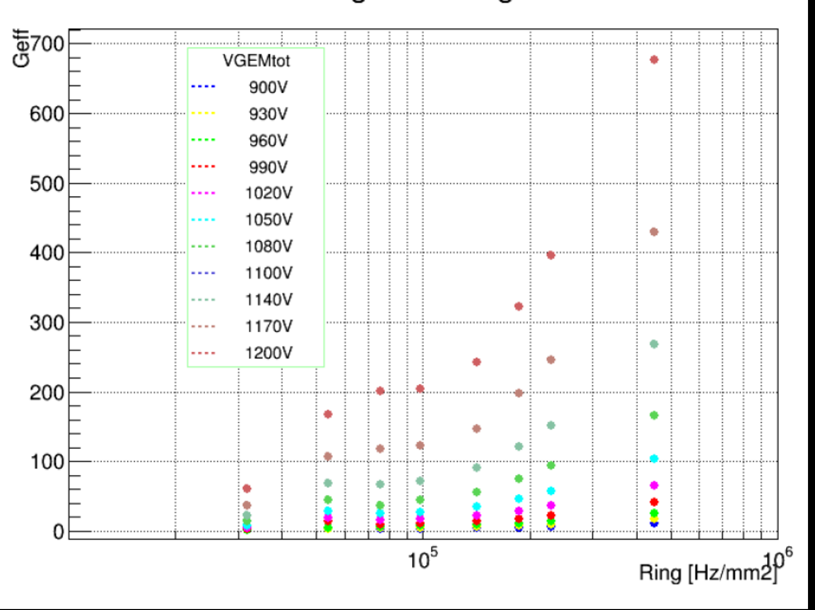

The IBF study on a TPG prototype, Thesis_2016 Bari University

GEM different shapes and readout board

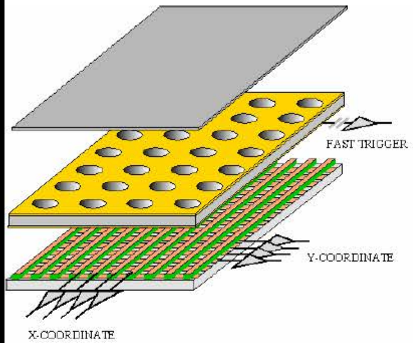

A. Bressan et al, Nucl. Instr. and Meth. A425(1999)254

Full decoupling of the charge amplification structure from the charge collection and readout structure.
Both structures can be optimized independently !

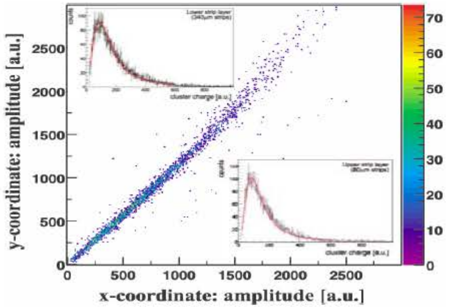

Charge correlation (Cartesian readout)

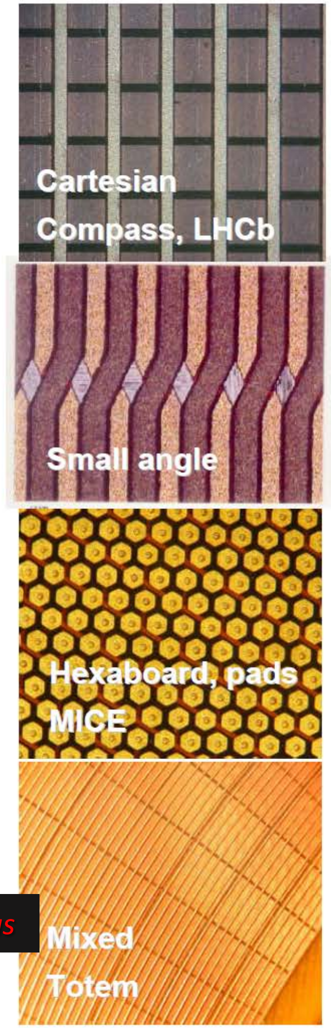

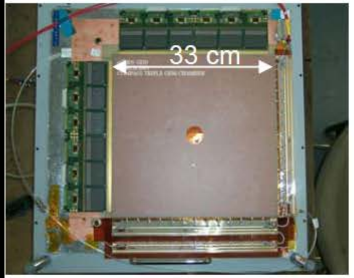

Compass

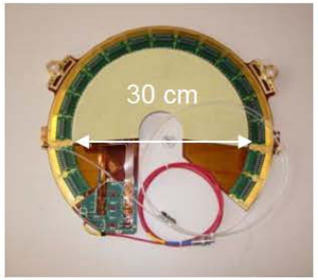

Totem

Triple-GEM tracker for KLOE apparatus

All detectors use three GEM foils in cascade for amplification to minimize discharge probability by reducing field strength.

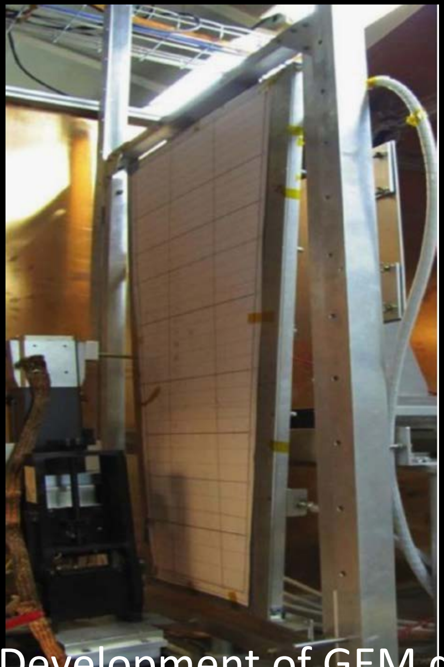

- Development of GEM detector of large area
- Triple GEM for CMS-End Cap Muon detector

Bidimensional XV readout plane for KLOE tracking detector

Gas Detestors in LHC experiments

ALICE:	TPC (tracker), TRD (transition rad.), TOF (MRPC), HMPID (RICH-pad chamber), Muon tracking (pad chamber), Muon trigger (RPC)
ATLAS:	TRD (straw tubes), MDT (muon drift tubes), Muon trigger (RPC, thin gap chambers)
CMS:	Muon detector (drift tubes, CSC), RPC (muon trigger)
LHCb:	Tracker (straw tubes), Muon detector (MWPC, GEM)
TOTEM:	Tracker & trigger (CSC , GEM)

Fast Timing architecture

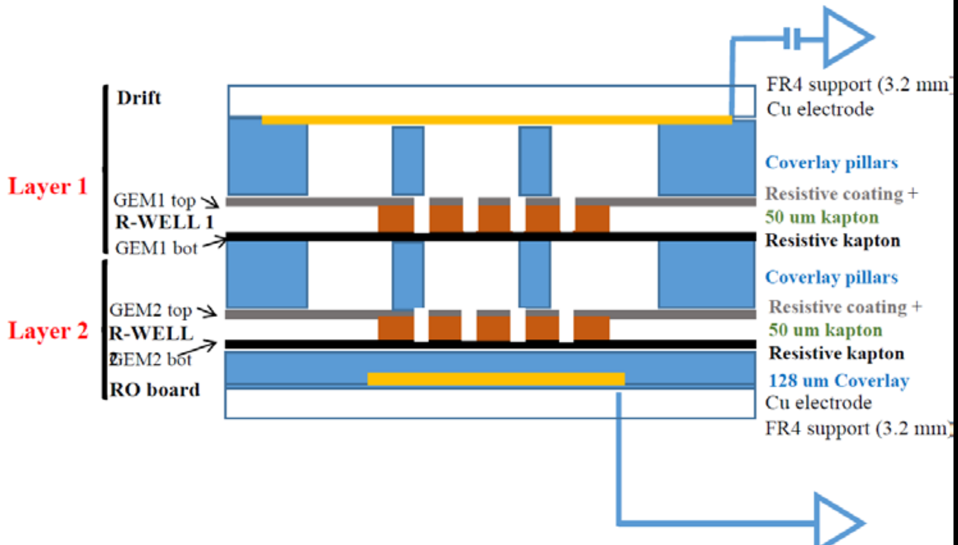

The detector is composed by two independent drift-amplification stages (Layer 1 & 2 in the picture above).

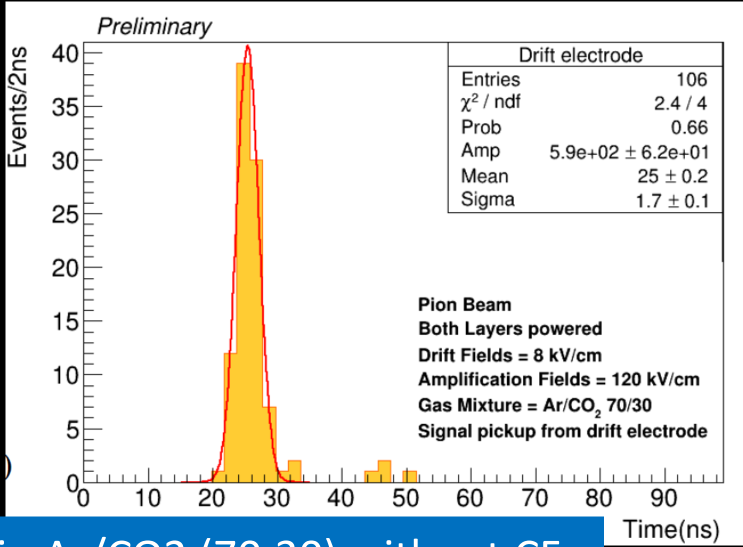

Only in Ar/CO2 (70:30) without CF_4

Each amplification region is based on ***a pair of polyimide foils*** stacked due to the electrostatic force induced by the polarization of the foils:

- The first foil, perforated with inverted truncated-cone-shaped holes (bases 100 µm and 70 µm, pitch 140 µm), is a 50 µm thick Apical KANECA, coated with diamond-like carbon technique, to reach up to 800 MΩ/□ resistivity.
- The second foil is 25 µm thick XC Dupont Kapton, with a resistivity of 2 MΩ/□.

The ***drift volumes are 250 µm thick***, with planarity ensured by coverlay pillars, with diameter 400 µm and pitch of ~3.3 mm.

The active area (circular) is about 20 cm^2.

D. Abbaneo et.al., "R&D on a new type of micropattern gaseous detector: The Fast Timing Micropattern detector", arXiv:1503.05330v1
European Patent Application 14200153.6
M. Maggi, A. Sharma, R. De Oliveira

Novel MPGD architecture

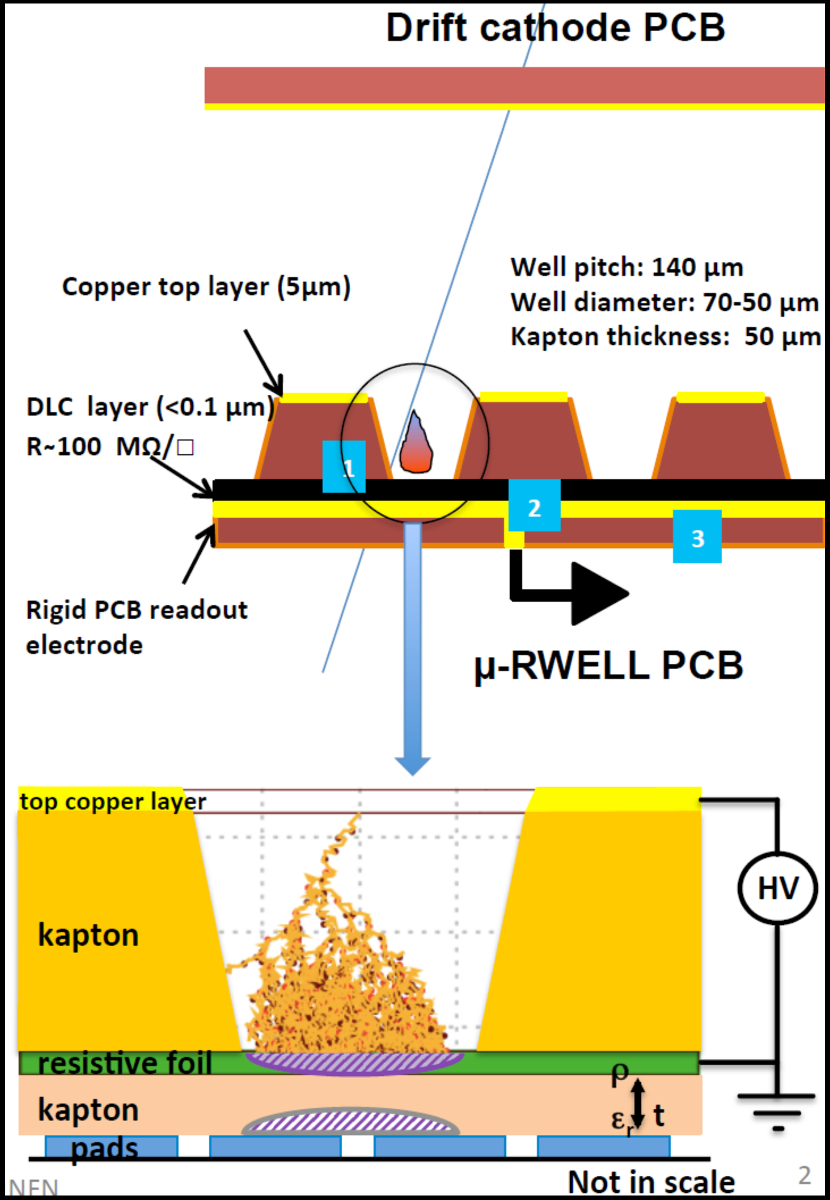

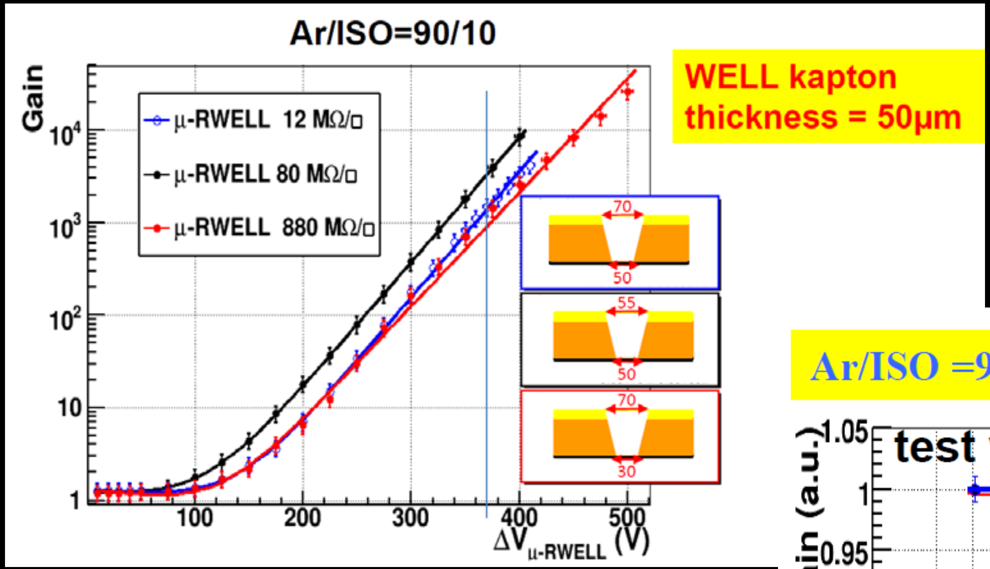

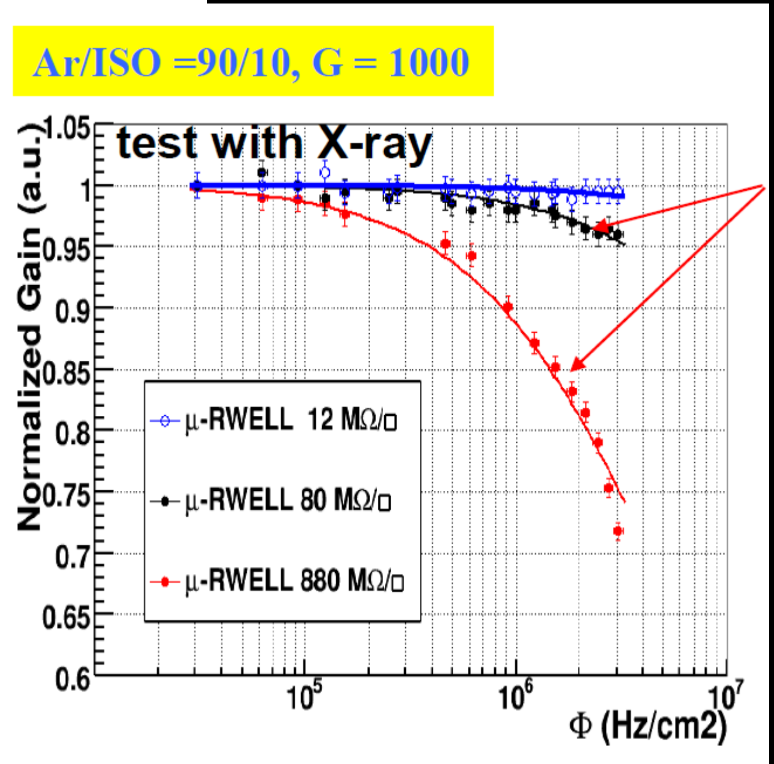

G. Bencivenni et.al.˝The micro-Resistive Well detector: a compact spark protected single amplificatio stage MPGD˝, JINST February 18, 2015

Laboratory measurements

1. Gain vs V_{GEM_TOT} for two gas mixtures
2. Transparency measurement:
   - @fixed V_{GEM} *Gain vs* E_d for different gas mixtures
   - Sensitivity measurements

$$G = \frac{I_a}{R \times n_T \times e}$$

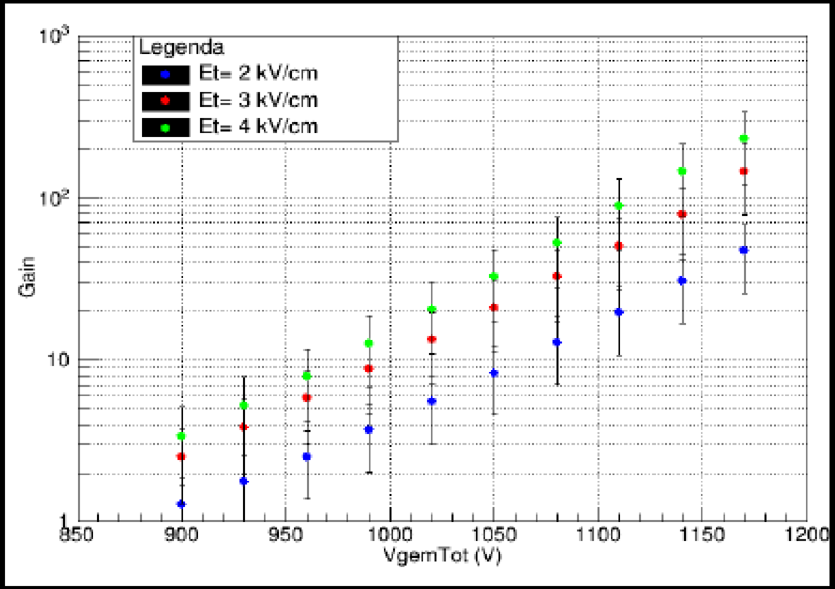

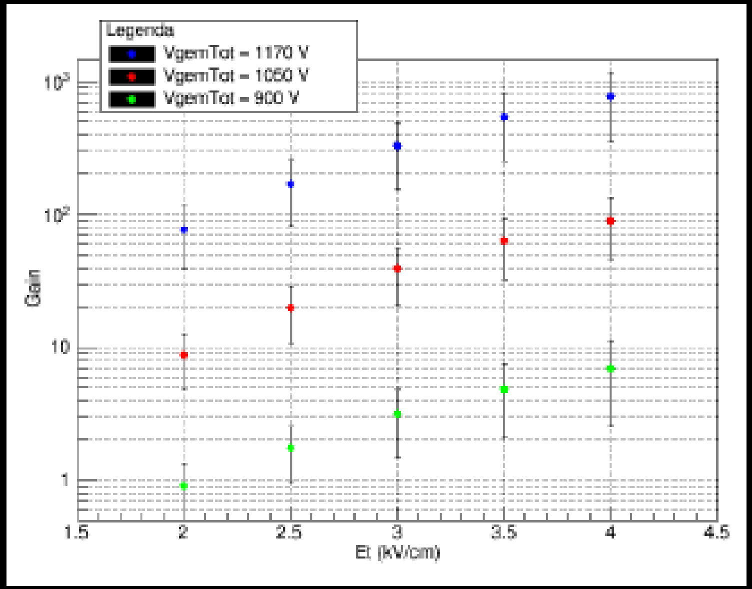

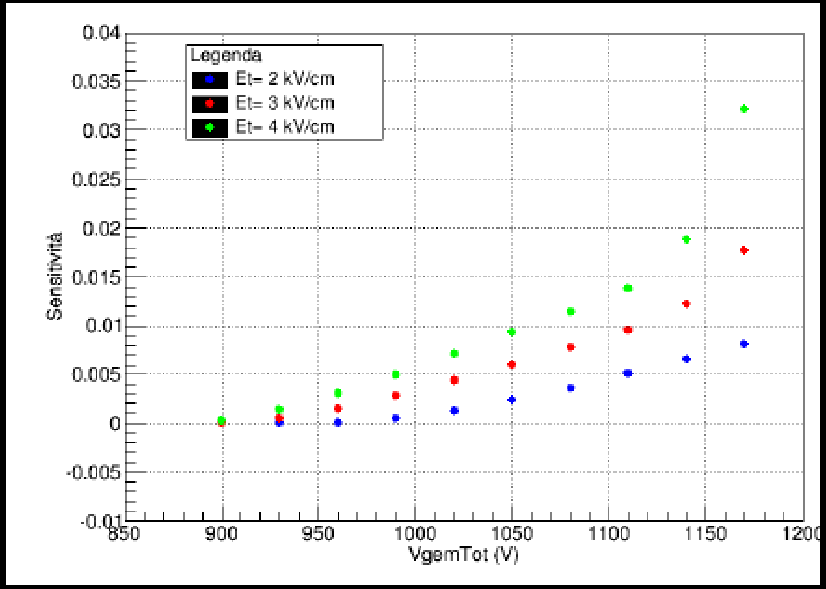

Suggestion for Gain measurements

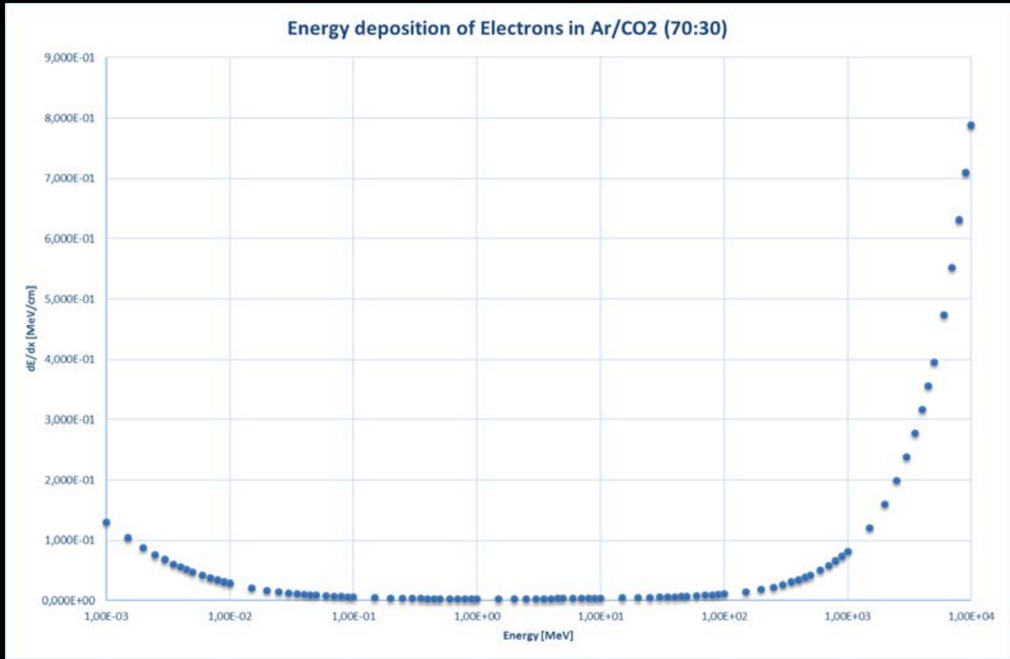

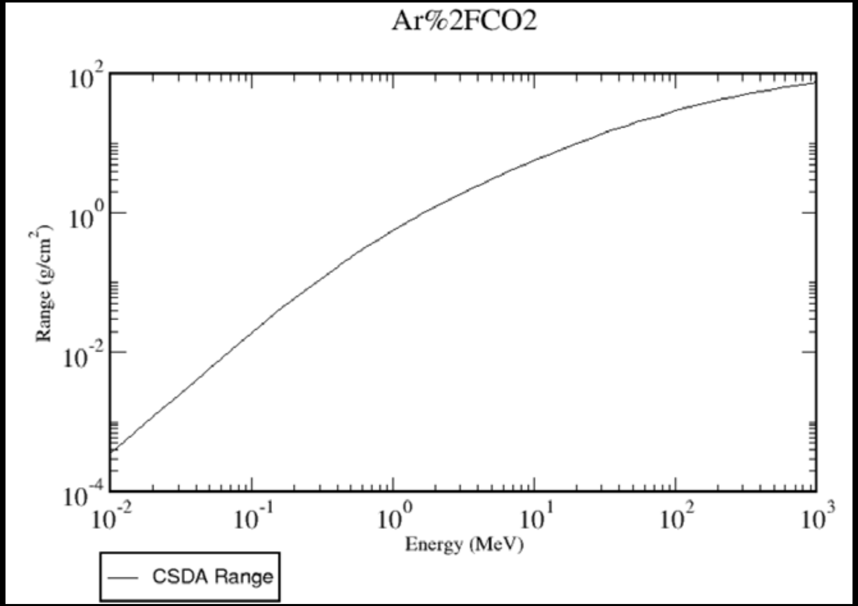

Evaluation of primary charge

Fe^{55} X-ray of 5.9 KeV → photoelectric effect
→ photoelectrons completely converted in drift gap
→ Range < 0.3 cm of drift gap

$$n_T = \Delta E \times \left[\frac{0.7}{W_i(Ar)} + \frac{0.3}{W_i(CO_2)}\right] = 5900 \times \left[\frac{0.7}{26} + \frac{0.3}{33}\right] \approx 212$$

Sr^{90} β^- of 0.546 MeV and 2.28MeV→ range » drft gap
→ we may assume $\langle N_T \rangle = 28\, e^-$

http://physics.nist.gov/PhysRefData/Star/Text/intro.html

Space charge effect

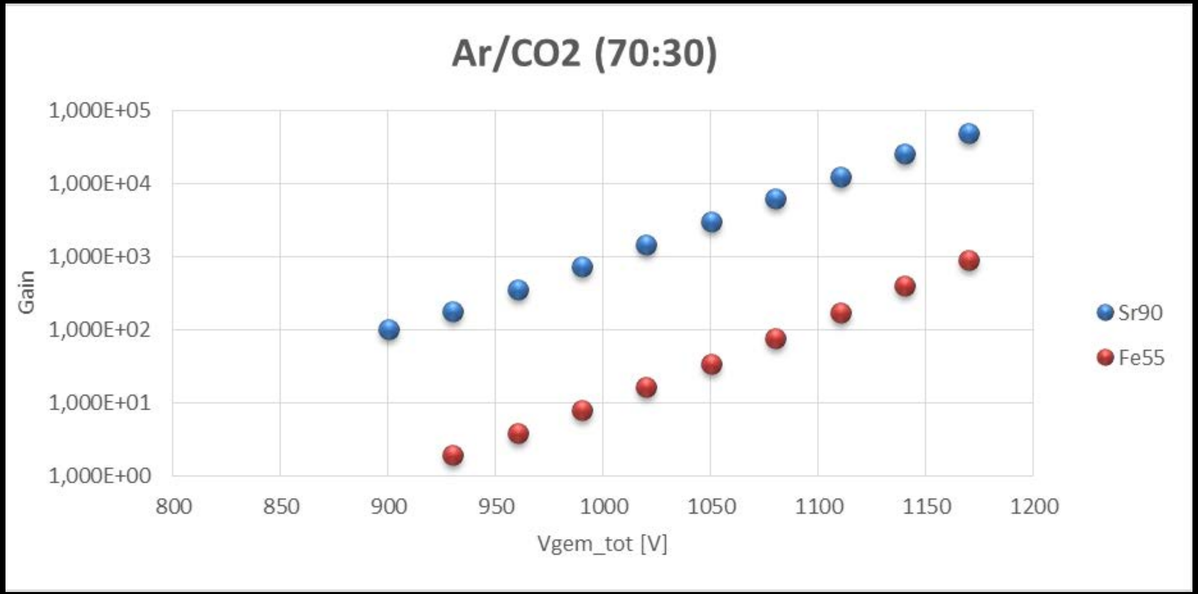

Triple-GEM detector 10x10 cm^2
Configuration: 3-1-2-1
Operated with:

- Ed = 1.5 KV/cm
- Et1 = Et2 = 3.0 KV/cm
- Ei = 5 KV/cm
- $V_{G1} > V_{G2} > V_{G3}$

Experimental setup

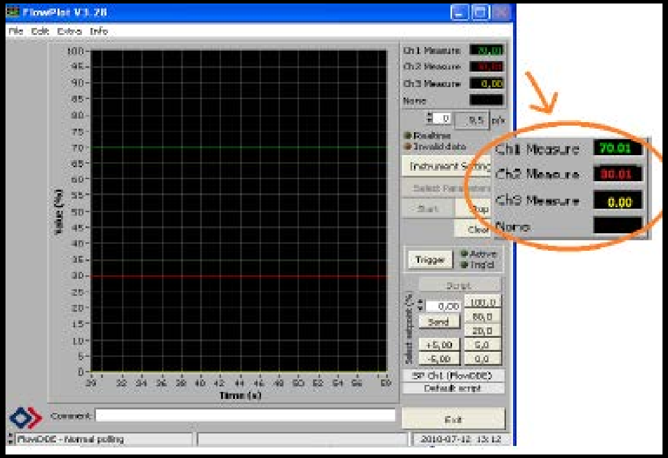

Triple gas system controlled by Bronkhorst Flowmter

Pico-ammeter Keithley 6487

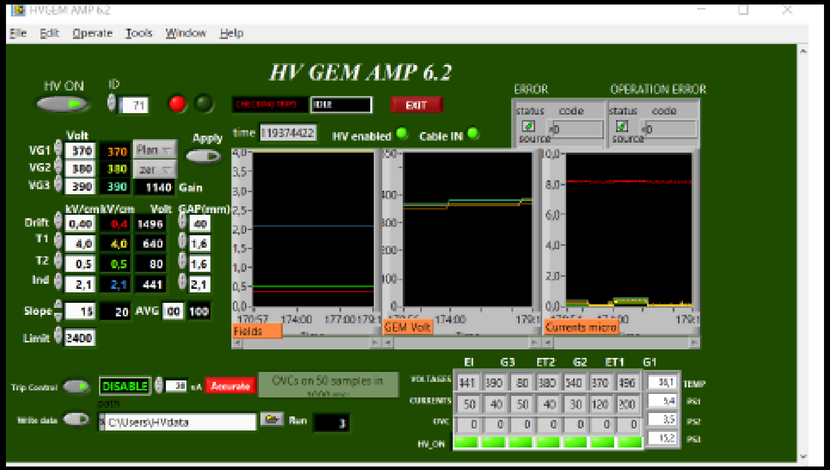

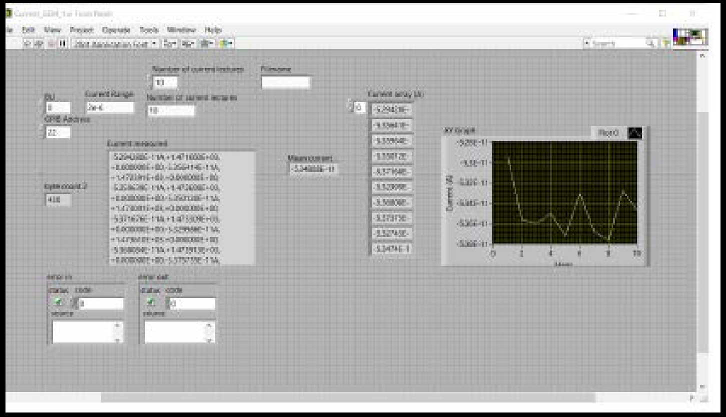

Special purpose custom-made HV system

The triple-GEM detector

Triple-GEM 10x10 single mask

Customized HV connection

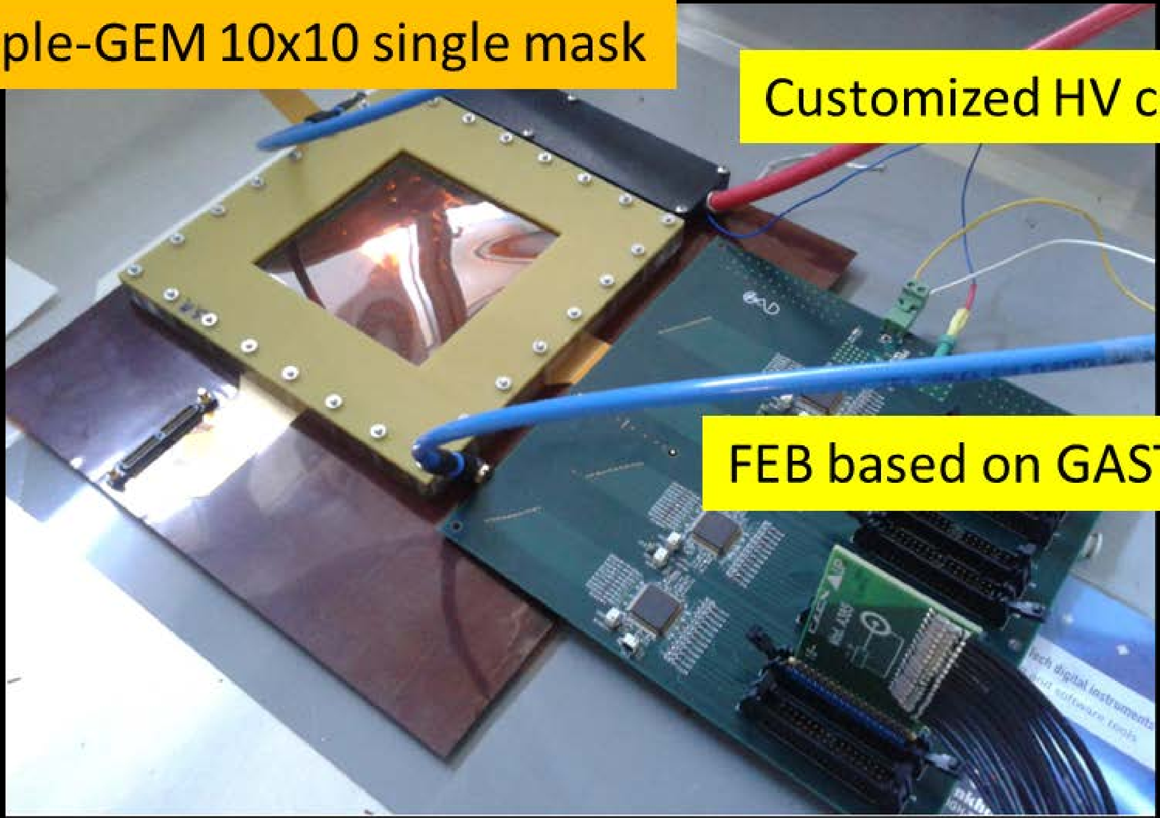

FEB based on GASTONE_32 ASIC

Anode plane readout with X-Y orthogonal strips
600μm width, 100μm pitch

GEM-Lab set-up

(FLOWDDE/FLOWPOT Flow-meter control software)

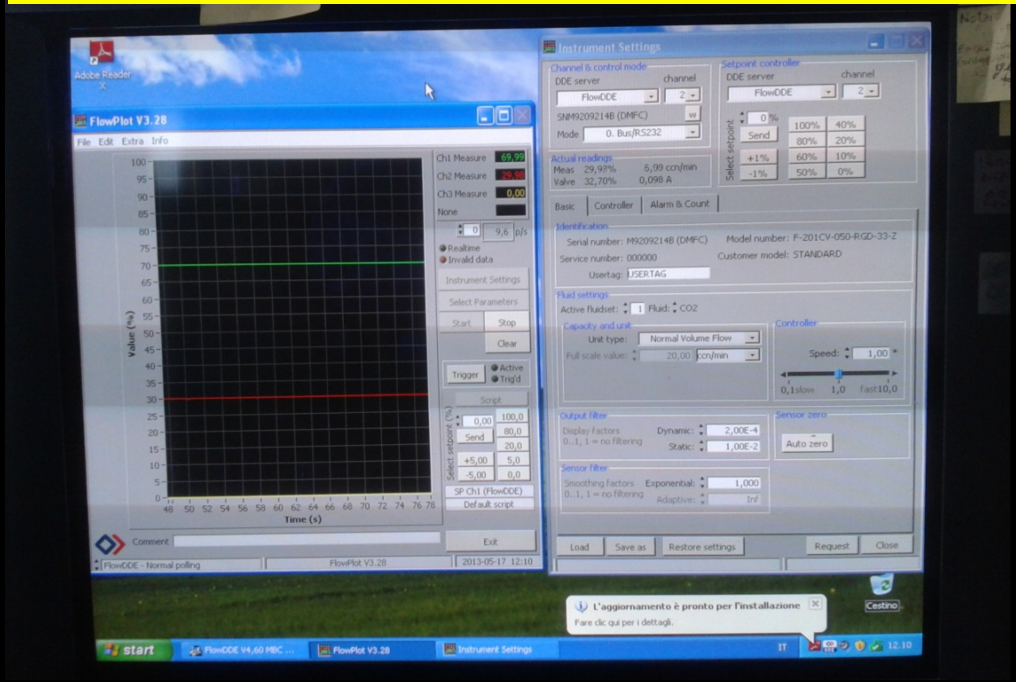

(EL-FLOW® Bronkhorst High Tech BV)

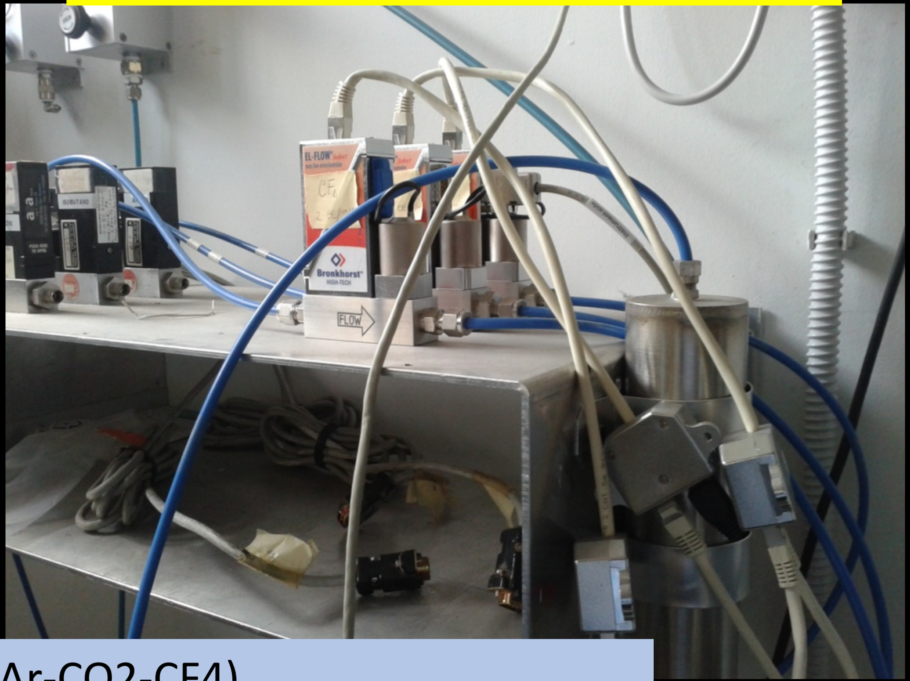

- The gas system is composed by three mixed lines (Ar-CO2-CF4)
- Each line is controlled by three Flow-mass meters

Ar (Max Capability = 20 cc/min), CO2 (20 cc/min), CF4 (2 cc/min) (precision of 1%)

- All the system is controlled by a PC software through an RS232 serial line interface

We foresee to use other gas type like Ne for instance for gas mixtures study

GEM-Lab set-up

- HV power supply based on Frascati HVGEM module and used in LHCb experiment (last release with Trip control on each channel
- 6 channels 150 μA-750 V_{MAX} /channel
- 1 channel 75μA – 1500 V_{MAX}
- HVGEM control is made through a LabView program
- Interfaced to PC through a USB connection

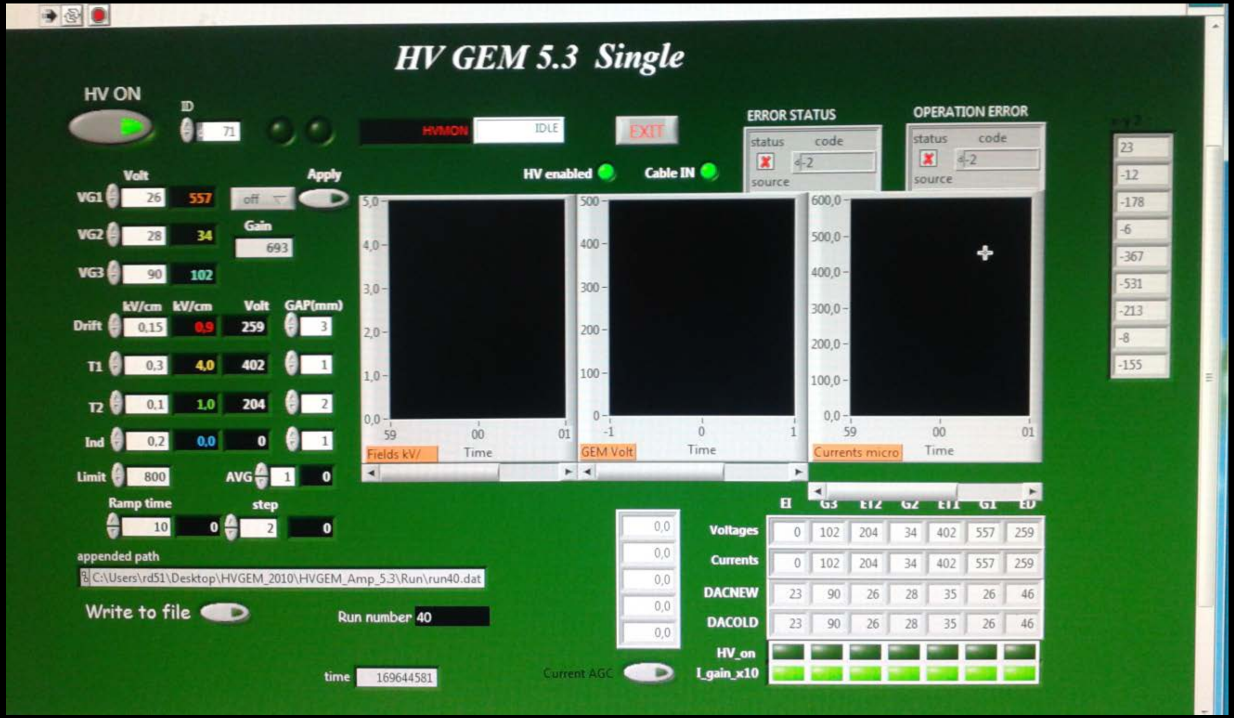

G. Corradi, F. Murtas and D.Tagnani, **A novel High Voltage System for a triple GEM detector.** *Nuclear Inst. and Methods in Physics Research, A (NIMA46 128)*

Front-End Readout Board

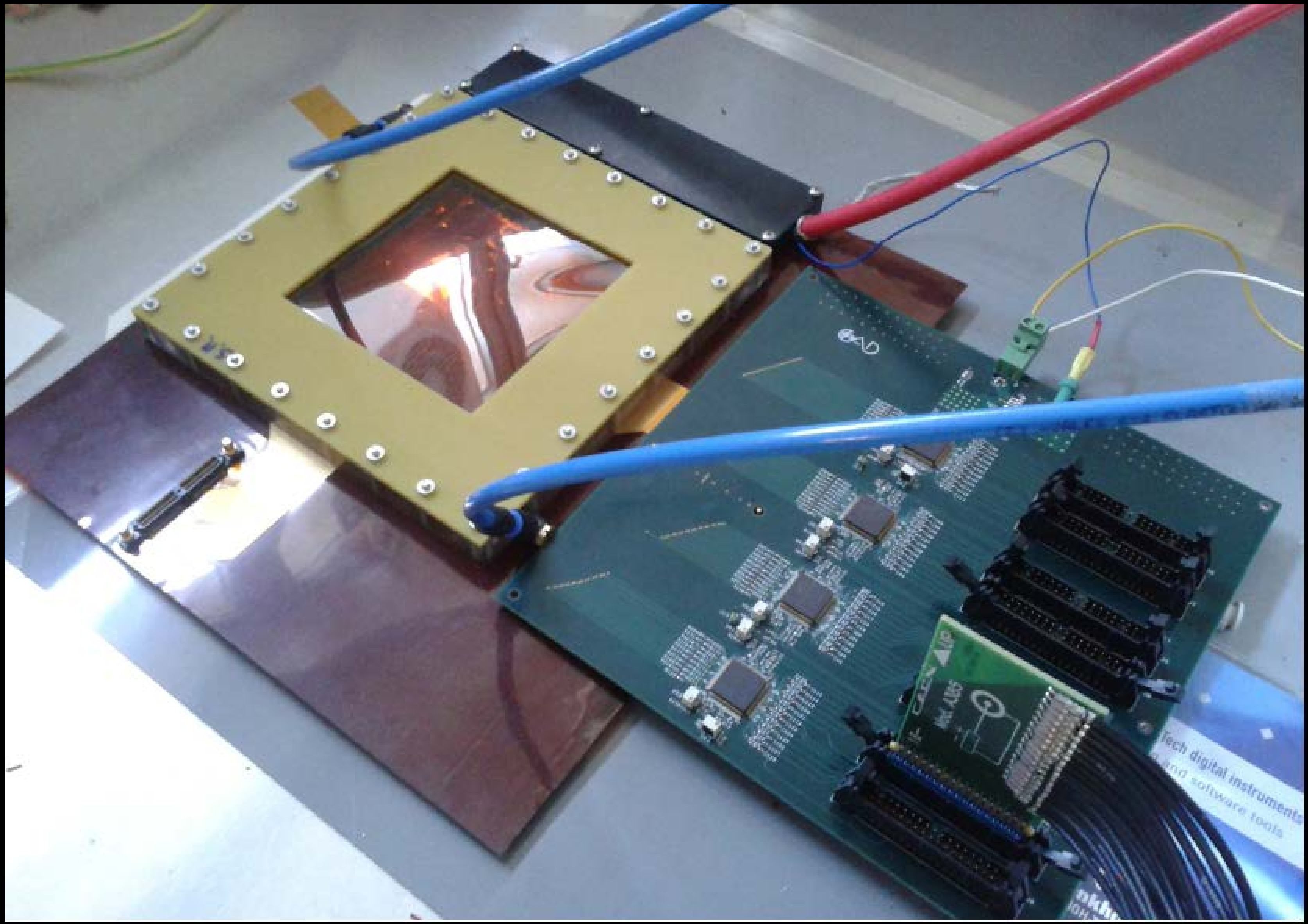

GASTONE_32 main features

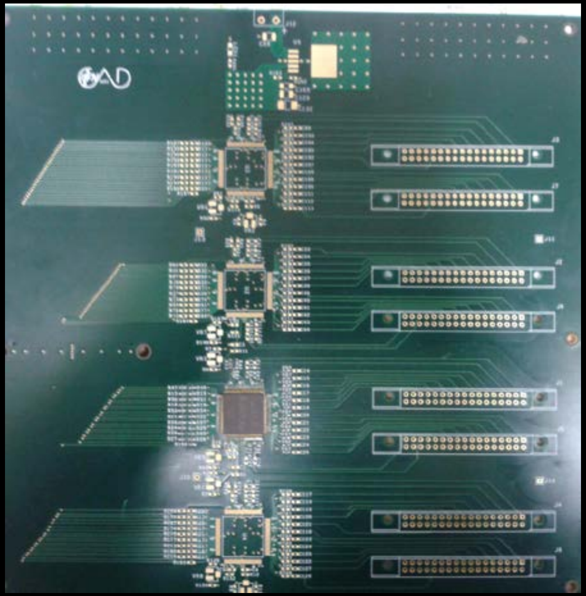

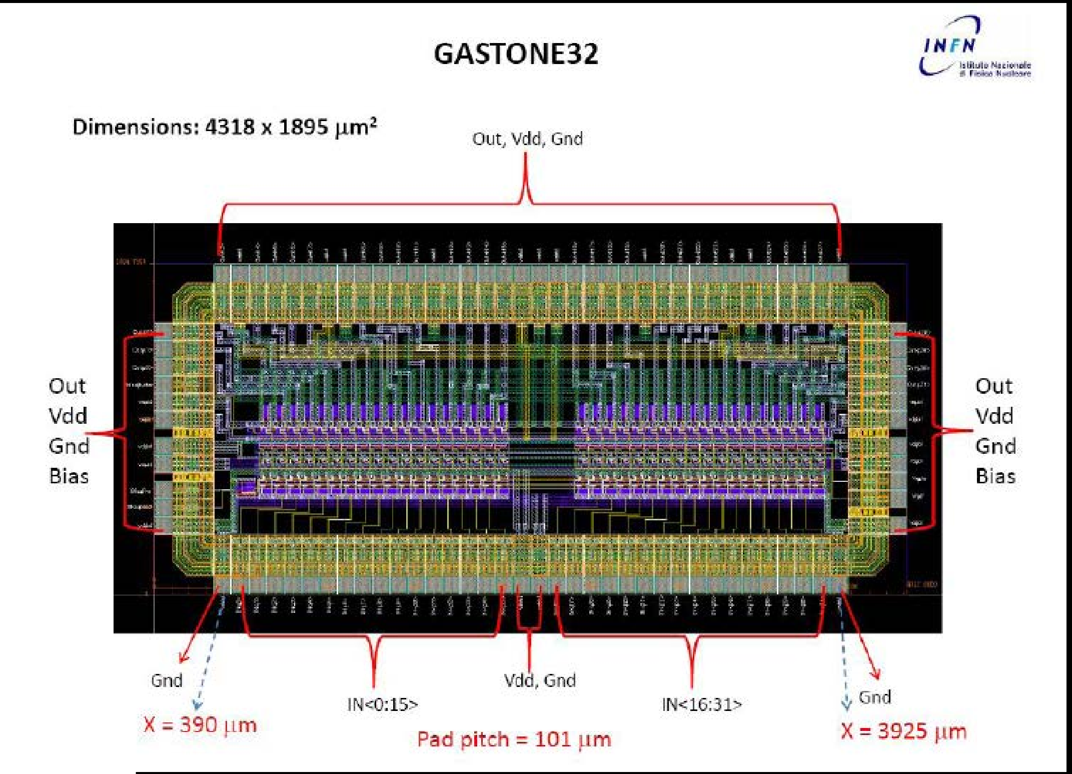

Input impedance	120 Ω
C_{det} range	0 – 150 pF
Number of channels	32
Baseline restorer	No
Total Gain sensitivity	20 mV/fC (C_{det} = 0 pF)
Peaking time	90 ns (C_D=100 pF)
Measured X-talk	< 1%
ENC (rms) measured on detector	800 e^- + 40 e^-/pF
Input protection circuitry	Integrated in each input channel
Power consumption	5 mW/Ch

- Capable to drive a 50Ω line
- Signal referred to GND

Backup

Charge induction – ionization chamber

SIGNAL DEVELOPMENT BY A MOVING CHARGE +Q

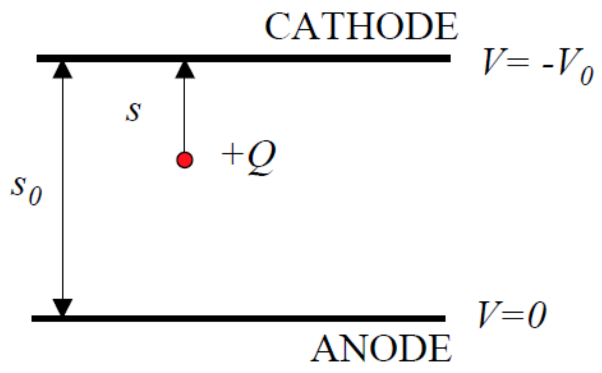

Charge induced on each electrode by +Q moving through the difference of potential dV:

$$dq = Q\frac{dV}{V_0} = Q\frac{ds}{s_0}$$

Integrating over s (or time t):

$$q(s) = \frac{Q}{s_0}s \quad q(t) = \frac{Q}{s_0}wt \quad i(t) = \frac{dq}{dt} = \frac{Q}{s_0}w$$

Electrons- ion pair (-Q and +Q) released at the same distance s from the cathode :

$$q(t) = Q\left(\frac{w^- t}{s_0} + \frac{w^+ t}{s_0}\right) \quad 0 \le t \le T^-$$

$$q(t) = Q\left(\frac{s - s_0}{s_0} + \frac{w^+ t}{s_0}\right) \quad T^- \le t \le T^+$$

$$q(T^+) = Q$$

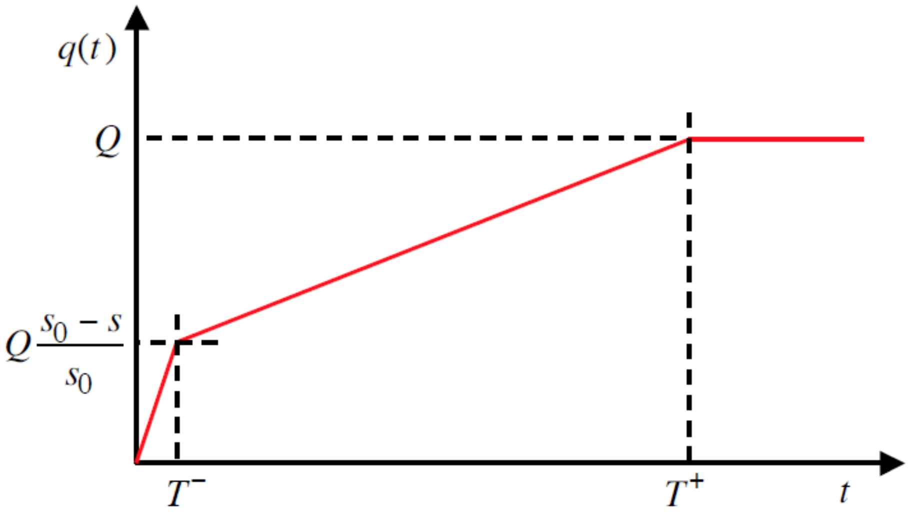

w^- (w^+) : electron (ion) drift velocity

T^- (T^+) : total electron (ion) drift time

($+Q$ on cathode , $-Q$ on anode)

Charge induction – avalanche multiplication – uniform field

PARALLEL PLATE COUNTERS:

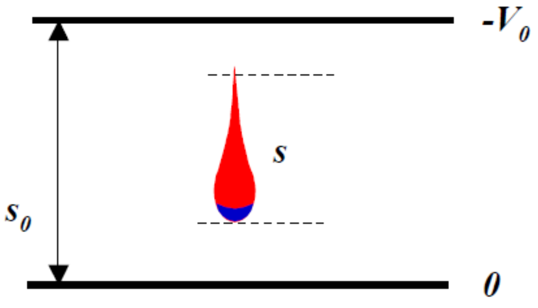

Increase in the number of charges after a path ds:

$$dn = n\alpha ds \qquad n = n_0 e^{\alpha s}$$

Charge induced by electrons: $dq^- = -en_0 e^{\alpha s} \dfrac{ds}{s_0}$

$$q^-(s) = \frac{en_0}{\alpha s_0}(e^{\alpha s} - 1) \approx \frac{en_0}{\alpha s_0} e^{\alpha s} = \frac{en_0}{\alpha s_0} e^{\alpha w^- t}$$

$$i^-(t) = \frac{dq^-}{dt} = \frac{en_0 w^-}{s_0} e^{\alpha w^- t} = \frac{en_0}{T^-} e^{\alpha w^- t}$$

Current signal induced by ions:

$$i^+(t) = \frac{en_0}{T^+}\left(e^{\alpha w^- t} - e^{\alpha w^* t}\right) \quad 0 \le t \le T^-$$

$$i^+(t) = \frac{en_0}{T^+}\left(e^{\alpha s} - e^{\alpha w^* t}\right) \quad T^- \le t \le T^+$$

$$\frac{1}{w^*} = \frac{1}{w^+} + \frac{1}{w^-}$$

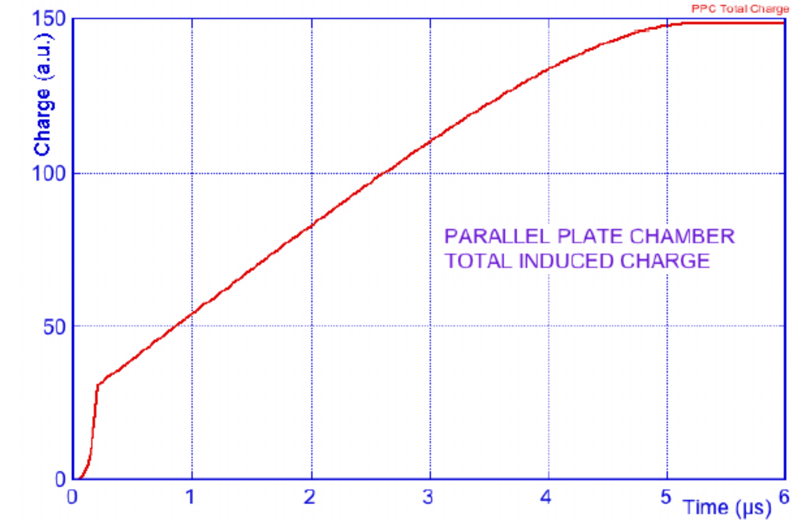

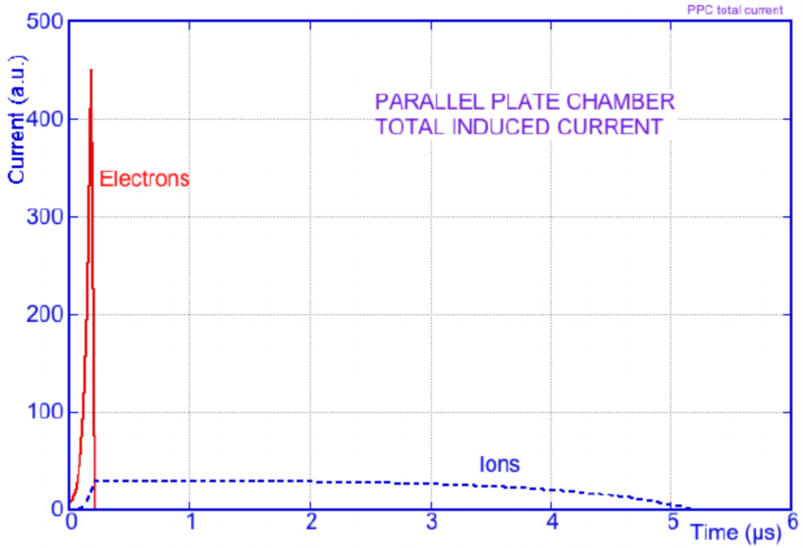

SWPC – signal formation

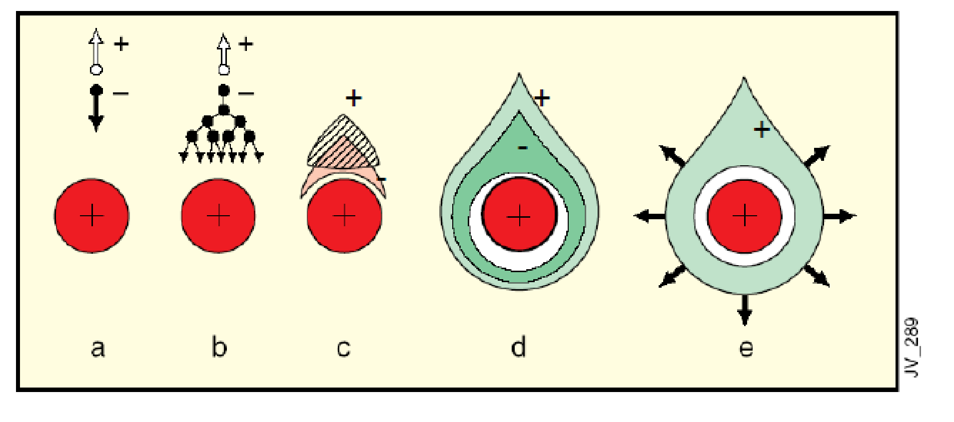

Avalanche formation within a few wire radii and within t < 1 ns.
Signal induction both on anode and cathode due to moving charges (both electrons and ions).

$$dv = \frac{Q}{lCV_0}\frac{dV}{dr}dr$$

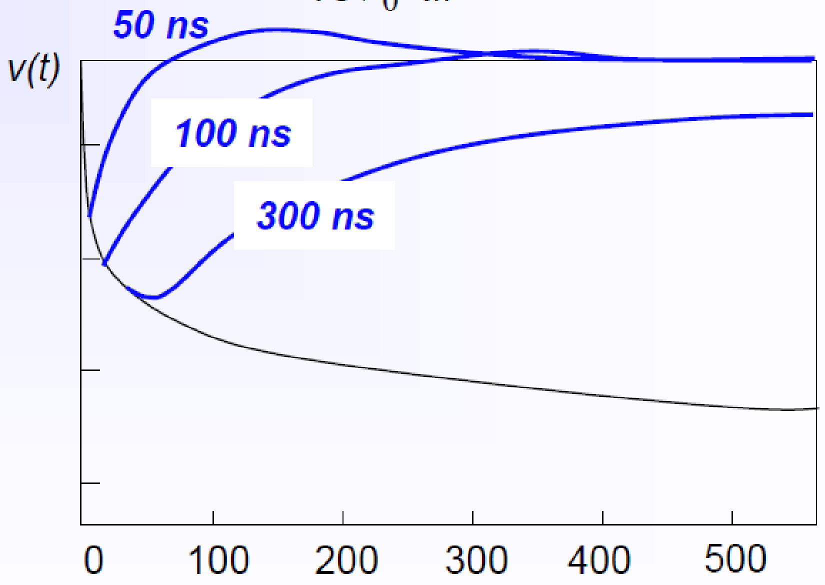

Electrons collected by the anode wire i.e. dr is very small (few μm). Electrons contribute only very little to detected signal (few %).
Ions have to drift back to cathode i.e. dr is large (few mm). Signal duration limited by total ion drift time.

Need electronic signal differentiation to limit dead time.

Energy spectrum of Sr^{90} radioactive decay

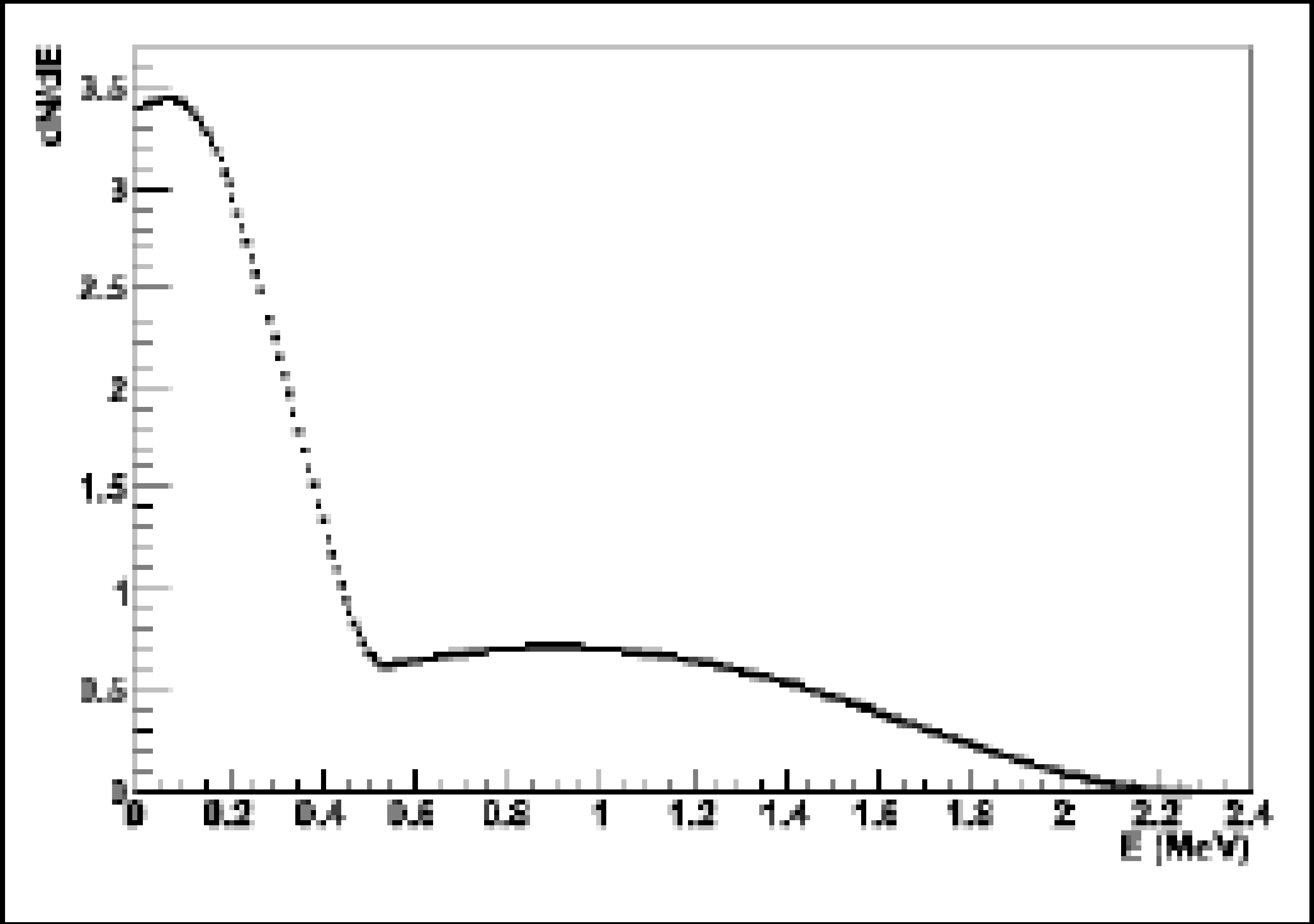

Two decay channels observed:

1. β^- of 546 KeV → Y^{90}
2. β^- of 2.28 MeV + Zr^{90} stable